INL/EXT-10-19627

Evaluation of Zero-Power, Elevated-Temperature Measurements at Japan's High Temperature Engineering Test Reactor

John D. Bess
Nozomu Fujimoto
James Sterbentz
Luka Snoj
Atsushi Zukeran

March 2011

The INL is a U.S. Department of Energy National Laboratory
operated by Battelle Energy Alliance

INL/EXT-10-19627

Evaluation of Zero-Power, Elevated-Temperature Measurements at Japan's High Temperature Engineering Test Reactor

John D. Bess
Nozomu Fujimoto[1]
James W. Sterbentz
Luka Snoj[2]
Atsushi Zukeran[3]

[1]Japan Atomic Energy Agency
[2]Jožef Stefan Institute
[3]Senior Reactor Physics Consultant

March 2011

Idaho National Laboratory
Idaho Falls, Idaho 83415

http://www.inl.gov

Prepared for the
U.S. Department of Energy
Office of Nuclear Energy
Under DOE Idaho Operations Office
Contract DE-AC07-05ID14517

NEA/NSC/DOC(2006)1

Gas Cooled (Thermal) Reactor - GCR

HTTR-GCR-RESR-003
CRIT-COEF

EVALUATION OF ZERO-POWER, ELEVATED-TEMPERATURE MEASUREMENTS AT JAPAN'S HIGH TEMPERATURE ENGINEERING TEST REACTOR

Evaluators

John D. Bess
Idaho National Laboratory

Nozomu Fujimoto
Japan Atomic Energy Agency

Internal Reviewers

James W. Sterbentz
Idaho National Laboratory

Independent Reviewers

Luka Snoj
Jožef Stefan Institute

Atsushi Zukeran
Senior Reactor Physics Consultant

Gas Cooled (Thermal) Reactor - GCR

HTTR-GCR-RESR-003
CRIT-COEF

Status of Compilation / Evaluation / Peer Review

Section 1	Compiled	Independent Review	Working Group Review	Approved
1.0 DETAILED DESCRIPTION	YES	YES	YES	YES
1.1 Description of the Critical and / or Subcritical Configuration	YES	YES	YES	YES
1.2 Description of Buckling and Extrapolation Length Measurements	NA	NA	NA	NA
1.3 Description of Spectral Characteristics Measurements	NA	NA	NA	NA
1.4 Description of Reactivity Effects Measurements	NA	NA	NA	NA
1.5 Description of Reactivity Coefficient Measurements	YES	YES	YES	YES
1.6 Description of Kinetics Measurements	NA	NA	NA	NA
1.7 Description of Reaction-Rate Distribution Measurements	NA	NA	NA	NA
1.8 Description of Power Distribution Measurements	NA	NA	NA	NA
1.9 Description of Isotopic Measurements	NA	NA	NA	NA
1.10 Description of Other Miscellaneous Types of Measurements	NA	NA	NA	NA
Section 2	**Evaluated**	**Independent Review**	**Working Group Review**	**Approved**
2.0 EVALUATION OF EXPERIMENTAL DATA	YES	YES	YES	YES
2.1 Evaluation of Critical and / or Subcritical Configuration Data	YES	YES	YES	YES
2.2 Evaluation of Buckling and Extrapolation Length Data	NA	NA	NA	NA
2.3 Evaluation of Spectral Characteristics Data	NA	NA	NA	NA
2.4 Evaluation of Reactivity Effects Data	NA	NA	NA	NA
2.5 Evaluation of Reactivity Coefficient Data	YES	YES	YES	YES
2.6 Evaluation of Kinetics Measurements Data	NA	NA	NA	NA
2.7 Evaluation of Reaction Rate Distributions	NA	NA	NA	NA
2.8 Evaluation of Power Distribution Data	NA	NA	NA	NA
2.9 Evaluation of Isotopic Measurements	NA	NA	NA	NA
2.10 Evaluation of Other Miscellaneous Types of Measurements	NA	NA	NA	NA

Gas Cooled (Thermal) Reactor - GCR

HTTR-GCR-RESR-003
CRIT-COEF

Section 3	Compiled	Independent Review	Working Group Review	Approved
3.0 BENCHMARK SPECIFICATIONS	YES	YES	YES	YES
3.1 Benchmark-Model Specifications for Critical and / or Subcritical Measurements	YES	YES	YES	YES
3.2 Benchmark-Model Specifications for Buckling and Extrapolation Length Measurements	NA	NA	NA	NA
3.3 Benchmark-Model Specifications for Spectral Characteristics Measurements	NA	NA	NA	NA
3.4 Benchmark-Model Specifications for Reactivity Effects Measurements	NA	NA	NA	NA
3.5 Benchmark-Model Specifications for Reactivity Coefficient Measurements	YES	YES	YES	YES
3.6 Benchmark-Model Specifications for Kinetics Measurements	NA	NA	NA	NA
3.7 Benchmark-Model Specifications for Reaction-Rate Distribution Measurements	NA	NA	NA	NA
3.8 Benchmark-Model Specifications for Power Distribution Measurements	NA	NA	NA	NA
3.9 Benchmark-Model Specifications for Isotopic Measurements	NA	NA	NA	NA
3.10 Benchmark-Model Specifications of Other Miscellaneous Types of Measurements	NA	NA	NA	NA
Section 4	**Compiled**	**Independent Review**	**Working Group Review**	**Approved**
4.0 RESULTS OF SAMPLE CALCULATIONS	YES	YES	YES	YES
4.1 Results of Calculations of the Critical or Subcritical Configurations	YES	YES	YES	YES
4.2 Results of Buckling and Extrapolation Length Calculations	NA	NA	NA	NA
4.3 Results of Spectral Characteristics Calculations	NA	NA	NA	NA
4.4 Results of Reactivity Effect Calculations	NA	NA	NA	NA
4.5 Results of Reactivity Coefficient Calculations	YES	YES	YES	YES
4.6 Results of Kinetics Parameter Calculations	NA	NA	NA	NA
4.7 Results of Reaction-Rate Distribution Calculations	NA	NA	NA	NA
4.8 Results of Power Distribution Calculations	NA	NA	NA	NA
4.9 Results of Isotopic Calculations	NA	NA	NA	NA
4.10 Results of Calculations of Other Miscellaneous Types of Measurements	NA	NA	NA	NA
Section 5	**Compiled**	**Independent Review**	**Working Group Review**	**Approved**
5.0 REFERENCES	YES	YES	YES	YES
Appendix A: Computer Codes, Cross Sections, and Typical Input Listings	YES	YES	YES	YES

EVALUATION OF ZERO-POWER, ELEVATED-TEMPERATURE MEASUREMENTS AT JAPAN'S HIGH TEMPERATURE ENGINEERING TEST REACTOR

IDENTIFICATION NUMBER: HTTR-GCR-RESR-003
CRIT-COEF

KEY WORDS: critical configurations, graphite-moderated, graphite-reflected, helium coolant, HTTR, isothermal, low enriched uranium (LEU), pin-in-block fuel, prismatic fuel, temperature coefficient, thermal reactor, TRISO, uranium oxide fuel

SUMMARY INFORMATION

1.0 DETAILED DESCRIPTION

The High Temperature Engineering Test Reactor (HTTR) of the Japan Atomic Energy Agency (JAEA) is a 30 MWth, graphite-moderated, helium-cooled reactor that was constructed with the objectives to establish and upgrade the technological basis for advanced high-temperature gas-cooled reactors (HTGRs) as well as to conduct various irradiation tests for innovative high-temperature research. The core size of the HTTR represents about one-half of that of future HTGRs, and the high excess reactivity of the HTTR, necessary for compensation of temperature, xenon, and burnup effects during power operations, is similar to that of future HTGRs. During the start-up core physics tests of the HTTR, various annular cores were formed to provide experimental data for verification of design codes for future HTGRs.[a]

The Japanese government approved construction of the HTTR in the 1989 fiscal year budget; construction began at the Oarai Research and Development Center in March 1991 and was completed May 1996. Fuel loading began July 1, 1998, from the core periphery. The first criticality was attained with an annular core on November 10, 1998 at 14:18, followed by a series of start-up core physics tests (Figure 1.1) until a fully-loaded core was developed on December 16, 1998. Criticality tests were carried out into January 1999. The first full power operation with an average core outlet temperature of 850 ºC was completed on December 7, 2001, and operational licensing of the HTTR was approved on March 6, 2002. The HTTR attained high temperature operation at 950 ºC in April 19, 2004. After a series of safety demonstration tests, it will be used as the heat source in a hydrogen production system by 2015. A short history of the HTTR project is shown in Figure 1.2.[b]

[a] N. Fujimoto, K. Yamashita, N. Nojiri, M. Takeuchi, and S. Fujisaki, "Annular Core Experiments in HTTR's Start-Up Core Physics Tests," *Nucl. Sci. Eng.*, **150**, 310-321 (2005).
[b] S. Shiozawa, S. Fujikawa, T. Iyoku, K. Kunitomi, and Y. Tachibana, "Overview of HTTR Design Features," *Nucl. Eng. Des.*, **233**:11-21 (2004).

Hot zero-power critical,[a] rise-to-power,[b] irradiation,[c] and safety demonstration testing[d,e] have also been performed with the HTTR, representing additional means for computational validation efforts. Power tests were performed in steps from 0 to 30 MW, with various tests performed at each step to confirm core characteristics, thermal-hydraulic properties, and radiation shielding (Ref. 1). The high-temperature test operation at 950 ºC represented the fifth and final phase of the rise-to-power tests.[f] The safety tests demonstrated inherent safety features of the HTTR such as slow temperature response during abnormal events due to the large heat capacity of the core and the negative reactivity feedback.[g] A more detailed summary of the rise-to-power with safety tests is shown in Table 1.1.

The experimental benchmark evaluated in this report pertains to the data available for two zero-power, warm-critical measurements with the fully-loaded HTTR core. Six isothermal temperature coefficients for the fully-loaded core from approximately 340 to 740 K have also been evaluated. These experiments were performed as part of the power-up tests (Refs. 1 and 2). Evaluation of the start-up core physics tests specific to the fully-loaded core (HTTR-GCR-RESR-001) and annular start-up core loadings (HTTR-GCR-RESR-002) have been previously evaluated.

---

[a] J. C. Kuijper, X. Raepsaet, J. B. M. de Haas, W. von Lensa, U. Ohlig, H-J. Ruetten, H. Brockmann, F. Damian, F. Dolci, W. Bernnat, J. Oppe, J. L. Kloosterman, N. Cerullo, G. Lomonaco, A. Negrini, J. Magill, and R. Seiler, "HTGR Reactor Physics and Fuel Cycle Studies," *Nucl. Eng. Des.*, **236**: 615-634 (2006).

[b] S. Nakagawa, Y. Tachibana, K. Takamatsu, S. Ueta, and S. Hanawa, "Performance Test of HTTR," *Nucl. Eng. Des.*, **233**: 291-300 (2004).

[c] T. Shibata, T. Kikuchi, S. Miyamoto, and K. Ogura, "Assessment of Irradiation Temperature Stability of the First Irradiation Test Rig in the HTTR," *Nucl. Eng. Des.*, **223**: 133-143 (2003).

[d] Y. Tachibana, S. Nakagawa, T. Takeda, A. Saikusa, T. Furusawa, K. Takamatsu, K. Sawa, and T. Iyoku, "Plan for the First Phase of Safety Demonstration Tests of the High Temperature Engineering Test Reactor (HTTR)," *Nucl. Eng. Des.*, **224**: 179-197 (2003).

[e] S. Nakagawa, K. Takamatsu, Y. Tachibana, N. Sakaba, and T. Iyoku, "Safety Demonstration Tests using High Temperature Engineering Test Reactor," *Nucl. Eng. Des.*, **233**: 301-308 (2004).

[f] S. Fujikawa, H. Hayashi, T. Nakazawa, K. Kawasaki, T. Iyoku, S. Nakagawa, and N. Sakaba, "Achievement of Reactor-Outlet Coolant Temperature of 950 ºC in HTTR," *J. Nucl. Sci. Tech.*, **41**(12): 1245-1254 (December 2004).

[g] S. Nakagawa, D. Tochio, K. Takamatsu, M. Goro, and T. Takeda, "Improvement of Analysis Technology for High Temperature Gas-Cooled Reactor by using Data Obtained in High Temperature Engineering Test Reactor," *J. Power Energy Syst.*, **2**(1): 83-91 (2008).

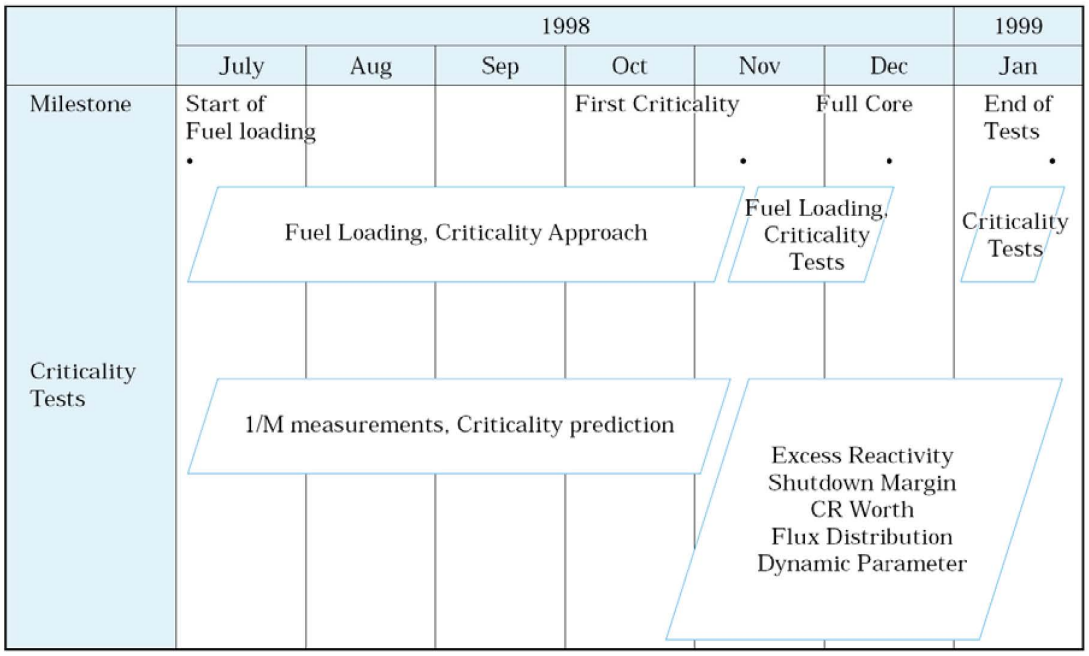

Figure 1.1. Progress of Start-Up Core Physics Tests.[a]

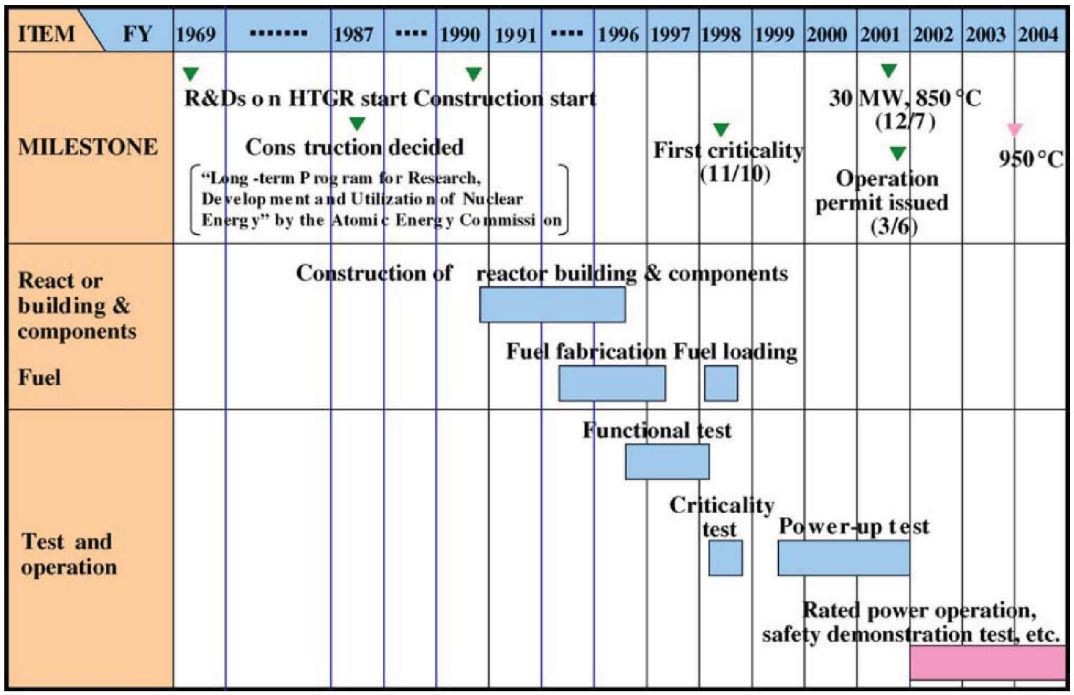

Figure 1.2. History of the HTTR Project.[b]

[a] "Present Status of HTGR Research and Development," Japan Atomic Energy Research Institute, Tokaimura, March 2004.

[b] S. Shiozawa, S. Fujikawa, T. Iyoku, K. Kunitomi, and Y. Tachibana, "Overview of HTTR Design Features," *Nucl. Eng. Des.*, **233**:11-21 (2004).

Table 1.1. HTTR Rise-to-Power and Safety Operation History.[a]

Operation name	Operation mode		Max. reactor thermal power (MW)	Duration	Operation time (MWd)	Remarks
1st phase rise-to-power test (PT-1)	●	▲	9	23 April–8 May 2000 11–26 May 2000	193	
		◆	9	30 May–6 June 2000		
2nd phase rise-to-power test (PT-2)	●	▲	20	3–8 July 2000 29 January–12 February 2001	63 423	a)
		◆	20	16 February–1 March 2001		
3rd phase rise-to-power test (PT-3)	■	▲	20	14 April–7 May 2001 11–16 May 2001 21 May–8 June 2001	689	b)
		◆	20			
4th phase rise-to-power test (PT-4)	●	▲	30	23 October–14 December 2001	1,293	Achievement of 850°C, 30 MW
		◆	30	25 January–6 March 2002	984	Operation permit issued.
1st operation cycle (RP/RS-1)	●	◆	30	30 May–17 June 2002	370	
		▲	9	21 June–1 July 2002	92	Safety demonstration test
2nd operation cycle (RS-2)	●	▲	30	5 February–14 March 2003	658	Safety demonstration test
3rd operation cycle (RP-3)	●	◆	20	16–21 May 2003	72	a)
4th operation cycle (RS-4)	●	▲	9	8–11 August 2003	25	Safety demonstration test
5th operation cycle (RS-5)	●	▲	30	27 anuary–25 February 2004	549	Safety demonstration test
			18	29 February–5 March 2004		Safety demonstration test
5th phase rise-to-power test (PT-5)	■	▲	30	31 March–1 May 2004	679	Achievement of 950°C, 30 MW
		◆	30	2 June–2 July 2004	626	Operation permit issued.
Total operation time (include other operations, *i.e.* core physics tests)					6,717	

●: Rated operation mode, ■: High-temperature test operation mode, ▲: Single-loaded operation mode, ◆: Parallel-loaded operation mode
a) Automatically reactor shut-down caused by a signal of PPWC flow-rate low
b) Automatically reactor shut-down caused by a loss of off-site electric power by a thunderbolt

1.1 Description of the Critical and / or Subcritical Configuration

1.1.1 Overview of Experiment

The initial start-up core physics tests for the High Temperature Engineering Test Reactor were performed between the months of July 1998 and January 1999. The HTTR facility is at the Oarai Research and Development Center of the Japan Atomic Energy Agency.

Core physics tests, including start-up and power-up operations, were planned in order to ensure core performance and reactor safety of an HTGR. Results were obtained for a core burn-up of up to 5 GWD/t. During these tests, the critical approach, the excess reactivity, the shutdown margin, the control rod worth, the reactivity coefficient, the neutron flux distribution, and the power distribution were measured and compared with the calculated results. Power-up tests began in April 2000 (Ref. 1).

Included in the initial IAEA benchmark study[b] is an analysis of the core isothermal temperature coefficients. These values were for analysis purposes only and did not represent actual core measurements. The accompanying warm critical rod position data for the HTTR at an isothermal temperature of 480 K was also provided only for evaluative purposes. However, subsequent publications from staff at the JAEA have provided elevated-temperature measurements in the HTTR, from which

[a] S. Fujikawa, H. Hayashi, T. Nakazawa, K. Kawasaki, T. Iyoku, S. Nakagawa, and N. Sakaba, "Achievement of Reactor-Outlet Coolant Temperature of 950 ºC in HTTR," *J. Nucl. Sci. Tech.*, **41**(12): 1245-1254 (December 2004).

[b] "Evaluation of High Temperature Gas Cooled Reactor Performance: Benchmark Analysis Related to Initial Testing of the HTTR and HTR-10," IAEA-TECDOC-1382, International Atomic Energy Agency, Vienna, November 2003.

isothermal temperature coefficients and warm critical conditions of the fully-loaded core can be evaluated.

Two zero-power, elevated-temperature, fully-loaded core configurations were evaluated in this benchmark analysis. The uncertainty range of k_{eff} is between -0.57 and +0.68% Δk (1σ). Dominant uncertainties are the impurities in the IG-110 graphite blocks and PGX graphite reflector blocks. Comprehensive biases could not be completed for all aspects of this experiment.

The calculations performed (Section 4.1) using the benchmark models (Section 3.1) have a k_{eff} approximately 1.8% greater than the experimental benchmark value and within 3σ. It is currently difficult to obtain the necessary information to further improve the confidence in the benchmark model and effectively reduce the overall uncertainty. The necessary data are proprietary and its release is being restricted, because the benchmark configuration of the HTTR core is the same that is currently in operation. Once this information is made available, the HTTR benchmark can be adjusted as appropriate.

1.1.2 Geometry of the Experiment Configuration and Measurement Procedure

The geometric information publicly available for this benchmark can be found compiled in Section 1.1.2 of HTTR-GCR-RESR-001.

1.1.2.1 Description of Criticality Measurements

The HTTR is shown in Figures 1.3 and 1.4. The control rod (CR) pairs were named center (C), ring 1 (R1), ring 2 (R2), and ring 3 (R3) from the center to the outside as shown in Figure 1.3 (also see Section 3.1.2.10 and Figure 3.15). Both R2 and R3 CRs are in the replaceable reflector region surrounding the core, where the six CR pairs on the sides of the hexagonal loading pattern are R2 CRs and the three remaining CR pairs at corners of the hex are R3 CRs. Control rods positions were defined with distance from the bottom of the fifth fuel layer.[a]

The active core contains 30 fuel columns. One column contains five fuel blocks. Each fuel block has 31 or 33 coolant channels, into which fuel rods are inserted. Fuel rods consist of a graphite sleeve containing 14 fuel compacts. Each fuel compact contains about 13,000 coated fuel particles (CFPs) randomly embedded in a graphite matrix (elsewhere is reported that each fuel compact contains about 13,500 particles[b]). Fuel-block assembly is depicted in Figure 1.5. A CFP is comprised of a spherical fuel kernel of low-enriched UO_2 with a coating of four layers.

The active core region in Figure 1.4 is comprised of columns of either fuel blocks or control blocks. The top of all fuel columns in the active region of the core is located on the same plane, which is higher than the plane at which the top of the control columns resides within the active region of the core. For this reason the active core region does not appear level.

All control rod insertion levels are adjusted on the same level except for the three pairs of control rods in the most outer region in the side reflectors. These three pairs of CRs are usually fully withdrawn. Effective corrections to critical rod position in the core include a sinking effect from the CR driving

[a] N. Fujimoto, K. Yamashita, N. Nojiri, M. Takeuchi, and S. Fujisaki, "Annular Core Experiments in HTTR's Start-Up Core Physics Tests," *Nucl. Sci. Eng.*, **150**, 310-321 (2005).

[b] K. Minato, H. Kikuchi, T. Tobita, K. Fukuda, M. Kaneko, N. Suzuki, S. Yoshimuta, and H. Tomimoto, "Improvements in Quality of As-Manufactured Fuels for High-Temperature Gas-Cooled Reactors," *J. Nucl. Sci. Tech.*, **34**(3): 325-333 (March 1997).

mechanism of about -14 mm and a temperature expansion effect of about +2 mm from 25 to 27 ºC.[a] Reported Japanese data typically had the sinking effect already accounted for in the reported rod positions. This sinking effect is caused by the added "weight" of the CR system when pushed upon by the forced helium coolant. Application of the temperature expansion effect, which seems unreasonably large, seems incorrect and is not discussed in other reference documents for the HTTR.

Two zero-power, warm-critical measurements were performed on the fully-loaded core at 122.0 and 144.9 ºC (395.15 and 418.05 K, respectively). The control rods (C, R1, and R2) were withdrawn to 1873 and 1903 mm, respectively. These criticals were performed just prior to power-up tests, in September 1999, to evaluate two temperature coefficients at zero power (Ref. 2); see Section 1.5 for a summary of the measured isothermal temperature coefficients.

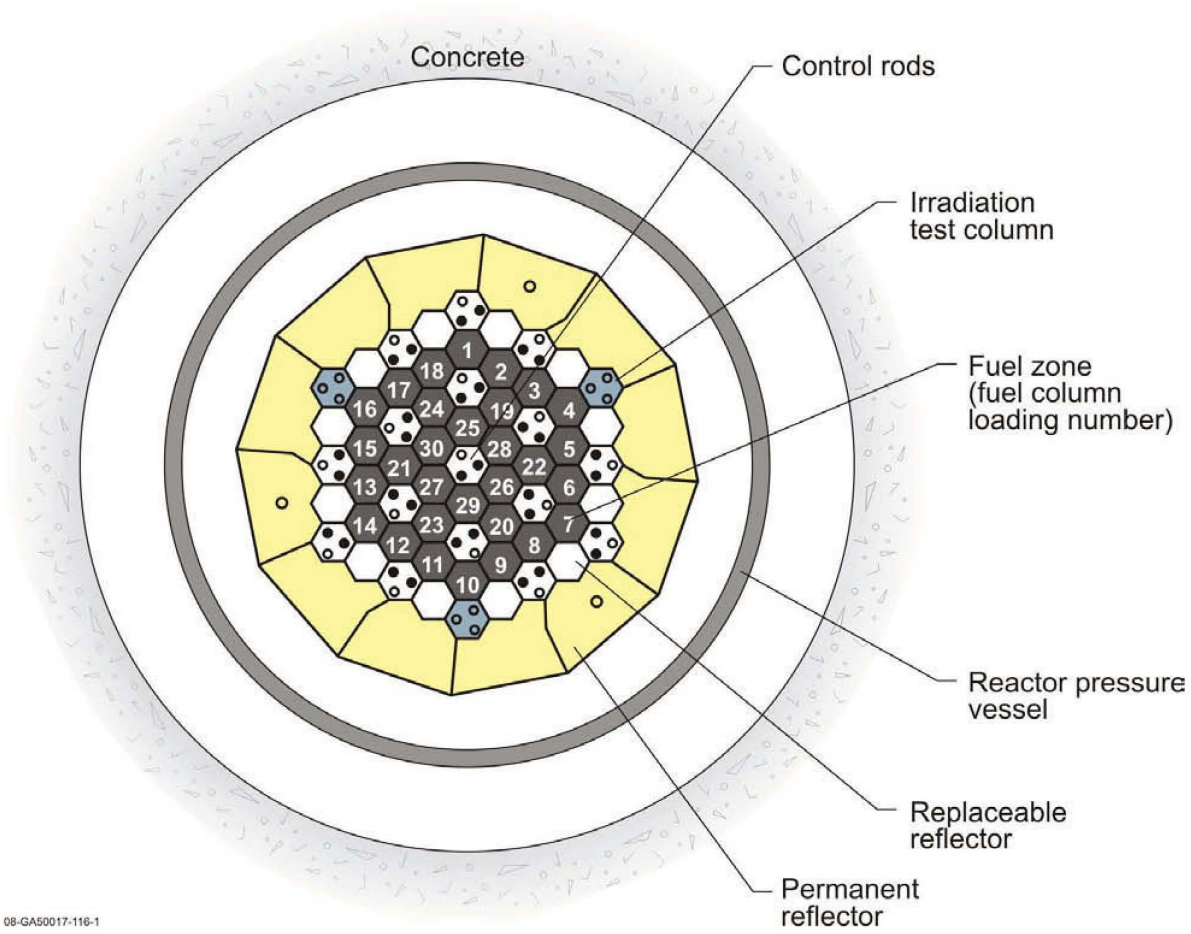

Figure 1.3. Loading Pattern of the HTTR.[b]

[a] "Evaluation of High Temperature Gas Cooled Reactor Performance: Benchmark Analysis Related to Initial Testing of the HTTR and HTR-10," IAEA-TECDOC-1382, International Atomic Energy Agency, Vienna, November 2003.

[b] N. Fujimoto, K. Yamashita, N. Nojiri, M. Takeuchi, and S. Fujisaki, "Annular Core Experiments in HTTR's Start-Up Core Physics Tests," *Nucl. Sci. Eng.*, **150**, 310-321 (2005).

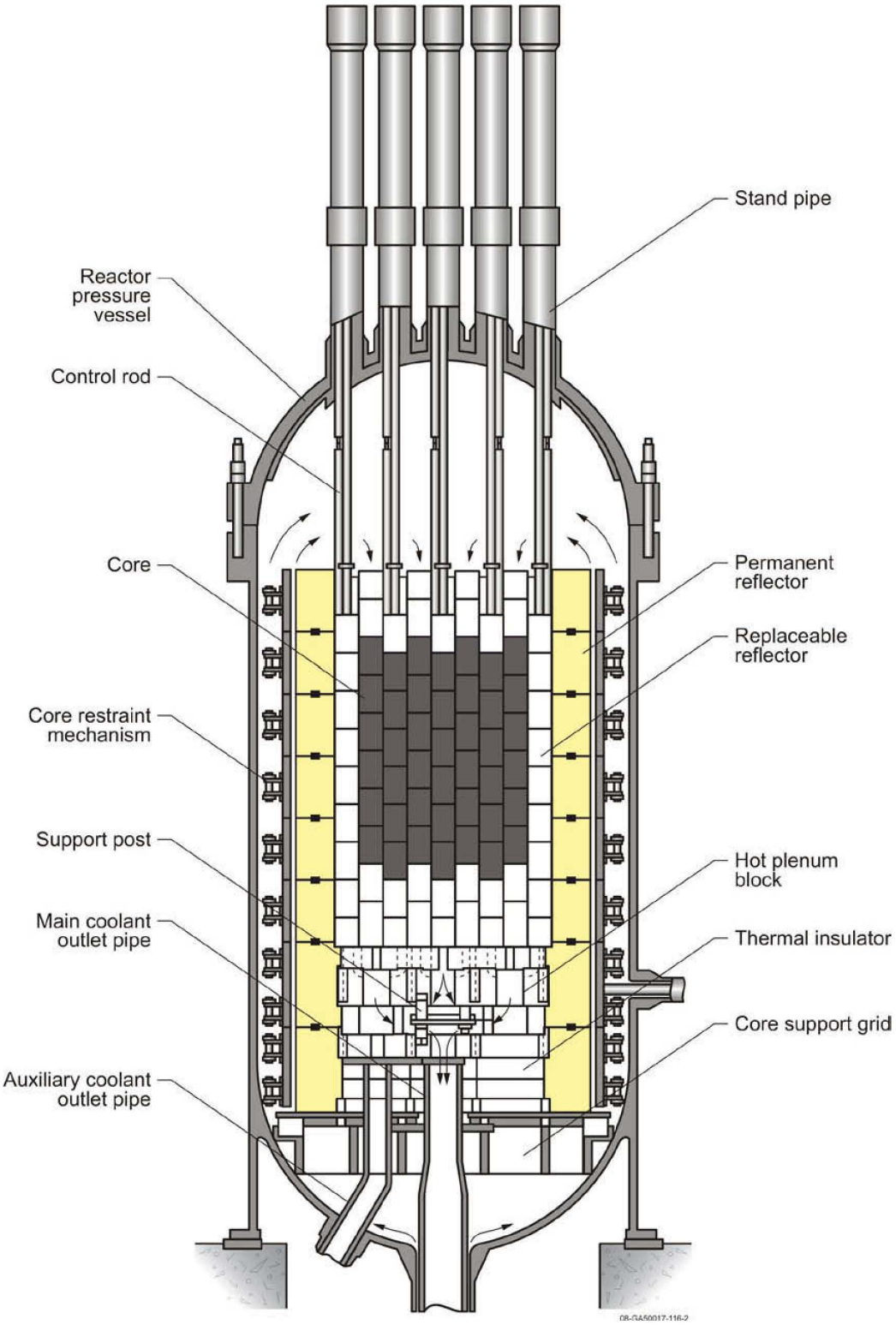

Figure 1.4. Vertical Cross Section of the HTTR.[a]

[a] N. Fujimoto, K. Yamashita, N. Nojiri, M. Takeuchi, and S. Fujisaki, "Annular Core Experiments in HTTR's Start-Up Core Physics Tests," *Nucl. Sci. Eng.*, **150**, 310-321 (2005).

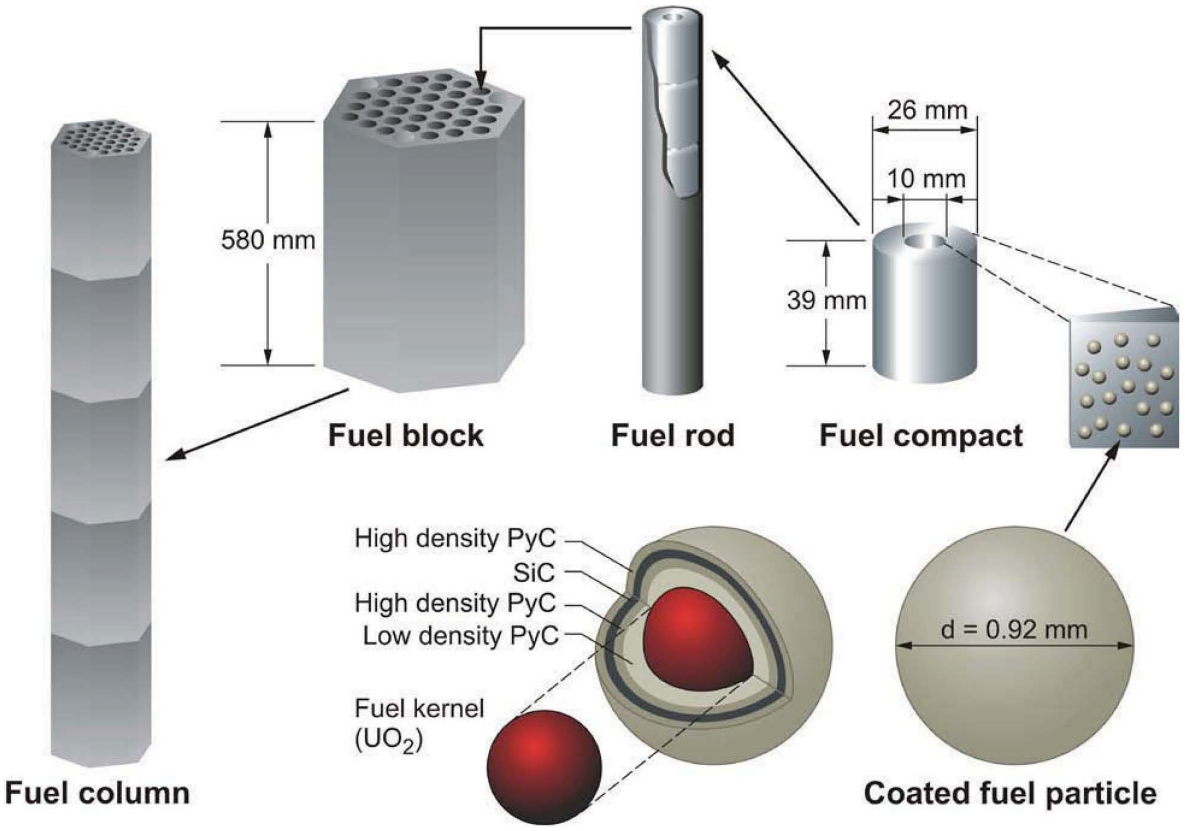

Figure 1.5. HTTR's Fuel Column, Fuel Block, Fuel Rod, Fuel Compact, and Coated Fuel Particle.[a]

1.1.3 Material Data

The material data publicly available for this benchmark can be found compiled in Section 1.1.3 of HTTR-GCR-RESR-001.

1.1.4 Temperature Data

The core was at isothermal temperatures of 122.0 and 144.9 ºC for the two warm critical measurements. Additional information regarding the equipment and method for performing temperature measurements was not available. Warm critical experiment data for the higher temperature isothermal temperature coefficients shown in Figure 1.6 were unavailable.

1.1.5 Additional Information Relevant to Critical and Subcritical Measurements

Additional information is not available.

[a] M. Goto, N. Nojiri, and S. Shimakawa, "Neutronics Calculations of HTTR with Several Nuclear Data Libraries," *J. Nucl. Sci. Tech.*, **43**(10): 1237-1244 (2006).

1.2 Description of Buckling and Extrapolation Length Measurements

Buckling and extrapolation length measurements were not made.

1.3 Description of Spectral Characteristics Measurements

Spectral characteristics measurements were not made.

1.4 Description of Reactivity Effects Measurements

Reactivity effects measurements were not made.

1.5 Description of Reactivity Coefficient Measurements

1.5.1 Overview of Experiment

Just prior to power-up tests, in September 1999, two warm critical measurements at zero power were performed to evaluate two temperature coefficients (See Section 1.1) (Ref. 2). Warm critical conditions here are considered to be core temperatures greater than room temperature but less than the HTTR full-power operational temperatures. Eleven additional isothermal temperature coefficients were measured that apply for core thermal power levels up to 20 MW (Ref. 1).

A total of six isothermal temperature coefficients for the fully-loaded core from approximately 340 to 740 K have also been evaluated. The lowest two measurements are derived from to the warm critical measurements discussed in Section 1.1. The eleven additional measurements in Figure 1.6, which do not have corresponding criticality data, were consolidated into four measurements due to repetition of measurements for given temperatures. One measurement at 421 K is acknowledged to have large measurement uncertainty and appears to be lower than expected when compared against the other coefficient measurements. Unknown internal heating effects not mentioned by the authors in Ref. 1 may also contribute to the difference between benchmark and calculated values at elevated temperatures. Additional unknown contributions to the uncertainty may include uncertainties in nuclear data and analysis tools and unknown experimental uncertainties in the measurement and evaluation of the isothermal temperature coefficients.

1.5.2 Geometry of the Experiment Configuration and Measurement Procedure

The geometric information publicly available for this benchmark can be found compiled in Section 1.1.2 of HTTR-GCR-RESR-001.

The fuel and reflector temperature coefficients of reactivity dominate the total measured reactivity coefficient of the HTTR. The temperature coefficient was obtained by comparing the reactivity difference caused by changes in core temperature. The core temperature was increased at a constant reactor power by reducing the heat removal via the secondary coolant system. The reactivity was then estimated from the control rod worth curve for each core temperature increase. Eleven different measurements were performed as part of the power-up tests between the isothermal core temperatures of approximately 150 and 470 ºC, that apply for core thermal power levels up to 20 MW (Ref. 1). These measurements are shown in Figure 1.6; multiple measurements were performed at given temperatures. The average coolant temperature represents the average isothermal temperature of the core. Additional information regarding power levels and control rod positions for production of Figure 1.6 is unavailable. The authors of Ref. 1 comment that “the experimental errors are very large” for measurements below 400 ºC (as shown in Figure 1.6).

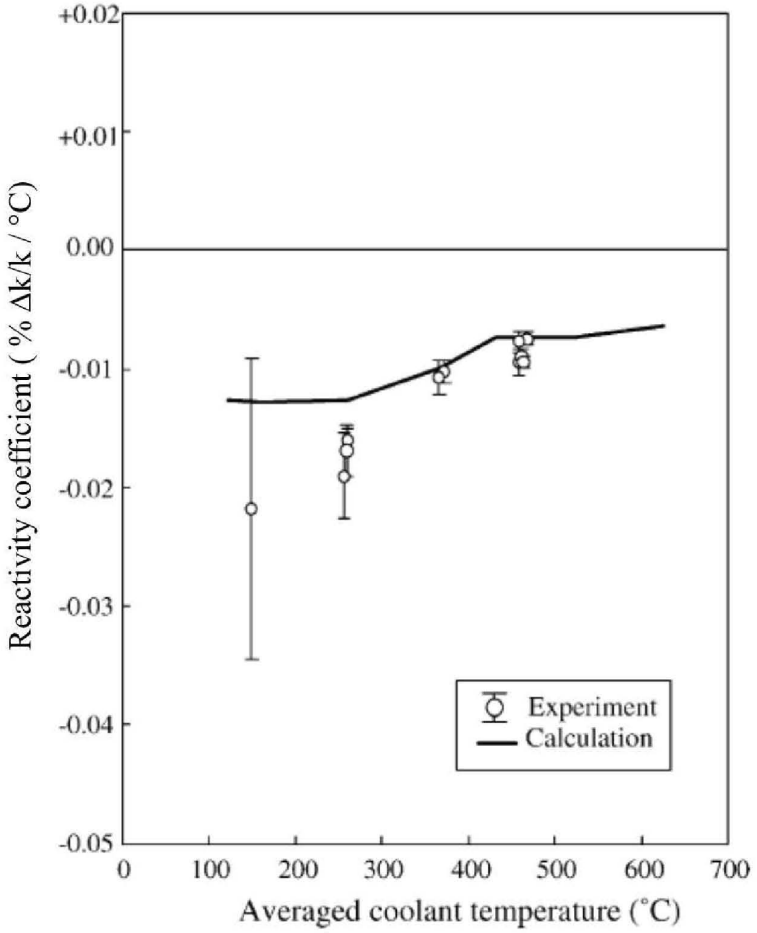

Figure 1.6. Temperature Coefficients vs. Average Coolant Temperature.

The original isothermal temperature coefficient data used to develop Figure 1.6 were not available.

Just prior to the power-up tests, two warm critical measurements (Section 1.1) were performed at zero-power to evaluate isothermal temperature coefficients at 72.4 and 133.5 ºC (345.55 and 406.65 K, respectively). The reported isothermal temperature coefficients at these two temperatures are -1.23×10^{-4} and -1.32×10^{-4} Δk/k/ºC (-12.3 and -13.2 pcm/ºC), respectively (Ref. 2). These measurements were separate from and were measured at lower temperatures than the eleven measurements provided in Figure 1.6.

The temperature coefficients are calculated using Equation 1.1, where the temperature coefficient worth at a given temperature is a function of the eigenvalues of two configurations with temperatures both above and below the temperature of the coefficient. The two lowest measurements were obtained from the criticality measurements described in Section 1.1 and the cold critical configuration described in HTTR-GCR-RESR-001. Warm critical experiment data for the higher temperature isothermal temperature coefficients shown in Figure 1.6 were unavailable.

$$\alpha_T = \frac{k_2 - k_1}{k_2 k_1}\left(\frac{1}{T_2 - T_1}\right). \qquad (1.1)$$

A summary of the six isothermal temperature coefficients evaluated in this benchmark is provided in Table 1.2. See Section 2.5 regarding the procedure for evaluation of the available data in Section 1.5 to obtain these benchmark experiment values with associated uncertainties. The values provided in Table 1.2 were derived from the original available data and best engineering judgment.

Table 1.2. Benchmark Experiment Isothermal Temperature Coefficients.

Data Point	Temperature (K)	Reactivity Coefficient (% Δk/k/K)	±	1σ Uncertainty
1	346	-0.0123	±	0.0032
2	407	-0.0132	±	0.0033
3	421	-0.0217	±	0.0130
4	533	-0.0165	±	0.0029
5	642	-0.0103	±	0.0028
6	736	-0.0086	±	0.0027

1.5.3 Material Data

The material data publicly available for this benchmark can be found compiled in Section 1.1.3 of HTTR-GCR-RESR-001.

1.5.4 Temperature Data

The reported isothermal temperature coefficient measurements are within the temperature range from approximately 70 to 470 ºC (~340 to 740 K). Additional information regarding the equipment and method for performing temperature measurements was not available.

1.5.5 Additional Information Relevant to Reactivity Coefficient Measurements

Additional information is not available.

1.6 Description of Kinetics Measurements

Kinetics measurements were not made.

1.7 Description of Reaction-Rate Distribution Measurements

Reaction-rate distribution measurements were not made.

1.8 Description of Power Distribution Measurements

Power distribution measurements were not made.

1.9 Description of Isotopic Measurements

Isotopic measurements were not made.

1.10 Description of Other Miscellaneous Types of Measurements

Other miscellaneous types of measurements were not made.

2.0 EVALUATION OF EXPERIMENTAL DATA

The overall uncertainty in the calculated value of k_{eff}, which is a function of multiple input parameters, is given by[a]

$$u_c^2(k_{eff}) = \sum_{i=1}^{N} (\Delta k_i)^2 + 2\sum_{i=1}^{N-1} \sum_{j=i+1}^{N} (\Delta k_i)(\Delta k_j) r_{i,j} \ . \qquad (2.1)$$

In Equation 2.1, Δk_i is the change in k_{eff} when parameter i is changed by the standard deviation in the parameter, and $r_{i,j}$ is the correlation coefficient for parameters i and j.

Where standard deviations are available, they are used for calculating the effects these uncertainties might have on k_{eff}, in terms of Δk_i. Where observed ranges are given, but not standard deviations, the limiting values of the observed ranges are usually applied, and plausible distribution functions are assumed for finding Δk_i. Where only tolerances are given, their limiting values are used, along with plausible distribution functions. Where no guidance is given on the variability of a parameter, engineering judgment is used to select a range of variation that will produce the largest reasonable uncertainty in k_{eff}. The bounding values in this range are then applied in the uncertainty analysis. If the overall uncertainty in k_{eff} predicted by this approach is small enough that the experiment can be judged an acceptable benchmark, one can be confident that the real experiment is actually even better. All uncertainties are adjusted to values of one standard deviation (1σ). No information is available on correlations among parameters, so all parameters and their uncertainties are assumed to be uncorrelated.

Usually, no information is publicly available about the distribution function of the deviation of a parameter from its nominal value. In most cases, it is reasonably assumed that the most relevant quantity is uniformly distributed. For example, if the change in k_{eff} from its nominal value is dependent on the change in the volume of a spatial region, then it is assumed that the deviation of the volume of that region from its nominal value is uniformly distributed.

The uncertainty analyses were performed in accordance with guidance provided in the ICSBEP Handbook.

It should be noted that assuming a uniform distribution of a parameter between its limits leads to overprediction of the effect on k_{eff}.

These observations are used repeatedly in the following analysis.

The following sections discuss the calculation of the effects of uncertainties in the parameters listed in tables in each section. The values of the tabulated parameters are computed in the benchmark critical configuration and in the configuration with each parameter assigned its maximum variation (or its standard deviation when available), one parameter at a time. The bases for the choices of the parameter values are discussed.

In all cases where tolerances or observed variations apply to large numbers of objects, such as TRISO fuel particles, both deterministic (or systematic) uncertainties (applying to all the objects equally) and random uncertainties (different from one object to the next) will occur. For the fuel particles and their subregions especially, the random uncertainties are extremely small (i.e., the tolerance limit for the random uncertainty divided by the square root of the number of fuel particles in the core). In all cases, division by such large numbers makes the random component of the uncertainty negligible. Positional dependence of objects within the assembly also influences the effective proportional effect on the

[a] *International Handbook of Evaluated Criticality Safety Benchmark Experiments,* NEA/NSC/DOC(95)03/I-VIII, OECD-NEA, "ICSBEP Guide to the Expression of Uncertainties," Revision 1, p. 29, September 30, 2004.

resultant uncertainty and bias calculations. However, since no information is available about how the uncertainties are divided between the systematic and random components, it is assumed throughout that the uncertainties are 25% systematic and 75% random for all uncertainties that exhibit a random component.

This assumption provides a basic prediction of the effect on k_{eff} until additional information regarding systematic uncertainties can be better evaluated. The 25% systematic uncertainty is bound by the fact that most systematic uncertainties would be below 50% of the total uncertainty and above the historic approach of ignoring the unknown systematic components (i.e., treat it with a 0% probability). In actuality, careful experimenters may have an unknown systematic uncertainty that is approximately 10-15% of their total reported uncertainty. Evaluated uncertainties are listed as calculated, such that the readers may themselves adjust results according to some desired systematic-to-random uncertainty ratio. The summary in Section 2.1.7 does list the systematic and random components of the uncertainty as separate entities based on the assumption that uncertainties with random components have 25% systematic uncertainty.

It is important to note that most parameters regarding the TRISO particles are normally distributed.

Thermal expansion effects upon material properties of the HTTR components are discussed in Section 3.1.1.2.

2.1 Evaluation of Critical and / or Subcritical Configuration Data

Monte Carlo n-Particle (MCNP) version 5.1.51 calculations were utilized to estimate the biases and uncertainties associated with the experimental results for HTTR critical configurations in this evaluation. MCNP is a general-purpose, continuous-energy, generalized-geometry, time-dependent, coupled n-particle Monte Carlo transport code.[a] The Evaluated Neutron Data File library, ENDF/B-VII.0,[b] was utilized in analysis of the experiment and benchmark model biases and uncertainties. The nuclear data processing system, NJOY-99.296,[c] was used to process the cross section libraries to the desired analysis temperatures (see example NJOY input file in Appendix A.1). Elemental data such as molecular weights and isotopic abundances were taken from the 16th edition of the Chart of the Nuclides.[d] These values are summarized in Appendix C.

Doppler-broadened neutron cross sections were generated for ^{234}U, ^{235}U, and ^{238}U with the NJOY computer code at 400 and 420 K. These two temperatures were selected to correspond to the warm critical temperatures of 391.15 and 418.05 K, respectively. The thermal neutron scattering data [$S(\alpha,\beta)$] for graphite and uranium dioxide were also generated with the NJOY computer code at the temperatures of 400 and 500 K. Thermal scattering data scaled linearly with temperature, and eigenvalue calculations at 420 K were corrected to the appropriate temperature. Additional uncertainty due to thermal scattering scaling was negligible.

Utility of the NJOY input files for nuclear data processing were verified by generating cross sections at room temperature and comparing computed eigenvalues with those calculated using previously compiled ENDF/B-VII.0 data for MCNP. A basic verification of the Doppler broadening of the ^{235}U total fission

[a] X-5 Monte Carlo Team, "MCNP – a General Monte Carlo n-Particle Transport Code, version 5," LA-UR-03-1987, Los Alamos National Laboratory (2003).

[b] M. B. Chadwick, et al., "ENDF/B-VII.0: Next Generation Evaluated Nuclear Data Library for Nuclear Science and Technology," *Nucl. Data Sheets*, **107**: 2931-3060 (2006).

[c] R. E. MacFarlane and D. W. Muir, "The NJOY Nuclear Data Processing System Version 91," LA-12740-M (October 1994).

[d] Nuclides and Isotopes: Chart of the Nuclides, 16th edition, (2002).

cross section was performed by plotting room temperature cross sections with cross sections processed at 780 K (Figure 2.1 and 2.2).

Only the primary components of the HTTR active core and surrounding reflector region were included in the analysis of uncertainties in this evaluation. The uncertainty analysis was performed using a model temperature of approximately 400 or 420 K for configurations 1 and 2, respectively. The fully-loaded core configuration at room temperature (300K) is analyzed in a separate report (HTTR-GCR-RESR-001). Five configurations representing the HTTR annular cores created during initial fuel loading are also analyzed in a separate report (HTTR-GCR-RESR-002).

For all impurity assessments, only the equivalent natural-boron content is utilized in the evaluation. In the compositions used in the evaluation models, the natural-boron content is adjusted to include only the primary absorber ^{10}B, according to an isotopic abundance of 19.9 at.%.

All MCNP calculations of k_{eff} have statistical uncertainties between 0.00011 and 0.00012, resulting in Δk statistical uncertainties of approximately 0.00016, assuming no correlation between the individual MCNP results.

Some of the calculated uncertainties are poorly estimated because they are very small and on the order of the statistical uncertainty of the analysis method. However, these uncertainties are insignificant in magnitude compared to the total benchmark uncertainty. Reanalysis of most of these parameters with larger variations would not significantly reduce their uncertainties below the statistical uncertainty of the Monte Carlo calculations.

Uncertainties less than 0.0002 are reported as negligible (neg). When calculated uncertainties in Δk_{eff} are less than their statistical uncertainties, the statistical uncertainties are used in the calculation of the total uncertainty.

The term “Scaling Factor” denotes the necessary correction to adjust the evaluated uncertainty in k_{eff} to a 1σ value. Often a larger uncertainty is evaluated such that the calculated Δk value is greater than the statistical uncertainty in the analysis method.

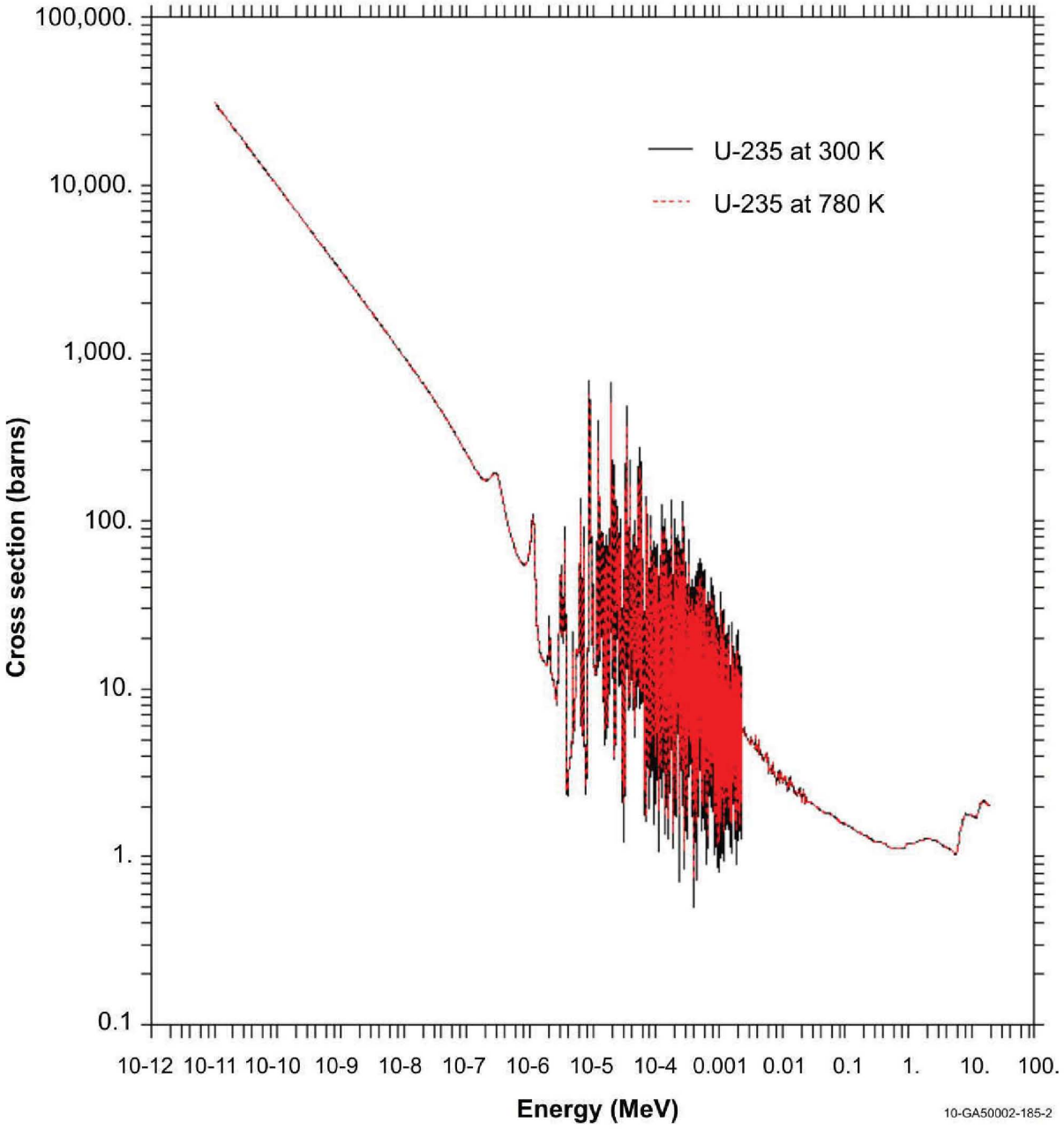

Figure 2.1. Comparison of Doppler Broadening of ^{235}U Fission Cross Section Data (full spectrum).

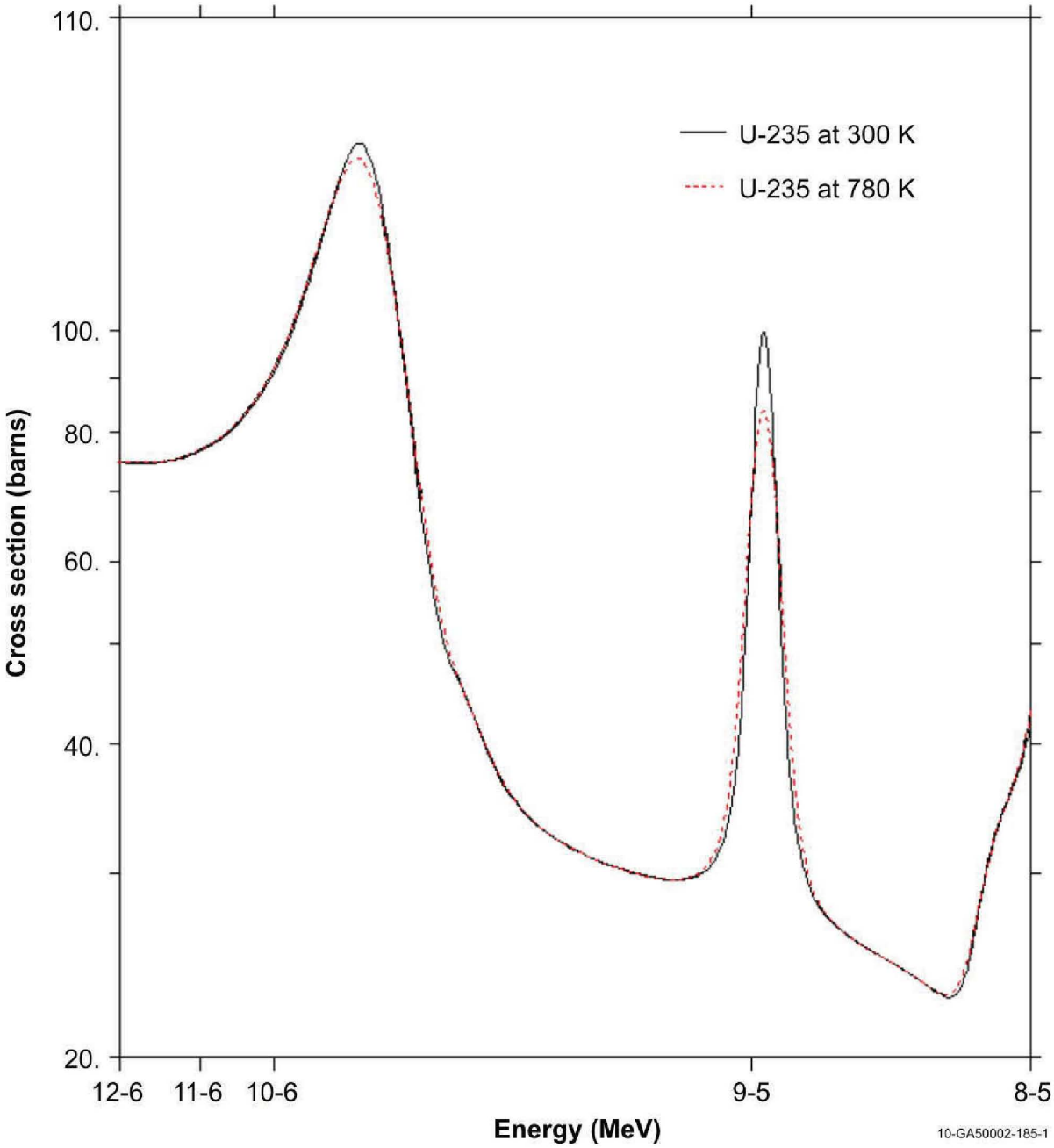

Figure 2.2. Comparison of Doppler Broadening of ^{235}U Fission Cross Section Data (0.8 to 3 eV).

2.1.1 Targeted Uncertainty Analysis

A significant number of perturbation analyses were performed for the cold critical, fully-loaded core configuration (HTTR-GCR-RESR-001) and annular core loadings (HTTR-GCR-RESR-002). Many of these uncertainties were insignificant. An analysis of the primary constituents contributing to the total uncertainty of the HTTR benchmark model for the fully-loaded core configuration was performed; approximately 98% of the total variance is contributed by the following sources:

- uranium enrichment,
- UO_2 impurity,
- graphite overcoat impurity,
- burnable poison pellet absorber content,
- isotopic abundance of boron,
- IG-110 graphite block density,
- IG-110 graphite block impurity,
- PGX permanent reflector block impurity,
- uranium mass density, and
- instrumentation.

The unknown impurity content in the IG-110 and PGX graphite blocks represent approximately 80% of the total uncertainty in the previous full-core benchmark model (HTTR-GCR-RESR-001). Only the uncertainties provided in this list were evaluated, via perturbation analysis, for the two warm critical configurations. The computed 1σ uncertainty values were then divided by the square root of ~0.98 to account for the minor contribution from all other uncertainty sources not explicitly evaluated.

Of the uncertainties evaluated in this section and presented above, all but four are considered to be 100% systematic. The absorber content of the burnable poison pellets (both 2.0 and 2.5 wt.%), the density of the IG-110 graphite blocks, and the uranium fuel mass are considered to have uncertainties that are 25% systematic and 75% random. Tables in this section provide results for all uncertainties treated as 100% systematic. Text is provided in the aforementioned individual sections regarding the treatment of their random uncertainties. The results shown in Tables 2.12 and 2.13 contain the uncertainties adjusted for their systematic and random components, where appropriate.

2.1.2 Geometrical Properties

2.1.2.1 Instrumentation

Insufficient information is available to comprehensively model and evaluate the uncertainties and biases related to the utility of instrumentation in the HTTR. Neglect of instrumentation inclusion in the model is a bias; uncertainty in the dimensions and composition of the instrumentation would provide uncertainty in that bias or uncertainty in the model should it have been included in the benchmark model. An approximation of the instrumentation in the HTTR was modeled using information from Section 1.1.2.3 of HTTR-GCR-RESR-001 and approximate diagrams shown in a presentation at the IAEA CRP-5 Meeting.[a] The expected bias in the instrumentation, from the aforementioned reference, is ~0.2% Δk/k.

Figures 2.3 through 2.6 provide basic geometric descriptions of the instrumentation utilized in the HTTR core. Figure 2.3 shows the respective heights. Figure 2.4, 2.5, and 2.6 provide additional information regarding channels 1, 2, and 3, respectively (columns E05, E13, and E21, respectively, in Figure 2.7). The 5-cm long 0.6-cm diameter BF_3 counters were modeled containing gas at 1 atm with 100 at.% ^{10}B

[a] N. Fujimoto, N. Nojiri, and K. Yamashita, "HTTR's Benchmark Calculation of Start-Up Core Physics Tests," Report of the 3rd Research Coordiation Meeting on the CRP, IAEA, Oarai, Japan, March 12-16 (2001).

content. All metallic components were modeled as aluminum. Approximate dimensions were used based on scaling of the Figures 2.4 through 2.6 and the known hole diameter of 123 mm.

Approximate biases were calculated for the warm critical core configurations (Table 3.1). The bias for the fully-loaded core critical was previously calculated to be 0.254 ± 0.073% Δk/k (Section 3.1.1.1 of HTTR-GCR-RESR-001). The instrumentation bias was calculated for the two warm critical configurations and provided in Table 3.1. The uncertainty in the biases was approximated by dividing the biases in half, and then treating it as a bounding uncertainty and dividing by $\sqrt{3}$. The uncertainty in the instrumentation is included in the total benchmark model uncertainty, and is provided in Table 3.1. The instrumentation is not included in the benchmark model but the bias is used to correct the experimental k_{eff}. Because the actual dimensions and material properties are approximated, this uncertainty is treated as completely systematic with no random components.

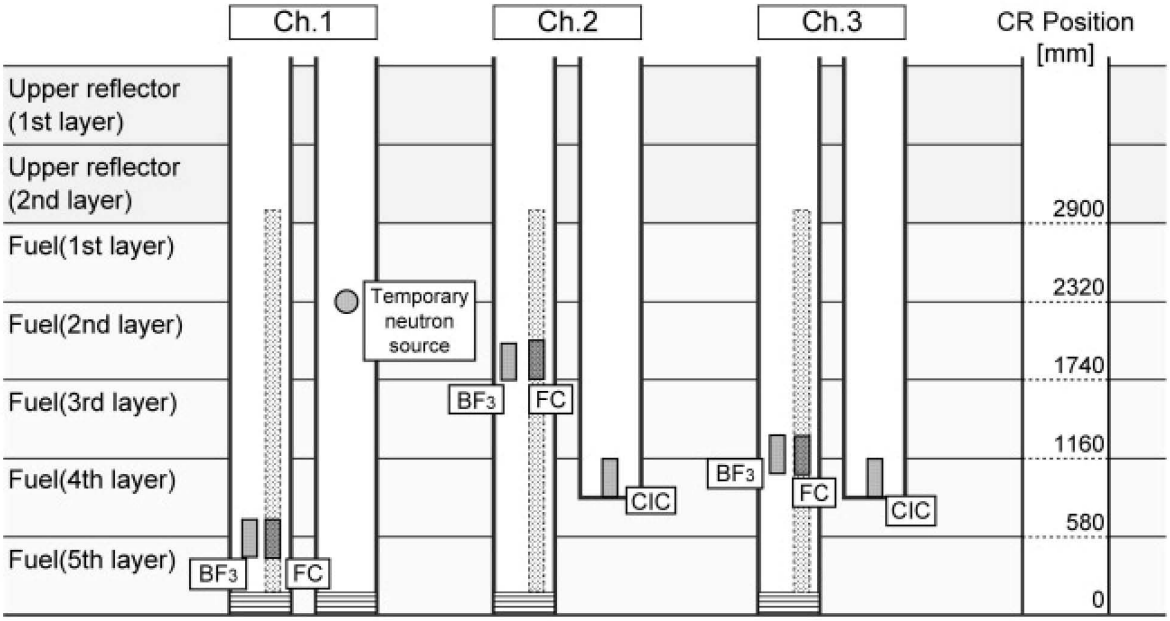

Figure 2.3. Vertical Position of the Temporary Neutron Detectors (Ref 1, p. 314).
BF_3 = boron-trifluoride neutron detector
CIC = gamma-ray compensated ionization chamber
FC = micro-fission chamber

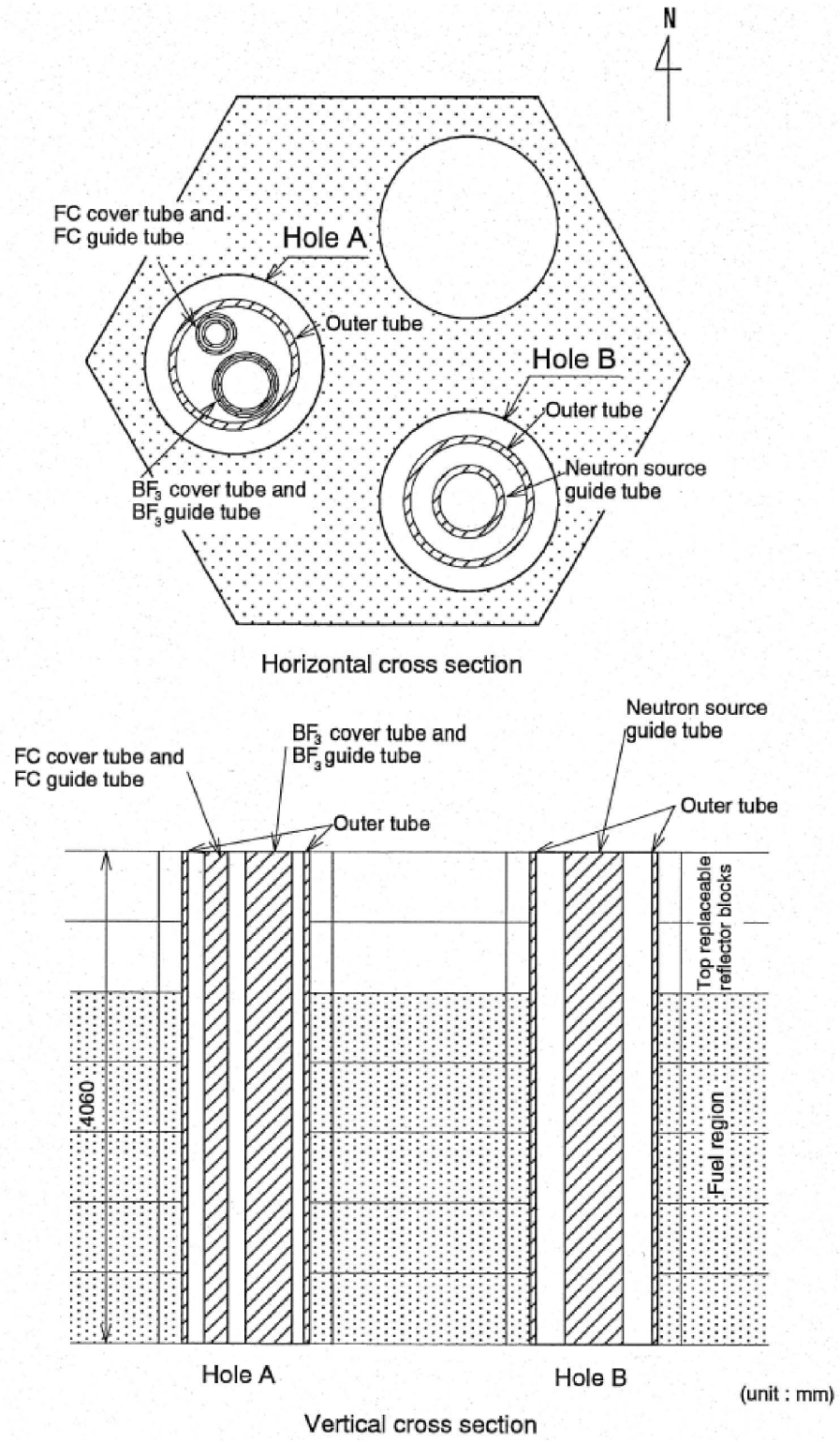

Figure 2.4. Approximation of Instrumentation Channel 1 (Column E05). [a]

[a] N. Fujimoto, N. Nojiri, and K. Yamashita, "HTTR's Benchmark Calculation of Start-Up Core Physics Tests," Report of the 3rd Research Coordination Meeting on the CRP, IAEA, Oarai, Japan, March 12-16 (2001).

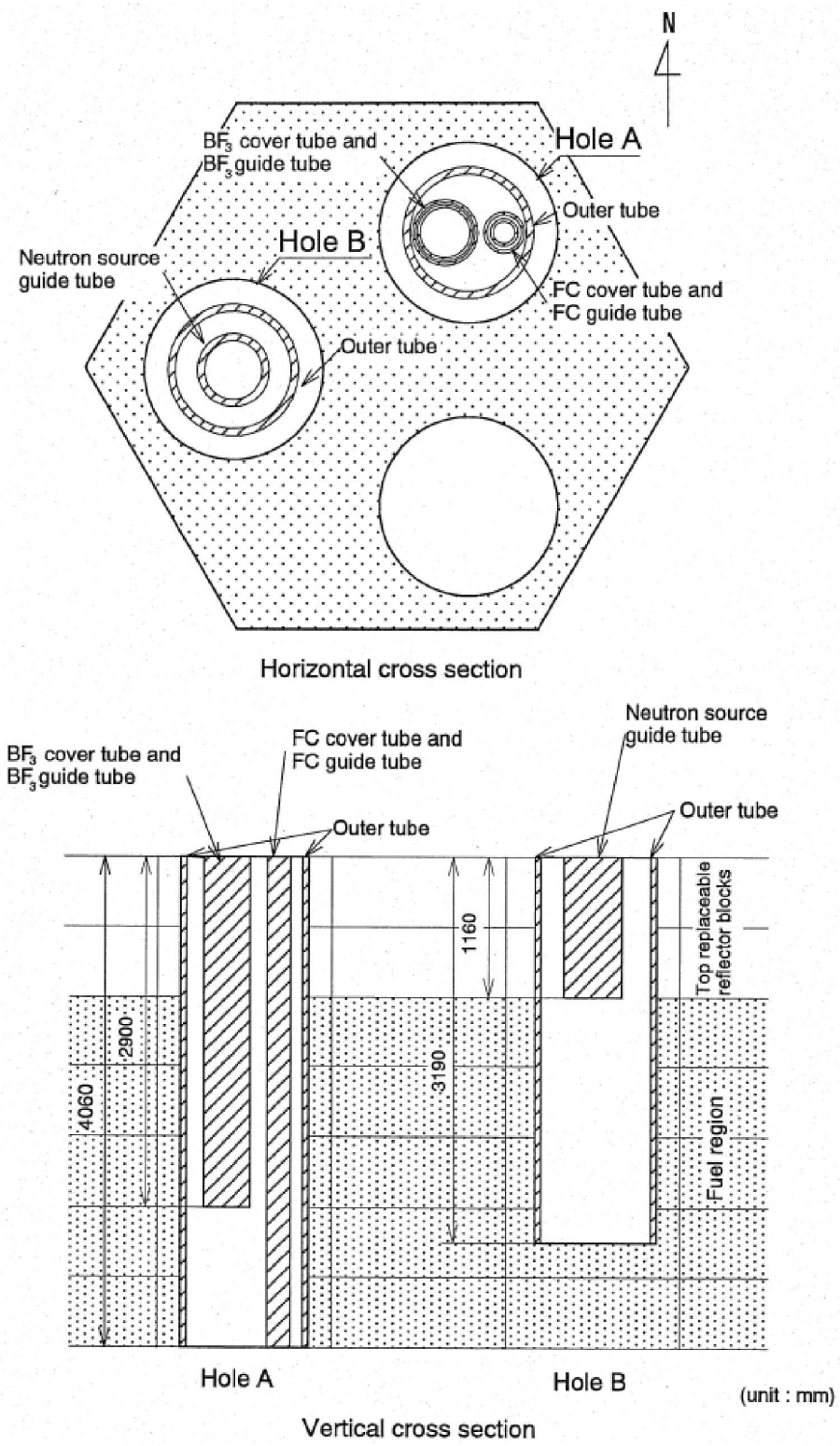

Figure 2.5. Approximation of Instrumentation Channel 2 (Column E13). [a]

[a] N. Fujimoto, N. Nojiri, and K. Yamashita, "HTTR's Benchmark Calculation of Start-Up Core Physics Tests," Report of the 3rd Research Coordination Meeting on the CRP, IAEA, Oarai, Japan, March 12-16 (2001).

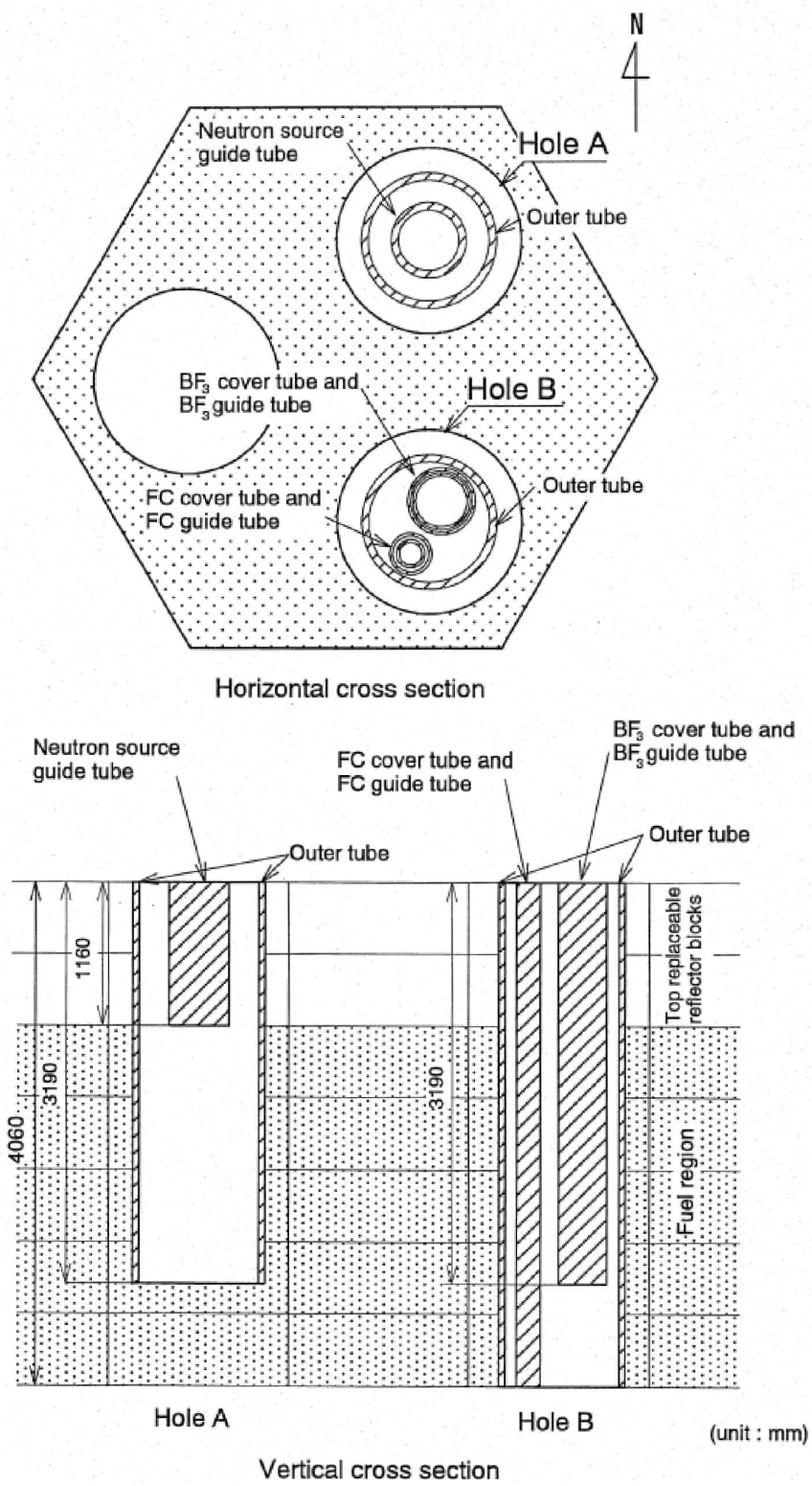

Figure 2.6. Approximation of Instrumentation Channel 3 (Column E21). [a]

[a] N. Fujimoto, N. Nojiri, and K. Yamashita, "HTTR's Benchmark Calculation of Start-Up Core Physics Tests," Report of the 3rd Research Coordination Meeting on the CRP, IAEA, Oarai, Japan, March 12-16 (2001).

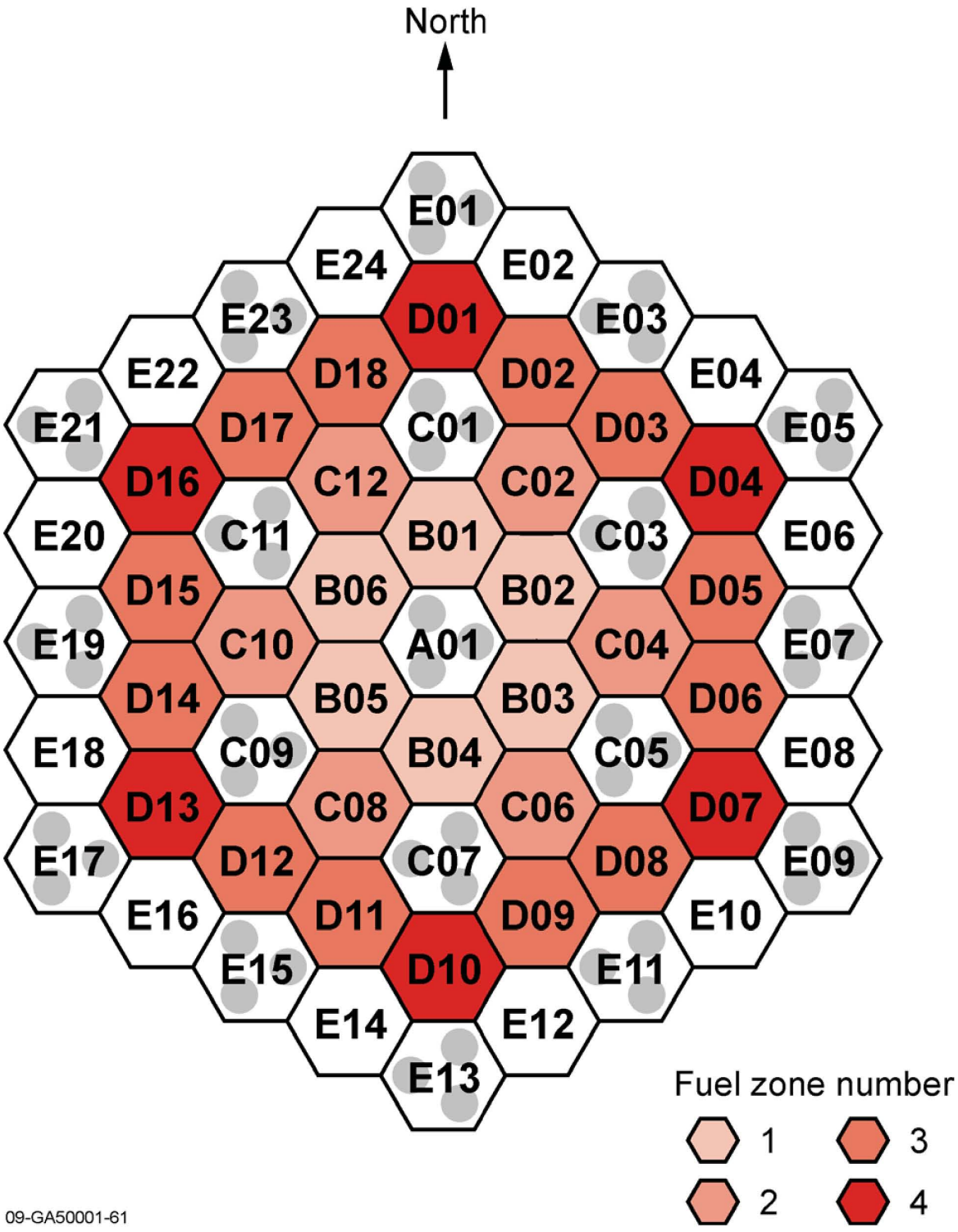

Figure 2.7. Fuel Column Name and Zone Number in the HTTR Core.

2.1.3 Compositional Variations

2.1.3.1 Coated Fuel Particles

Uranium Enrichment

The concentration of ^{234}U expected in the TRISO fuel had to be determined, as it was not provided. First the weight fractions of isotopes in natural uranium dioxide were determined. Then the enriched weight percent of ^{235}U was multiplied by the natural weight percent of ^{234}U (0.0055 at.%) and divided by the natural weight percent of ^{235}U (0.72 at.%). Thus an approximate concentration of "enriched" ^{234}U content could be determined for this evaluation, which may slightly underestimate the actual ^{234}U content.

$$\gamma_{^{234}U}^{Enriched} = \frac{\gamma_{^{234}U}^{Natural}}{\gamma_{^{235}U}^{Natural}} \gamma_{^{235}U}^{Enriched} .$$

Information was not provided regarding the uncertainty in the uranium enrichment of the TRISO kernels. It is reported elsewhere that the manufacturing tolerance limit for the enrichment is 4.5% of the reported weight percent. [a] For example, the enrichment of 3.4 wt.% is bound within a tolerance of ±0.153 wt.%. The ^{234}U content adjusted to match the effective increase or decrease in enrichment of ^{235}U, to determine the effective uncertainty in k_{eff}. The nominal enrichment values are shown in Figure 1.46 and Table 1.11 of HTTR-GCR-RESR-001. Results are shown in Tables 2.1 and 2.2 for Cases 1 and 2 (400 and 420 K), respectively. The actual uncertainty in the uranium enrichment is much smaller than the manufacturing limits; however this information is not publicly available. Therefore, the bounding limits are treated with a normal distribution instead of one with uniform probability.

Configurations 1 through 4 do not contain uranium fuel with the enrichments of 3.40 and 6.70 wt.%.

The uncertainty in the uranium enrichment is considered all systematic with no random component.

UO_2 Impurity

The kernel impurity was varied from 0-3 ppm by weight of equivalent natural-boron content to determine the bounding uncertainty in k_{eff}. The maximum impurity limit was scaled by a factor of 10 so as to quantify the effective upper uncertainty in the UO_2 impurity. The average value is 1.5 ppm by weight (Tables 1.13 and 1.14 of HTTR-GCR-RESR-001). Results are shown in Table 2.3.

The uncertainty in the UO_2 impurity is considered all systematic with no random component.

[a] S. Maruyama, K. Yamashita, N. Fujimoto, I. Murata, R. Shindo, and Y. Sudo, "Determination of Hot Spot Factors for Calculation of the Maximum Fuel Temperatures in the Core Thermal and Hydraulic Design of HTTR," JAERI-M 88-250, JAEA (November 18, 1988). [in Japanese].

Table 2.1. Effect of Uncertainty in Uranium Enrichment (Case 1).

Deviation	Δk	±	$\sigma_{\Delta k}$	Scaling Factor	Δk_{eff} (1σ)	±	$\sigma_{\Delta keff}$
-0.153 wt.% of 3.4 wt.%	-0.00244	±	0.00016	3	-0.00081	±	0.00005
+0.153 wt.% of 3.4 wt.%	0.00212	±	0.00016	3	0.00071	±	0.00005
-0.1755 wt.% of 3.9 wt.%	-0.00226	±	0.00016	3	-0.00075	±	0.00005
+0.1755 wt.% of 3.9 wt.%	0.00191	±	0.00016	3	0.00064	±	0.00005
-0.1935 wt.% of 4.3 wt.%	-0.00421	±	0.00016	3	-0.00140	±	0.00005
+0.1935 wt.% of 4.3 wt.%	0.00351	±	0.00016	3	0.00117	±	0.00005
-0.216 wt.% of 4.8 wt.%	-0.00145	±	0.00016	3	-0.00048	±	0.00005
+0.216 wt.% of 4.8 wt.%	0.00123	±	0.00016	3	0.00041	±	0.00005
-0.234 wt.% of 5.2 wt.%	-0.00141	±	0.00016	3	-0.00047	±	0.00005
+0.234 wt.% of 5.2 wt.%	0.00087	±	0.00016	3	0.00029	±	0.00005
-0.2655 wt.% of 5.9 wt.%	-0.00154	±	0.00016	3	-0.00051	±	0.00005
+0.2655 wt.% of 5.9 wt.%	0.00117	±	0.00016	3	0.00039	±	0.00005
-0.2835 wt.% of 6.3 wt.%	-0.00107	±	0.00016	3	-0.00036	±	0.00005
+0.2835 wt.% of 6.3 wt.%	0.00038	±	0.00016	3	0.00013	±	0.00005
-0.3015 wt.% of 6.7 wt.%	-0.00029	±	0.00016	3	-0.00010	±	0.00005
+0.3015 wt.% of 6.7 wt.%	-0.00018	±	0.00016	3	-0.00006	±	0.00005
-0.324 wt.% of 7.2 wt.%	-0.00042	±	0.00016	3	-0.00014	±	0.00005
+0.324 wt.% of 7.2 wt.%	0.00015	±	0.00016	3	0.00005	±	0.00005
-0.3555 wt.% of 7.9 wt.%	-0.00046	±	0.00016	3	-0.00015	±	0.00005
+0.3555 wt.% of 7.9 wt.%	0.00004	±	0.00016	3	0.00001	±	0.00005
-0.423 wt.% of 9.4 wt.%	-0.00031	±	0.00016	3	-0.00010	±	0.00005
+0.423 wt.% of 9.4 wt.%	-0.00006	±	0.00016	3	-0.00002	±	0.00005
-0.4455 wt.% of 9.9 wt.%	-0.00039	±	0.00016	3	-0.00013	±	0.00005
+0.4455 wt.% of 9.9 wt.%	-0.00018	±	0.00016	3	-0.00006	±	0.00005

Table 2.2. Effect of Uncertainty in Uranium Enrichment (Case 2).

Deviation	Δk	±	$\sigma_{\Delta k}$	Scaling Factor	Δk_{eff} (1σ)	±	$\sigma_{\Delta keff}$
-0.153 wt.% of 3.4 wt.%	-0.00222	±	0.00016	3	-0.00074	±	0.00005
+0.153 wt.% of 3.4 wt.%	0.00209	±	0.00016	3	0.00070	±	0.00005
-0.1755 wt.% of 3.9 wt.%	-0.00181	±	0.00016	3	-0.00060	±	0.00005
+0.1755 wt.% of 3.9 wt.%	0.00195	±	0.00016	3	0.00065	±	0.00005
-0.1935 wt.% of 4.3 wt.%	-0.00407	±	0.00016	3	-0.00136	±	0.00005
+0.1935 wt.% of 4.3 wt.%	0.00395	±	0.00016	3	0.00132	±	0.00005
-0.216 wt.% of 4.8 wt.%	-0.00132	±	0.00016	3	-0.00044	±	0.00005
+0.216 wt.% of 4.8 wt.%	0.00130	±	0.00016	3	0.00043	±	0.00005
-0.234 wt.% of 5.2 wt.%	-0.00089	±	0.00016	3	-0.00030	±	0.00005
+0.234 wt.% of 5.2 wt.%	0.00124	±	0.00016	3	0.00041	±	0.00005
-0.2655 wt.% of 5.9 wt.%	-0.00146	±	0.00016	3	-0.00049	±	0.00005
+0.2655 wt.% of 5.9 wt.%	0.00107	±	0.00016	3	0.00036	±	0.00005
-0.2835 wt.% of 6.3 wt.%	-0.00097	±	0.00016	3	-0.00032	±	0.00005
+0.2835 wt.% of 6.3 wt.%	0.00083	±	0.00016	3	0.00028	±	0.00005
-0.3015 wt.% of 6.7 wt.%	0.00004	±	0.00016	3	0.00001	±	0.00005
+0.3015 wt.% of 6.7 wt.%	0.00013	±	0.00016	3	0.00004	±	0.00005
-0.324 wt.% of 7.2 wt.%	-0.00022	±	0.00016	3	-0.00007	±	0.00005
+0.324 wt.% of 7.2 wt.%	0.00011	±	0.00016	3	0.00004	±	0.00005
-0.3555 wt.% of 7.9 wt.%	-0.00026	±	0.00016	3	-0.00009	±	0.00005
+0.3555 wt.% of 7.9 wt.%	0.00017	±	0.00016	3	0.00006	±	0.00005
-0.423 wt.% of 9.4 wt.%	-0.00003	±	0.00016	3	-0.00001	±	0.00005
+0.423 wt.% of 9.4 wt.%	0.00020	±	0.00016	3	0.00007	±	0.00005
-0.4455 wt.% of 9.9 wt.%	-0.00003	±	0.00016	3	-0.00001	±	0.00005
+0.4455 wt.% of 9.9 wt.%	-0.00002	±	0.00016	3	-0.00001	±	0.00005

Table 2.3. Effect of Uncertainty in UO_2 Impurity.

Case	Deviation	Δk	±	$\sigma_{\Delta k}$	Scaling Factor	Δk_{eff} (1σ)	±	$\sigma_{\Delta keff}$
1	0 ppm	0.00047	±	0.00016	$\sqrt{3}$	0.00027	±	0.00009
	30 ppm	-0.01314	±	0.00016	$10\sqrt{3}$	-0.00076	±	0.00001
2	0 ppm	0.00053	±	0.00016	$\sqrt{3}$	0.00031	±	0.00009
	30 ppm	-0.01311	±	0.00016	$10\sqrt{3}$	-0.00076	±	0.00001

Overcoat Impurity

The overcoat impurity was varied from 0-5 ppm by weight of equivalent natural-boron content to determine the bounding uncertainty in k_{eff}. The average value of the coated fuel particles is 1.5 ppm by weight (Table 1.13 of HTTR-GCR-RESR-001); it is assumed that the overcoat would have a comparable impurity amount. The alternative is to use the impurity of the compact (matrix) material, which is 0.82 ppm by weight (Table 1.27 of HTTR-GCR-RESR-001). The larger amount is selected, i.e. 1.5 ppm, to represent the mean impurity content in the graphite overcoat. Results are shown in Table 2.4.

The uncertainty in the overcoat impurity is considered all systematic with no random component.

Table 2.4. Effect of Uncertainty in Overcoat Impurity.

Case	Deviation	Δk	±	$\sigma_{\Delta k}$	Scaling Factor	Δk_{eff} (1σ)	±	$\sigma_{\Delta keff}$
1	0 ppm	0.00035	±	0.00016	√3	0.00020	±	0.00009
	5 ppm	-0.00142	±	0.00016	√3	-0.00082	±	0.00009
2	0 ppm	0.00042	±	0.00016	√3	0.00024	±	0.00009
	5 ppm	-0.00143	±	0.00016	√3	-0.00083	±	0.00009

2.1.3.2 Burnable Poisons

Absorber Content

The uncertainty in the absorber content was not provided and the variation provided in Table 1.29 of HTTR-GCR-RESR-001 appears too excessive for the quantities utilized in the BP pellets. A variation of approximately ±0.25% by weight was assumed for each of the two absorber pellet types, and the effective uncertainty in k_{eff} was determined. This value is treated as a bounding limit. The uncertainty of ±0.25% is based upon the assumption that burnable poison pellets with boron contents between 1.75 and 2.25 wt.% would have an average content of 2.00 wt.% and boron contents between 2.25 and 2.75 wt.% would have an average content of 2.50 wt.%. Further information is necessary to reduce the range of the uncertainty. Results are shown in Tables 2.5 and 2.6.

The total number of burnable poison pellets with weight percents of 2.00 and 2.50 used in the fully-loaded core is 3,600 and 1,920, respectively. For determining the random component of the uncertainty (Tables 2.12 and 2.13), the results in Tables 2.5 and 2.6 are divided by their respective √N value.

Table 2.5. Effect of Uncertainty in BP Absorber Content (nominal 2.00 wt.%).

Case	Deviation	Δk	±	$\sigma_{\Delta k}$	Scaling Factor	Δk_{eff} (1σ)	±	$\sigma_{\Delta keff}$
1	-0.25 wt.%	0.00562	±	0.00016	√3	0.00324	±	0.00009
	+0.25 wt.%	-0.00515	±	0.00016	√3	-0.00297	±	0.00009
2	-0.25 wt.%	0.00575	±	0.00016	√3	0.00332	±	0.00009
	+0.25 wt.%	-0.00488	±	0.00016	√3	-0.00282	±	0.00009

Table 2.6. Effect of Uncertainty in BP Absorber Content (nominal 2.50 wt.%).

Case	Deviation	Δk	$\pm$	$\sigma_{\Delta k}$	Scaling Factor	Δk_{eff} (1σ)	$\pm$	$\sigma_{\Delta keff}$
1	-0.25 wt.%	0.00183	$\pm$	0.00016	$\sqrt{3}$	0.00106	$\pm$	0.00009
	+0.25 wt.%	-0.00205	$\pm$	0.00016	$\sqrt{3}$	-0.00118	$\pm$	0.00009
2	-0.25 wt.%	0.000241	$\pm$	0.00016	$\sqrt{3}$	0.00139	$\pm$	0.00009
	+0.25 wt.%	-0.00209	$\pm$	0.00016	$\sqrt{3}$	-0.00121	$\pm$	0.00009

Absorber Isotopic Abundance

According to the 16th edition of the Chart of the Nuclides, the natural isotopic abundance of ^{10}B has been measured between 19.1 and 20.3 at.% with a nominal value of 19.9 at.%.[a] The abundance of ^{10}B in the BPs was therefore evaluated at the minimum and maximum bounding values to determine the effective uncertainty in k_{eff}. Table 1.28 of HTTR-GCR-RESR-001 states that the abundance of ^{10}B is 18.7 wt.%, which correlates to approximately 20.2 at.%. The benchmark model was evaluated at 19.9 at.%. Results are shown in Table 2.7.

The uncertainty in the absorber isotopic abundance is considered all systematic with no random component.

Table 2.7. Effect of Uncertainty in BP Isotopic Abundance of ^{10}B.

Case	Deviation	Δk	$\pm$	$\sigma_{\Delta k}$	Scaling Factor	Δk_{eff} (1σ)	$\pm$	$\sigma_{\Delta keff}$
1	19.1%	0.00270	$\pm$	0.00016	$\sqrt{3}$	0.00156	$\pm$	0.00009
	20.3%	-0.00156	$\pm$	0.00016	$\sqrt{3}$	-0.00090	$\pm$	0.00009
2	19.1%	0.00265	$\pm$	0.00016	$\sqrt{3}$	0.00153	$\pm$	0.00009
	20.3%	-0.00113	$\pm$	0.00016	$\sqrt{3}$	-0.00065	$\pm$	0.00009

2.1.3.3 Graphite Blocks

Density

The IG-110 graphite density was varied ±0.04 g/cm^3 from a nominal value selected as 1.76 g/cm^3 (ranging from 1.75 to 1.78 g/cm^3, Tables 1.13, 1.19, and 1.27 of HTTR-GCR-RESR-001) to determine the effective uncertainty in k_{eff}. A variation of 0.03 g/cm^3 accounts for the difference in density between the various samples of IG-110 blocks, and a variation of 0.01 g/cm^3 is assumed to encompass the variability in the volume fraction caused by eliminating various features such as the dowels, sockets, fuel handling position, and ridged features on the fuel rods. The assumed uncertainty of 0.03 g/cm^3 for the IG-110 graphite encompasses the range of reported densities found throughout Section 1 of HTTR-GCR-RESR-001. Results are shown in Table 2.8. This value is treated as bounding.

[a] Nuclides and Isotopes: Chart of the Nuclides, 16th edition, (2002).

Previous results[a] state that a graphite weight difference of less than 1% should result in a bias of -0.3% Δk/k. Scaling the results provided in Table 2.8 provides an uncertainty comparable to the previously published information.

The total number of IG-110 graphite blocks used in the fully-loaded core is 549. For determining the random component of the uncertainty (Tables 2.12 and 2.13), the results in Table 2.8 is divided by √549.

Table 2.8. Effect of Uncertainty in IG-110 Density in Graphite Blocks.

Case	Deviation	Δk	±	$\sigma_{\Delta k}$	Scaling Factor	Δk_{eff} (1σ)	±	$\sigma_{\Delta keff}$
1	-0.04 g/cm^3	-0.00583	±	0.00016	√3	-0.00337	±	0.00009
	+0.04 g/cm^3	0.00511	±	0.00016	√3	0.00295	±	0.00009
2	-0.04 g/cm^3	-0.00551	±	0.00016	√3	-0.00318	±	0.00009
	+0.04 g/cm^3	0.00530	±	0.00016	√3	0.00306	±	0.00009

Impurity

The graphite block impurity was varied from 0-3 ppm by weight of equivalent natural-boron content (Table 1.13 of HTTR-GCR-RESR-001), where the 3 ppm value is 3 times the bounding limit, to determine the bounding uncertainty in k_{eff}. The nominal impurity is 0.40 ppm or 0.37 ppm of natural boron by weight for the fuel/control blocks and reflector blocks, respectively (Table 1.27 of HTTR-GCR-RESR-001). However, characterization of the graphite first loaded into the reactor determined the equivalent boron content for IG-110 graphite to be 0.59 ppm.[b] This latter value is used in the benchmark model. Results are shown in Table 2.9.

It has been reported that the estimated air content in the graphite blocks would provide -0.4% Δk/k to the computational model.[c] Reference 1 states that an uncertainty factor of ~0.52% Δk/k should be used. The inclusion of air in the benchmark model did not produce a noticeable change in reactivity; this was done by modeling air, at atmospheric pressure, distributed throughout the block in the quantity equivalent to the volume fraction to the void space generated for the dowels, sockets, fuel handling position, and other miscellaneous block features. However, it is unclear exactly how much air is entrapped within the graphite blocks. Air can be entrapped during the graphitization process or absorbed onto the graphite surface. Typically, significant contribution to the equivalent boron content in a graphite block is caused by impurities in the graphite. Methods to measure the impurity content in graphite have improved over the past several years, and the impurity content of the HTTR graphite may need to be reassessed.[d]

---

[a] Fujimoto, N., Nakano, M., Takeuchi, M., Fujisaki, S., and Yamashita, K., "Start-Up Core Physics Tests of High Temperature Engineering Test Reactor (HTTR), (II): First Criticality by an Annular Form Fuel Loading and Its Criticality Prediction Method," *J. Atomic Energy Society Japan*, **42**(5), 458-464 (2000).

[b] Sumita, J., Shibata, T., Hanawa, S., Ishihara, M., Iyoku, T., and Sawa, K., "Characteristics of First Loaded IG-110 Graphite in HTTR Core," *JAEA Technol 2006-048*, October (2006).

[c] Fujimoto, N., Nakano, M., Takeuchi, M., Fujisaki, S., and Yamashita, K., "Start-Up Core Physics Tests of High Temperature Engineering Test Reactor (HTTR), (II): First Criticality by an Annular Form Fuel Loading and Its Criticality Prediction Method," *J. Atomic Energy Society Japan*, **42**(5), 458-464 (2000).

[d] Private communication with Rob Bratton at Idaho National Laboratory (November 20, 2008).

Graphite is also somewhat hydroscopic and can absorb water into its pores after fabrication. At low temperatures, the water would still be present in the graphite. Information regarding possible water content in the graphite blocks is unavailable, however.

The uncertainty in the graphite block impurity is considered all systematic with no random component.

Table 2.9. Effect of Uncertainty in IG-110 Impurity in Graphite Blocks.

Case	Deviation	Δk	$\pm$	$\sigma_{\Delta k}$	Scaling Factor	Δk_{eff} (1σ)	$\pm$	$\sigma_{\Delta keff}$
1	0 ppm	0.00738	±	0.00016	$\sqrt{3}$	0.00426	±	0.00009
	3 ppm	-0.02808	±	0.00016	$3\sqrt{3}$	-0.00540	±	0.00009
2	0 ppm	0.00743	±	0.00016	$\sqrt{3}$	0.00429	±	0.00009
	3 ppm	-0.02770	±	0.00016	$3\sqrt{3}$	-0.00533	±	0.00009

2.1.3.4 Permanent Reflectors

Impurity

The permanent reflector impurity was varied from 0-5 ppm by weight of equivalent natural-boron content (Table 1.16 of HTTR-GCR-RESR-001) to determine the bounding uncertainty in k_{eff}. The nominal impurity is 1.91 ppm of natural boron by weight (Table 1.27 of HTTR-GCR-RESR-001). Results are shown in Table 2.10.

The uncertainty in the permanent reflector impurity is considered all systematic with no random component.

Table 2.10. Effect of Uncertainty in PGX Impurity in Permanent Reflector.

Case	Deviation	Δk	$\pm$	$\sigma_{\Delta k}$	Scaling Factor	Δk_{eff} (1σ)	$\pm$	$\sigma_{\Delta keff}$
1	0 ppm	0.00350	±	0.00016	$\sqrt{3}$	0.00202	±	0.00009
	5 ppm	-0.00537	±	0.00016	$\sqrt{3}$	-0.00310	±	0.00009
2	0 ppm	0.00394	±	0.00016	$\sqrt{3}$	0.00227	±	0.00009
	5 ppm	-0.00513	±	0.00016	$\sqrt{3}$	-0.00296	±	0.00009

2.1.4 Additional Analyses

2.1.4.1 Room Return

Insufficient information is available to model and evaluate the uncertainties and biases related to any room return effects in the HTTR. Shielding plugs, plates, and blocks are incorporated within the HTTR vessel and would considerably reduce room return effects from the surrounding reactor vessel, reactor internals, and HTTR infrastructure and facility due to the content of sintered B_4C/C neutron absorber.

A conservative analysis of the HTTR benchmark model of the fully-loaded core (HTTR-GCR-RESR-001) surrounded by shielding material, steel, and concrete provided an insignificant effect because the slight increase in the effective multiplication factor was well below the range of statistical uncertainty for the analysis. Actual room return effects are assumed to be quite negligible.

2.1.4.2 Simplification Biases and Uncertainties

Whereas insufficient information is publicly available, a comprehensive analysis of simplification biases and their respective uncertainties could not be appropriately assessed. Currently only an approximate bias for the instrumentation components in the reactor has been assessed (Section 2.1.2.1). As additional information becomes available, highly detailed and simplified benchmark models can be generated and their biases can be adequately determined.

2.1.4.3 Temperature

Insufficient information is available to model and evaluate the uncertainties and biases related to temperature effects.

2.1.5 Systematic Biases and Uncertainties

There was no information regarding systematic biases or uncertainties publicly available for these experiments. Previous efforts of the Japanese in analyzing the 19-fuel-column core (Case 1) obtained an analytical excess reactivity of 2.7% $\Delta k/k$, with an estimated Monte Carlo calculation overestimate of 1.2% $\Delta k/k$.[a] Additional information is necessary to completely verify published results to generate an analytical bias for MCNP.

As discussed at the beginning of Section 2, all uncertainties are treated as 25% systematic, with no reduction in uncertainty due to the multiplicity of core components, and as 75% random.

2.1.6 Analysis of HTTR Uranium Content

The parameters (dimensions, density, etc.) of the TRISO particles fabricated during the manufacturing process are very normally distributed, except for any defective particles. The fuel content, or mass, is the most well-known specification and measured with the highest accuracy.[b]

Because of the overspecification of the TRISO particles in Table 1.14 of HTTR-GCR-RESR-001 and the correlation of uranium kernel diameter, density, packing fraction, and mass, the effect of the uncertainties in the kernel diameter, density, and packing fraction are not included in the total uncertainty as separate entities. The uranium content of the fuel rods of 188.58 ± 5.66 g (Table 1.14 of HTTR-GCR-RESR-001) is the parameter most likely known with the greatest accuracy. Therefore, the diameter of the kernels will be fixed at 600 μm, and the density will be varied ± 0.32 g/cm^3 from a nominal value of 10.39 g/cm^3 to determine the effective uncertainty in k_{eff} due to the uranium mass uncertainty. Results are shown in Table 2.11. This value is treated as a bounding limit.

The total number of fuel rods used in the fully-loaded core is approximately 4,770. For determining the random component of the uncertainty (Tables 2.12 and 2.13), the results in Table 2.11 is divided by $\sqrt{4,770}$.

---

[a] Fujimoto, N., Nakano, M., Takeuchi, M., Fujisaki, S., and Yamashita, K., "Start-Up Core Physics Tests of High Temperature Engineering Test Reactor (HTTR), (II): First Criticality by an Annular Form Fuel Loading and Its Criticality Prediction Method," *J. Atomic Energy Society Japan*, **42**(5), 458-464 (2000).

[b] Personal communication with David Petti from the Idaho National Laboratory (September 28, 2009).

Table 2.11. Effect of Uncertainty in Uranium Mass.

Case	Deviation	Δk	±	$\sigma_{\Delta k}$	Scaling Factor	Δk_{eff} (1σ)	±	$\sigma_{\Delta keff}$
1	-0.32 g/cm^3	-0.00531	±	0.00016	√3	-0.00307	±	0.00009
	+0.32 g/cm^3	0.00469	±	0.00016	√3	0.00271	±	0.00009
2	-0.32 g/cm^3	-0.00515	±	0.00016	√3	-0.00297	±	0.00009
	+0.32 g/cm^3	0.00481	±	0.00016	√3	0.00278	±	0.00009

2.1.7 Total Experimental Uncertainty

A compilation of the total evaluated uncertainty in the HTTR model is shown in Tables 2.12 and 2.13 for configurations 1 and 2, respectively. As discussed earlier, each of the evaluated uncertainties is divided into a systematic component (25%) and random component (75%), where appropriate. The random component is then divided by the square-root of the number of random objects reported in the subsection containing the calculated base uncertainty values. The root-mean square of each subcomponent is taken to determine the uncertainty in either the random or systematic components of the total evaluated uncertainty. The total evaluated uncertainty is then the root-mean square of the random and systematic uncertainties. The total evaluated uncertainty is also divided by the square root of ~0.98 as discussed in Section 2.1.1.

Uncertainties less than 0.0002 are reported as negligible (neg). When calculated uncertainties in Δk_{eff} are less than their statistical uncertainties, the statistical uncertainties are used in the calculation of the total uncertainty. Table listings where calculations were not performed or otherwise not available are labeled with 'NA'. For uncertainties where a random component is not applicable, the uncertainty is denoted with '--'.

The most significant contributions to the overall uncertainty from the systematic uncertainties include the impurities in the IG-110 graphite blocks and PGX graphite reflector blocks. All uncertainties providing at least 0.1% Δk_{eff} are highlighted in gray in Tables 2.12 and 2.13. All of the random uncertainties are less than 0.1% Δk_{eff}. The overall uncertainty is less than 1% Δk_{eff}; it is expected that the total uncertainty will be reduced as additional parameters that characterize the HTTR are obtained.

Table 2.12. Total Experimental Uncertainty (Case 1).

Varied Parameter	Systematic Uncertainty		Random Uncertainty	
	$-\Delta k_{eff}$ (1σ)	$+\Delta k_{eff}$ (1σ)	$-\Delta k_{eff}$ (1σ)	$+\Delta k_{eff}$ (1σ)
Instrumentation	0.00073	0.00073	--	--
3.4 wt.% Enrichment	0.00081	0.00071	--	--
3.9 wt.% Enrichment	0.00075	0.00064	--	--
4.3 wt.% Enrichment	0.00140	0.00117	--	--
4.8 wt.% Enrichment	0.00048	0.00041	--	--
5.2 wt.% Enrichment	0.00047	0.00029	--	--
5.9 wt.% Enrichment	0.00051	0.00039	--	--
6.3 wt.% Enrichment	0.00036	neg	--	--
6.7 wt.% Enrichment	neg	neg	--	--
7.2 wt.% Enrichment	neg	neg	--	--
7.9 wt.% Enrichment	neg	neg	--	--
9.4 wt.% Enrichment	neg	neg	--	--
9.9 wt.% Enrichment	neg	neg	--	--
UO_2 Impurity	0.00027	0.00076	--	--
Overcoat Impurity	0.00020	0.00082	--	--
BP Absorber Content, 2.0 wt.%	0.00081	0.00074	neg	neg
BP Absorber Content, 2.5 wt.%	0.00026	0.00030	neg	neg
BP Isotopic Abundance of ^{10}B	0.00156	0.00090	--	--
IG-110 Density in Blocks	0.00084	0.00074	neg	neg
IG-110 Impurity in Blocks	0.00426	0.00540	--	--
PGX Impurity	0.00202	0.00310	--	--
Uranium Fuel Mass (Sec. 2.1.6)	0.00077	0.00068	neg	neg
Uncertainty of Components	0.00560	0.00676	neg	neg
Total Uncorrected Uncertainty	0.00560	0.00676		
Correction Factor	√(97.6%)	√(98.1%)		
Total Evaluation Uncertainty	0.00567	0.00683		

Table 2.13. Total Experimental Uncertainty (Case 2).

Varied Parameter	Systematic Uncertainty		Random Uncertainty	
	$-\Delta k_{eff}$ (1σ)	$+\Delta k_{eff}$ (1σ)	$-\Delta k_{eff}$ (1σ)	$+\Delta k_{eff}$ (1σ)
Instrumentation	0.00076	0.00076	--	--
3.4 wt.% Enrichment	0.00074	0.00070	--	--
3.9 wt.% Enrichment	0.00060	0.00065	--	--
4.3 wt.% Enrichment	0.00136	0.00132	--	--
4.8 wt.% Enrichment	0.00044	0.00043	--	--
5.2 wt.% Enrichment	0.00030	0.00041	--	--
5.9 wt.% Enrichment	0.00049	0.00036	--	--
6.3 wt.% Enrichment	0.00032	0.00028	--	--
6.7 wt.% Enrichment	neg	neg	--	--
7.2 wt.% Enrichment	neg	neg	--	--
7.9 wt.% Enrichment	neg	neg	--	--
9.4 wt.% Enrichment	neg	neg	--	--
9.9 wt.% Enrichment	neg	neg	--	--
UO_2 Impurity	0.00031	0.00076	--	--
Overcoat Impurity	0.00024	0.00083	--	--
BP Absorber Content, 2.0 wt.%	0.00083	0.00070	neg	neg
BP Absorber Content, 2.5 wt.%	0.00035	0.00030	neg	neg
BP Isotopic Abundance of ^{10}B	0.00153	0.00065	--	--
IG-110 Density in Blocks	0.00080	0.00076	neg	neg
IG-110 Impurity in Blocks	0.00429	0.00533	--	--
PGX Impurity	0.00227	0.00296	--	--
Uranium Fuel Mass (Sec. 2.1.6)	0.00074	0.00069	neg	neg
Uncertainty of Components	0.00566	0.00666	neg	neg
Total Uncorrected Uncertainty	0.00566	0.00666		
Correction Factor	√(97.6%)	√(98.1%)		
Total Evaluation Uncertainty	0.00573	0.00672		

2.2 Evaluation of Buckling and Extrapolation Length Data

Buckling and extrapolation length measurements were not made.

2.3 Evaluation of Spectral Characteristics Data

Spectral characteristics measurements were not made.

2.4 Evaluation of Reactivity Effects Data

Reactivity effects measurements were not made.

2.5 Evaluation of Reactivity Coefficient Data

2.5.1 Isothermal Temperature Coefficients

The uncertainty in the evaluation of the isothermal temperature coefficient measurements comes from four different sources:

1. measurement of the coefficients,
2. temperature,
3. control rod positions, and
4. extrapolation of control rod positions for this analysis.

Typically experimental measurement uncertainty is much greater than uncertainties obtainable via a perturbation analysis of a model of the experiment. Therefore it is assumed that uncertainties in the HTTR core configuration, or the model used to evaluate the HTTR, are negligible compared to the assumed experimental uncertainty for these two coefficients. The reported data are converted to units more applicable to this evaluation (Table 2.14).

Information regarding the methods and instrumentation utilized to measure reactivity changes and the isothermal temperature of the core were not provided. Uncertainty in the measurement of the coefficients was not available for the coefficients measured prior to the power-up tests. Uncertainties in the measurement of coefficients during the power-up tests are shown in Figure 1.6.

Temperature coefficients obtained just prior to the power-up tests were calculated from criticality measurements for room temperature (HTTR-GCR-RESR-001) and two elevated temperature measurements (Section 1.1). Information regarding the uncertainty in the determination of the coefficients at 346 and 407 ºC (Ref. 2) is unavailable. Without further information, an uncertainty of 15% was assumed to apply to these two coefficients. This assumed uncertainty may appear rather large when typically a 10% uncertainty might be assumed. However, the authors in Ref. 1 indicate that larger measurement errors existed for their measurements below 400 ºC; this statement was assumed to partially apply towards the measurements in Ref. 2.

Table 2.14. Warm Critical Isothermal Temperature Coefficients.

Temperature (K)	Reactivity Coefficient (% Δk/k/K)	±	1σ Uncertainty
346	-0.0123	±	0.0018
407	-0.0132	±	0.0020

The original isothermal temperature coefficient data used to develop Figure 1.6 were not available. Therefore, this temperature coefficient chart (Ref. 1) was digitized to allow for further comparative analysis with computational results. There are approximately 11 data points reported with multiple coefficients reported near specific temperature intervals. The digitization of the chart was performed by Chris White at the Idaho National Laboratory using Marisoft Digitizer.[a] A digital copy of the chart is imported into the program and then bound within a grid system; each individual data point is then marked and exported as numerical data. The most practical means to determine the accuracy of the digitization process is to compare a known data point to that determined using the digitization process. No known isothermal temperature coefficient points were found that correspond to this chart. An example chart with known values, similar to the data shown in Figure 1.6, was prepared and digitized to estimate the uncertainty in the digitization procedure. The uncertainty in the digitization process was determined to be approximately 0.3%. This uncertainty is negligible compared to experimental measurement uncertainty.

Perturbation analysis of model parameters was also not performed for these temperature coefficients as their associated uncertainties would be negligible compared to the experimental uncertainty in these measurements.

The results of the digitization process are shown in Table 2.15. A variance-weighted average (Equation 2.2) and deviation (Equation 2.3) were used to obtain a single temperature, isothermal temperature coefficient, and 1σ uncertainty for four temperatures using the digitized data from Figure 1.6. The uncertainty in the reactivity coefficient was also used to variance-weight the average temperature for repeated measurements, where higher quality coefficient measurements weigh heavier than those with larger uncertainties (Equation 2.4).

$$\overline{x} = \frac{\sum_i \frac{x_i}{\sigma_i^2}}{\sum_i \frac{1}{\sigma_i^2}}. \tag{2.2}$$

$$\sigma_{\overline{x}}^2 = \frac{1}{\sum_i \frac{1}{\sigma_i^2}}. \tag{2.3}$$

$$\overline{T} = \frac{\sum_i \frac{T_i}{\sigma_{x_i}^2}}{\sum_i \frac{1}{\sigma_{x_i}^2}}. \tag{2.4}$$

The uncertainty in the temperature was assumed to be negligible compared to the range over which these measurements were taken.

Reference 1 stated that during the power-up operation tests a core burn-up of up to 5 GWD/t was obtained. Measurements in Table 2.14 were obtained prior to power-up operations. Information regarding the actual burnup condition of the core when the measurement data in Figure 1.6 and Table 2.15 were obtained is unavailable. It is assumed that burnup effects and their associated uncertainty, if any, are negligible.

[a] M. Mitchell, Marisoft Digitizer Application Version 3.3, http://digitizer.sourceforge.net/, © 1997.

Table 2.15. Digitized and Consolidated Temperature Coefficient Data.

Digitized Data Points (Figure 1.6)			
Temperature [ºC(K)]	Reactivity Coefficient (% Δk/k/K)	±	1σ Uncertainty
148.08 (421.23)	-0.02173	±	0.012690
255.77 (528.92)	-0.01900	±	0.003645
259.51 (532.66)	-0.01688	±	0.001985
260.26 (533.42)	-0.01601	±	0.001360
354.96 (638.11)	-0.01061	±	0.001420
370.94 (644.09)	-0.01023	±	0.000900
458.44 (731.59)	-0.00762	±	0.000735
459.19 (732.34)	-0.00942	±	0.000920
431.43 (734.58)	-0.00893	±	0.000640
463.68 (736.83)	-0.00942	±	0.000485
467.41 (740.56)	-0.00746	±	0.000575
Variance-Weighted Consolidation of Data Points			
Temperature (K)	Reactivity Coefficient (% Δk/k/K)	±	1σ Uncertainty
421	-0.0217	±	0.0127
533	-0.0165	±	0.0011
642	-0.0103	±	0.0008
736	-0.0086	±	0.0003

It should be noted that estimation of core reactivity from the control rod worth curve is not very precise as the control rod worth curve can have a relatively high uncertainty and is dependent upon the position of other control rods, the neutron flux distribution, and measurement technique. Typically it is more reliable to measure the isothermal temperature reactivity coefficient using a digital reactivity meter.[a] A digital reactivity meter typically uses a compensated ionization chamber probe to measure neutron flux, period, and reactivity during online reactor operations. However, this method was not used in the performance of these measurements.

Exact control rod positions are known for the three configurations of the HTTR in Ref. 2. These positions are shown in Table 2.16.

The uncertainty in the control rod positions (±5 mm) is reported in Section 1.1.2.4 of HTTR-GCR-RESR-001. This uncertainty is equivalent to approximately ±0.0060 Δk_{eff} (Section 2.1.1.2 of HTTR-GCR-RESR-001). If this uncertainty is treated as 25% systematic and the random component is divided by the square-root of the number of control rod pairs (16), the uncertainty in a given critical measurement used to assess a temperature coefficient is ±0.0019 Δk. Then uncertainty in the reactivity worth between two critical temperature measurements is ±0.0019 Δk × √2, or ±0.0027 Δk.

[a] Personal communication with Javier Ortensi at INL (February 2010).

Due to a lack of information regarding the control rod positions for the measurement of isothermal temperature coefficients above 400 K, a means of estimating their positions was devised using available control rod worth curve data and extrapolation of known control rod position data in Table 2.16. The estimated control rod positions can then be utilized to estimate isothermal temperature coefficients for temperatures above 400 K.

Table 2.16. Known Control Rod Positions.

Temperature (K)	Control Rod Positions (mm)			
	C	R1	R2	R3[(a)]
295.85	1765	1765	1765	4049
395.15	1873	1873	1873	4049
418.05	1903	1903	1903	4049

(a) R3 control rods are fully withdrawn and the height is taken from the benchmark model in HTTR-GCR-RESR-001.

Control rod worth curve data were evaluated in the appendices of Ref. 2. The worth of the control rods is approximately linear for measurements up to withdrawal positions of 2500 mm (Figure 2.8). The linearity of withdrawn control rod positions up to approximately 2350 mm was evaluated by digitizing Figure 2.8 and fitting data points pulled from the curve "Measured (corrected)" with a linear trend line. Figure 2.9 shows the linear fit of control rod measurements with respect to reactivity worth measurements.

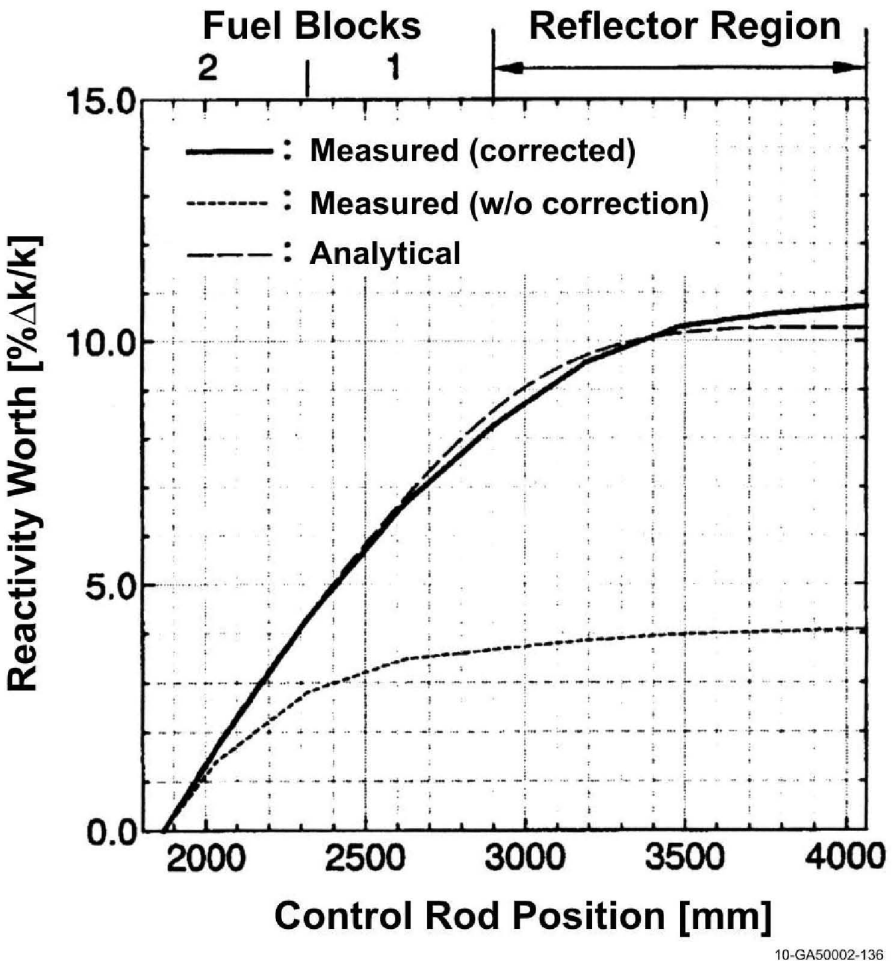

Figure 2.8. Evaluated Control Rod Worth Curve for HTTR (Redrawn and translated from Ref. 2).

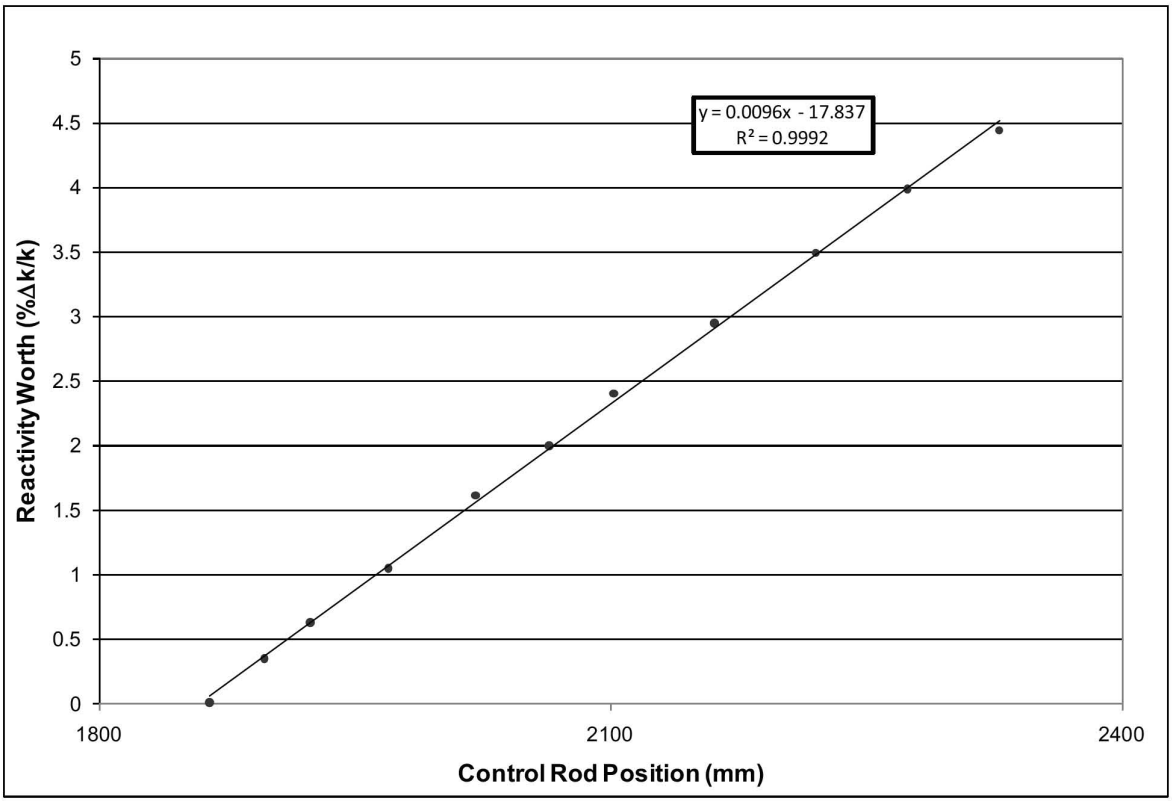

Figure 2.9. Linear Trend Fit of Measured Control Rod Worth Curve (Digitized Data from Figure 2.8).

The data provided for the three known critical configuration measurements (Table 2.16) were then used to extrapolate control rod positions as a function of isothermal core temperature (Figure 2.10). The linear extrapolation (equation shown in Figure 2.10) was then used to estimate control rod positions for elevated temperature conditions at 380, 480, 580, 680, and 780 K (Table 2.17), where h represents the withdrawn height of the control rods (excluding R3 positions) in mm, and T represents the isothermal core temperature. Whereas the extrapolated control rod positions are less than 2500 mm, it is assumed that significant deviation from linearity is not present.

The uncertainty in the extrapolation of control rod positions is assumed to already be included with the uncertainty in the control rod positions when the critical measurements were performed in support of the isothermal temperature coefficient measurements.

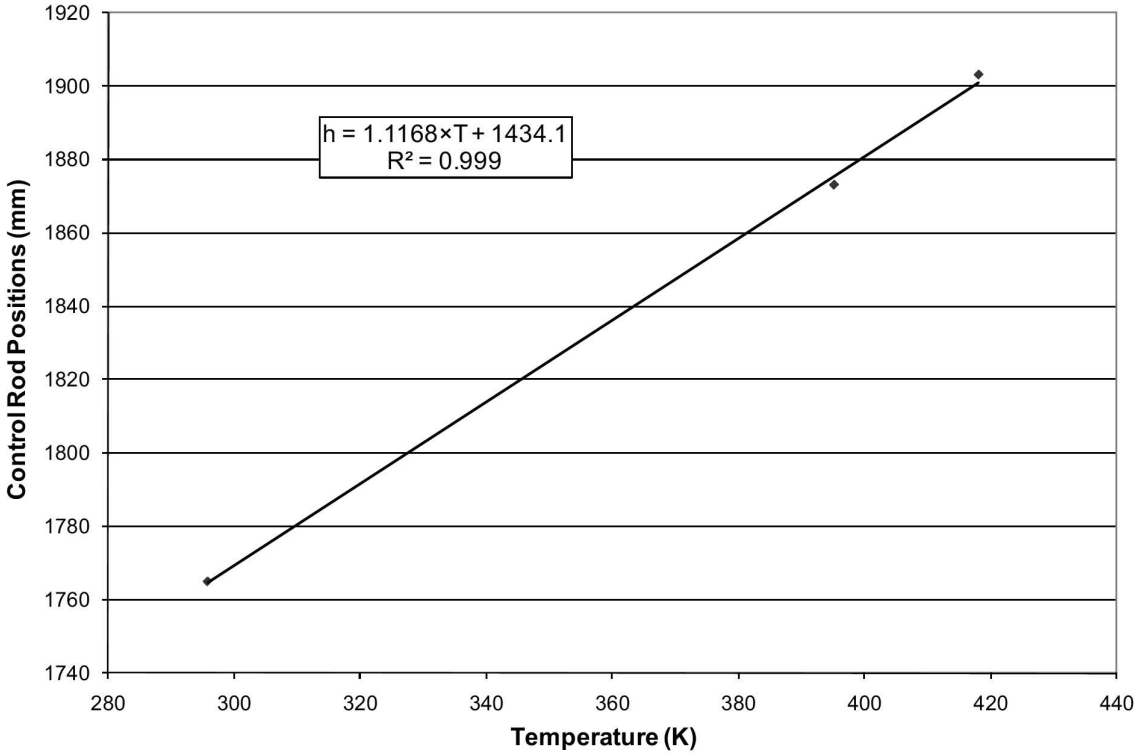

Figure 2.10. Linear Fit of Known Control Rod Position Measurements.

Table 2.17. Extrapolated Control Rod Positions.

Temperature (K)	Control Rod Positions (mm)			
	C	R1	R2	R3[(a)]
380	1859	1859	1859	4049
480	1970	1970	1970	4049
580	2082	2082	2082	4049
680	2194	2194	2194	4049
780	2305	2305	2305	4049

(a) R3 control rods are fully withdrawn and the height is taken from the benchmark model in HTTR-GCR-RESR-001.

A summary of the evaluated uncertainties for the six isothermal temperature coefficients is shown in Table 2.18.

Table 2.18. Total Uncertainty in Isothermal Temperature Coefficients.

Temperature (K)	Reactivity Coefficient (% Δk/k/K)	Measurement Uncertainty	Temperature Uncertainty	Control Rod Position and Extrapolation Uncertainty	Total 1σ Uncertainty
346	-0.0123	0.0018	negligible	0.0027	0.0032
407	-0.0132	0.0020	negligible	0.0027	0.0033
421	-0.0217	0.0127	negligible	0.0027	0.0130
533	-0.0165	0.0011	negligible	0.0027	0.0029
642	-0.0103	0.0008	negligible	0.0027	0.0028
736	-0.0086	0.0003	negligible	0.0027	0.0027

The temperature coefficients are calculated using Equation 2.5, where the temperature coefficient worth at a given temperature is a function of the eigenvalues of two configurations with temperatures both above and below the temperature of the coefficient. Critical core configurations at temperatures of 300 (room temperature, 380, 400, 480, 580, 680, and 780 K are used to evaluate the isothermal temperature coefficients. The configurations at 300 (HTTR-GCR-RESR-001) and 400 K (Case 1, Section 3.1) represent actual experimental configurations, while those at the elevated temperatures use variants of the benchmark models in Section 3.1 with the control rod positions shown in Tables 2.16 and 2.17.

$$\alpha_T = \frac{k_2 - k_1}{k_2 k_1}\left(\frac{1}{T_2 - T_1}\right). \tag{2.5}$$

Eigenvalues were calculated for critical configurations with temperatures above and below the temperature at which the isothermal temperature coefficients were measured. These configurations were then evaluated using the control rod positions of the opposite configuration to obtain eigenvalues, which represent the effective addition or subtraction of reactivity worth due to control rod movement. An example calculation is provided below.

To calculate the isothermal temperature coefficient at 421 K, first eigenvalues were calculated for critical configurations at 380 and 480 K using the extrapolated control rod positions in Table 2.17, 1859 and 1970 mm, respectively. Example eigenvalues are 1.01909 and 1.01517, respectively. Then the control rod configurations were swapped between the two temperatures, such that the positions are 1970 and 1859 mm at 380 and 480 K, respectively. The eigenvalues at these two temperatures with the control rod positions switched are 1.03184 and 1.00157, respectively. The reactivity worth of control rod movements was then used to estimate reactivity effects due to temperature changes in the core. The average reactivity difference between the high and low temperature analyses was then used to calculate the isothermal temperature coefficient. Equations 2.6 and 2.7 summarize the analytical method utilized with the computed eigenvalues to calculate the isothermal temperature coefficient. Equations 2.8 and 2.9 use the example eigenvalues to demonstrate the use of Equations 2.6 and 2.7.

$$\left(\frac{\Delta k}{k}\right)_{T=421K} = -\frac{1}{2}\left[\frac{\left(k_{\substack{T=380K \\ CR=1970mm}}\right) - \left(k_{\substack{T=380K \\ CR=1859mm}}\right)}{k_{\substack{T=380K \\ CR=1970mm}} \times k_{\substack{T=380K \\ CR=1859mm}}} + \frac{\left(k_{\substack{T=480K \\ CR=1859mm}}\right) - \left(k_{\substack{T=480K \\ CR=1970mm}}\right)}{k_{\substack{T=480K \\ CR=1859mm}} \times k_{\substack{T=480K \\ CR=1970mm}}}\right]. \tag{2.6}$$

$$\alpha_{T=421K} = \frac{\left(\frac{\Delta k}{k}\right)_{T=421K}}{\Delta T} \times 100\% . \tag{2.7}$$

$$\left(\frac{\Delta k}{k}\right)_{T=421K} = -\frac{1}{2}\left[\frac{1.03184-1.01909}{1.03184\times 1.01909} + \frac{1.01517-1.00157}{1.01517\times 1.00157}\right] = -0.0128\frac{\Delta k}{k}. \tag{2.8}$$

$$\alpha_{T=421K} = \frac{-0.0128\frac{\Delta k}{k}}{100K} \times 100\% = -0.0128\frac{\%\Delta k}{k\cdot K}. \tag{2.9}$$

MCNP was utilized for the eigenvalue calculations with ENDF/B-VII.0 cross section data processed by NJOY, as discussed in Section 2.1. Cross section were generated, including Doppler broadening of the uranium isotopes, with the NJOY computer code at 380, 400, 480, 580, 680, and 780 K. The thermal neutron scattering data [S(α,β)] for graphite and uranium dioxide were also generated with the NJOY computer code at the temperatures of 400, 500, 600, 700, 800, and 1000 K. Thermal scattering data scaled linearly with temperature, and eigenvalue calculations were corrected to the appropriate temperature. Additional uncertainty due to thermal scattering scaling was negligible.

Calculated isothermal temperature coefficients using the method discussed in the previous paragraph are shown in Table 2.19. These can be compared against the measured isothermal temperature coefficient data in Tables 2.14 and 2.15.

Table 2.19. Calculated Isothermal Temperature Coefficients.

Isothermal Temperature of Coefficient Measurement (K)	Low/High Evaluated Temperature Range (K)	α_T (% Δk/k/K)	±	1σ
346	300/400	-0.0116	±	0.0002
407 & 421	380/480	-0.0128	±	0.0002
533	480/580	-0.0129	±	0.0002
642	580/680	-0.0126	±	0.0002
736	680/780	-0.0121	±	0.0002

2.6 Evaluation of Kinetics Measurements Data

Kinetics measurements were not made.

2.7 Evaluation of Reaction-Rate Distributions

Reaction-rate distribution measurements were not made.

2.8 Evaluation of Power Distribution Data

Power distribution measurements were not made.

2.9 Evaluation of Isotopic Measurements

Isotopic measurements were not made.

2.10 Evaluation of Other Miscellaneous Types of Measurements

Other miscellaneous types of measurements were not made.

3.0 BENCHMARK SPECIFICATIONS

3.1 Benchmark-Model Specifications for Critical and / or Subcritical Measurements

Whereas insufficient information is publicly available, a finely-detailed benchmark model could not be established. A benchmark of the HTTR was prepared and analyzed with as much detail as feasible. The simplification bias for this model could also not be fully determined. However, the uncertainties in the benchmark model are believed to be of sufficient magnitude to encompass any biases incurred due to the simplification process of the benchmark model and a bias for the removal of the core instrumentation has been estimated. It is currently difficult to obtain the necessary information to improve the confidence in the benchmark model; the necessary data are proprietary and its released is being restricted, because the benchmark configuration of the HTTR core is the same that is currently in operation. Once this information is made available, the HTTR benchmark can be adjusted as appropriate.

Analysis of the fully-loaded, 30-fuel-column, cold-critical core can be found in HTTR-GCR-RESR-001. The benchmark models for the two warm critical benchmarks are identical in material properties and dimensions to the cold-critical core; only the isothermal temperatures of the core and positions to which the control rods are withdrawn have changed.

3.1.1 Description of the Benchmark Model Simplifications

Significant simplifications were required to develop a benchmark model of the HTTR because of a lack of publicly available information on dimensions and compositions. Simplifications will be discussed where applicable in the descriptions of the dimension and material properties of the model.

Most biases in the model were not quantified, and many are believed to be small. Biases that have been partially investigated are listed in Section 3.1.1.1.

The fuel handling positions, dowels, and sockets were not included in the model due to insufficient data specifications, but were accounted for with a 0.5% reduction in graphite density (based upon volume calculations using dimensions provided in Figure 1.52 of HTTR-GCR-RESR-001). The burnable poison insertion holes were placed on the same pitch as the fuel channels to simplify the model.

It is apparent from a comparison of Figures 1.65 and 1.67 of HTTR-GCR-RESR-001 that the depth to which the control rod, reserve shutdown system, and instrumentation holes are drilled varies. A depth of 1060 mm above the bottom of the core was selected for all positions to simplify the model. No bias was assessed.

Insufficient information was available to model the bottom-most reflector block according to actual design; therefore it was modeled with the same design as the two top reflector blocks and the other bottom reflector block. The top and bottom of each coolant channel is expected to taper from the 21-mm diameter to the 41-mm diameter of the fuel assemblies, but information was unavailable to describe the taper in the model. Therefore channels in the reflector blocks were modeled with 21-mm diameters.

Individual sections of the dodecagon-block-shaped permanent reflector were not modeled due to insufficient information. It was modeled as a cylindrical region surrounding the core columns. A bias was not assessed and is believed to be negligible.

Insufficient information was available to model the shielding blocks surrounding the core and shielding plugs in the core. Therefore, they were not included in the benchmark model. It is assumed that all neutrons reaching the core boundaries are lost and not scattered back by the shielding material. A conservative estimate of room-return effects demonstrated a negligible change in k_{eff}.

In the materials section, impurity contents in the materials are based upon natural boron equivalency. In the model, however, only the ^{10}B component is included, as the effect of the ^{11}B content is insignificant.

The density is the same (1.80 g/cm^3) for both types of burnable poison pellets. The boron content in the pellets is based on the reported weight percents instead of the atomic percents.

Available information overspecify the TRISO fuel particle parameters. Because the fuel mass of an individual rod would most probably be the most accurate measured parameter, it was preserved in the benchmark model with some variation to other parameters as necessary. The TRISO kernel diameter is maintained at the nominal value of 600 μm and the density of the fuel is 10.39 g/cm^3, which is within approximately 95% of the theoretical density of UO_2. The number of TRISO particles in a given compact was reduced from 13,000 to 12,987, with a packing fraction of 30%, in order to conserve a nominal fuel mass per rod of 188.58 g.

3.1.1.1 Assessed Biases

Although some biases have been partially investigated, there is incomplete information regarding the HTTR to accurately quantify simplification biases in order to adjust the benchmark k_{eff}. As stated previously, a conservative estimate of potential room-return effects provided negligible results. As shown in Section 2.1.3.2 in Table 2.37 of HTTR-GCR-RESR-001, the effect of neglecting the free uranium content of the fuel compacts was negligible. Finally, the effect of modeling the helium coolant as void material was also negligible (as shown in Section 2.1.3.10, Table 2.59 of HTTR-GCR-RESR-001). The reported literature bias for air content in the graphite could not be verified (Section 2.1.3.7 of HTTR-GCR-RESR-001).

Previous efforts of the Japanese in analyzing the 19-fuel-column core (Case 1) obtained an analytical excess reactivity of 2.7% Δk/k, with an estimated Monte Carlo calculation overestimate of 1.2% Δk/k.[a]

An approximate bias for the removal of reactor instrumentation from the three instrumentation columns in the core was calculated, as discussed in Section 2.1.2.1. Calculated biases with uncertainties are shown in Table 3.1.

Table 3.1. Estimated Bias for the Removal of Instrumentation Components.

Case	Δk	±	$\sigma_{\Delta k}$
1	0.00254	±	0.00073
2	0.00263	±	0.00076

The benchmark temperature of the two critical experiments was 395.15 and 418.05 K for configurations 1 and 2, respectively. Adjustment of the temperature to 400 and 420 K, respectively, to facilitate use of the benchmark models in calculations, provides a small additional bias. The effective bias due to the slight adjustment in temperature can be accounted for using the isothermal temperature coefficient at 407 K of -0.0132 ± 0.0020% Δk/k/K (Table 3.15). The calculated biases with uncertainties are shown in Table 3.2.

[a] Fujimoto, N., Nakano, M., Takeuchi, M., Fujisaki, S., and Yamashita, K., "Start-Up Core Physics Tests of High Temperature Engineering Test Reactor (HTTR), (II): First Criticality by an Annular Form Fuel Loading and Its Criticality Prediction Method," *J. Atomic Energy Society Japan*, **42**(5), 458-464 (2000).

Table 3.2. Estimated Bias for the Correction of Benchmark Temperature.

Case	ΔT (K)	Δk	±	$\sigma_{\Delta k}$
1	4.85	-0.00064	±	0.00010
2	1.95	-0.00026	±	0.00004

3.1.1.2 Neglect of Thermal Expansion Effects

The effect of thermal expansion upon the dimensions and densities of the major components of the HTTR have been evaluated for temperatures up to 780 K. Thermal expansion coefficients were obtained from available reference material and are summarized in Table 3.3. New dimensions and densities were calculated for the following thermally expanded components:

- graphite sleeves,
- graphite blocks,
- permanent reflector,
- fuel compacts, and
- control rod cladding.

These components were evaluated at temperatures of 380, 480, 580, 680, and 780 K. The dimensions and densities were then updated in a variant of the benchmark models and the eigenvalues were recalculated. The bias for neglecting the thermal expansion of major core components in the HTTR was determined to be negligible, as the changes in the calculated eigenvalues were insignificant compared to the statistical uncertainty in the calculations. Furthermore, the calculated adjustments to the benchmark model dimensions and densities were much less than their respective uncertainties evaluated in Section 2 of this report and HTTR-GCR-RESR-001.

Table 3.3. Thermal Expansion Coefficients.

Material	Mean Thermal Expansion Coefficient (10^{-6} K^{-1})	Temperature Range (K)
IG-110 Graphite[a][b]	4.06	293 – 673
PGX Graphite[a][b]	2.34	293 – 673
Fuel Compacts[c]	0.15	--
Alloy 800H[d]	14.2 – 17.8	294 – 1033

(a) Ishihara, M., Sumita, J., Shibata, T., Iyoku, T, and Oku, T., "Principle Design and Data of Graphite Components," *Nucl. Eng. Des.*, **233**, 251-260 (2004).
(b) Sumita, J., Shibata, T., Hanawa, S., Ishihara, M., Iyoku, T., and Sawa, K., "Characteristics of First Loaded IG-110 Graphite in HTTR Core," JAEA-Technology 2006-048 (October 2006).
(c) Maruyama, S., Yamashita, K., Fujimoto, N., Murata, I., Shindo, R., and Sudo, Y., "Determination of Hot Spot Factors for Calculation of the Maximum Temperatures in the Core Thermal and Hydraulic Design of HTTR," JAERI-M 88-250 (1998) [in Japanese].
(d) "Specification Sheet: Alloy 800, 800H, and 800AT," Sandmeyer Steel Company, http://www.sandmeyersteel.com, Last Accessed July 7, 2010.

3.1.2 Dimensions

3.1.2.1 Prismatic Pin-in-Block Fuel

TRISO Particles

The basic ingredient for HTTR fuel is the TRISO particle. A UO_2 kernel is surrounded by four coatings: a low density porous pyrolytic carbon (PyC) buffer layer, a high density inner isotropic PyC layer, a SiC layer, and a final outer PyC layer. A resinated graphite overcoat is then deposited around each TRISO particle. Figure 3.1 depicts the TRISO layers and their respective dimensions.

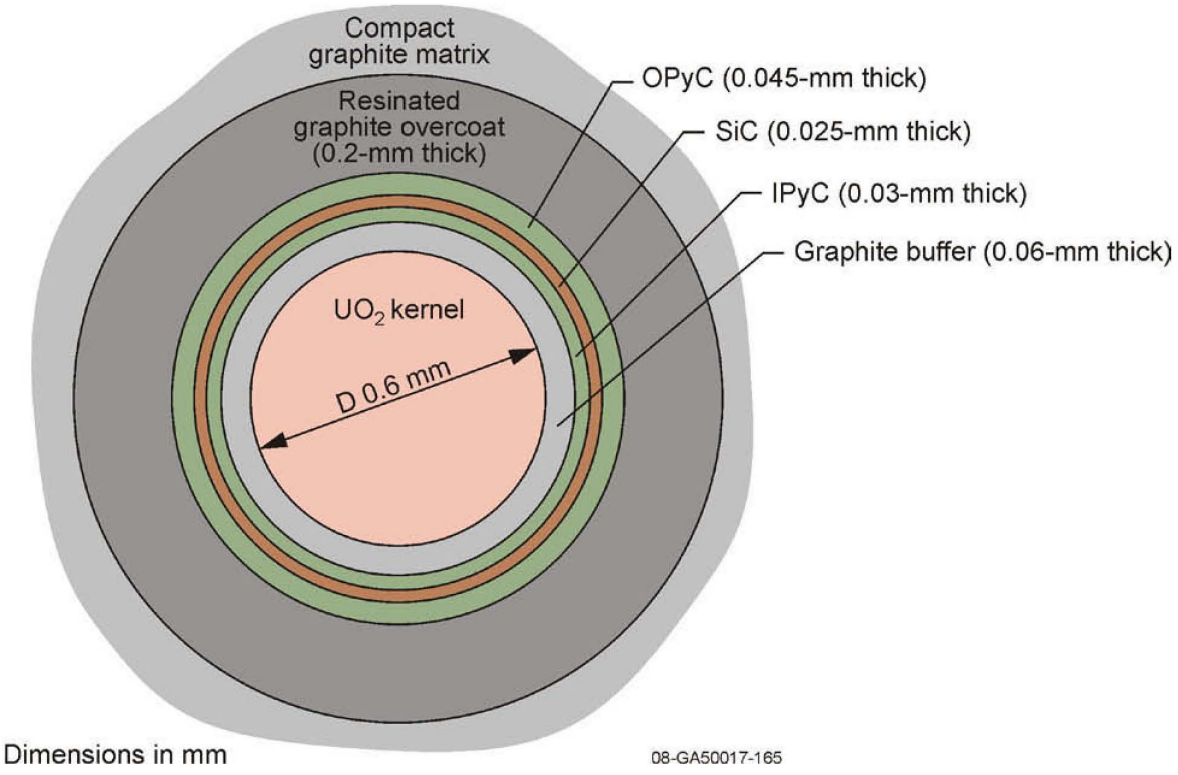

Figure 3.1. TRISO-Coated Fuel Particle.

Compacts

All fourteen fuel compacts in a single fuel rod are modeled as a single unit filled with the TRISO lattice. The stacked compacts have an inner diameter of 1 cm, an outer diameter of 2.6 cm, and an overall height of 54.6 cm.

A horizontal cross section of the compacts is shown in Figure 3.2. In the benchmark model, 12,987 TRISO particles are randomly distributed throughout the compact matrix in a single compact. For a stack of 14 compacts, as modeled in this benchmark, the total number of TRISO particles is 181,818.

A key parameter is that the total fuel mass of a single fuel rod (14 stacked compacts) is 188.58 g.

While this benchmark model retains randomness in TRISO particle distribution (Figure 3.2), many computer codes cannot properly model such configurations. It is up to the user to determine which

method is most appropriate while accounting for its impact on the reactivity of the model. Example means for analyzing this model are provided in Section 4.1. The difference in methods for accurately modeling random TRISO particles in a full-core reactor has been discussed in Section 2.1.4.2 of HTTR-GCR-RESR-001.

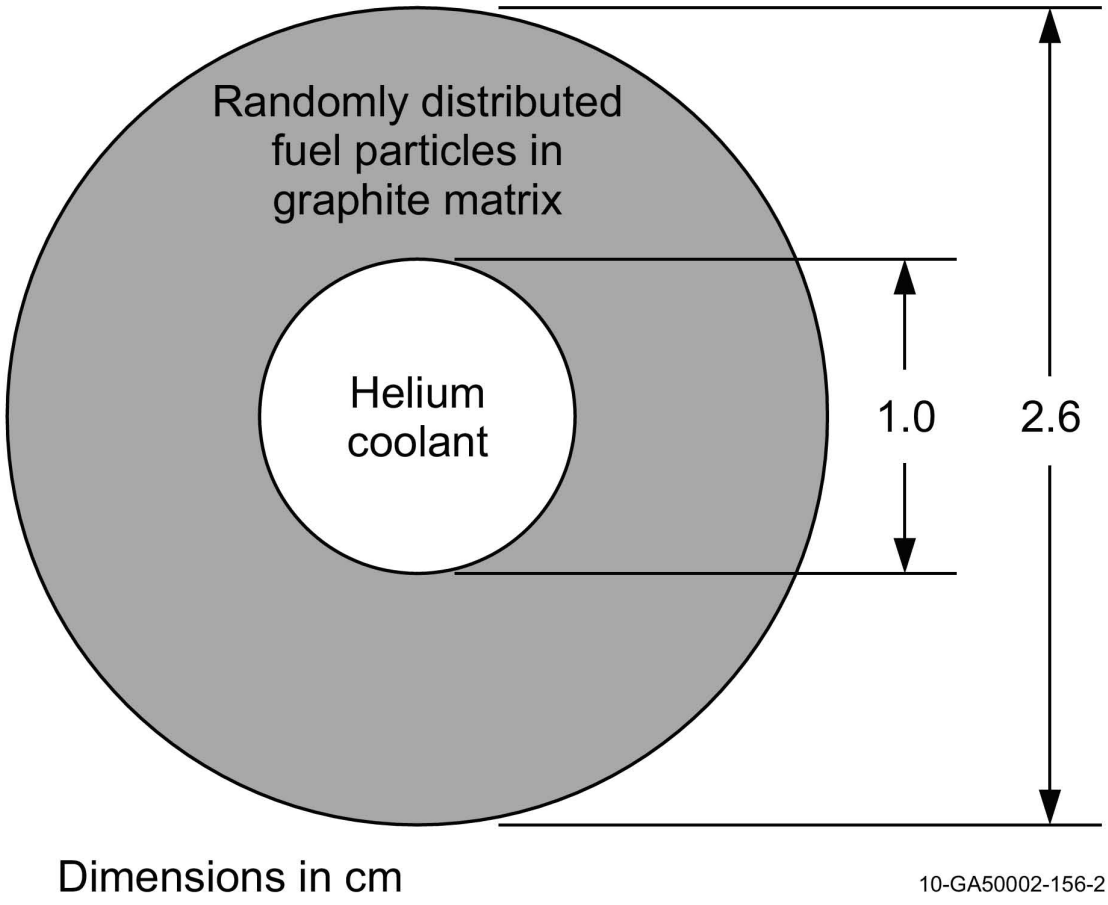

Figure 3.2. Fuel Compact Filled with Randomly Distributed TRISO Particles (Particles Not Shown).

Fuel Rod

A description of the HTTR fuel rod is modeled (Figure 3.3). Coolant channels through the graphite sleeve are not preserved in this neutronics model.

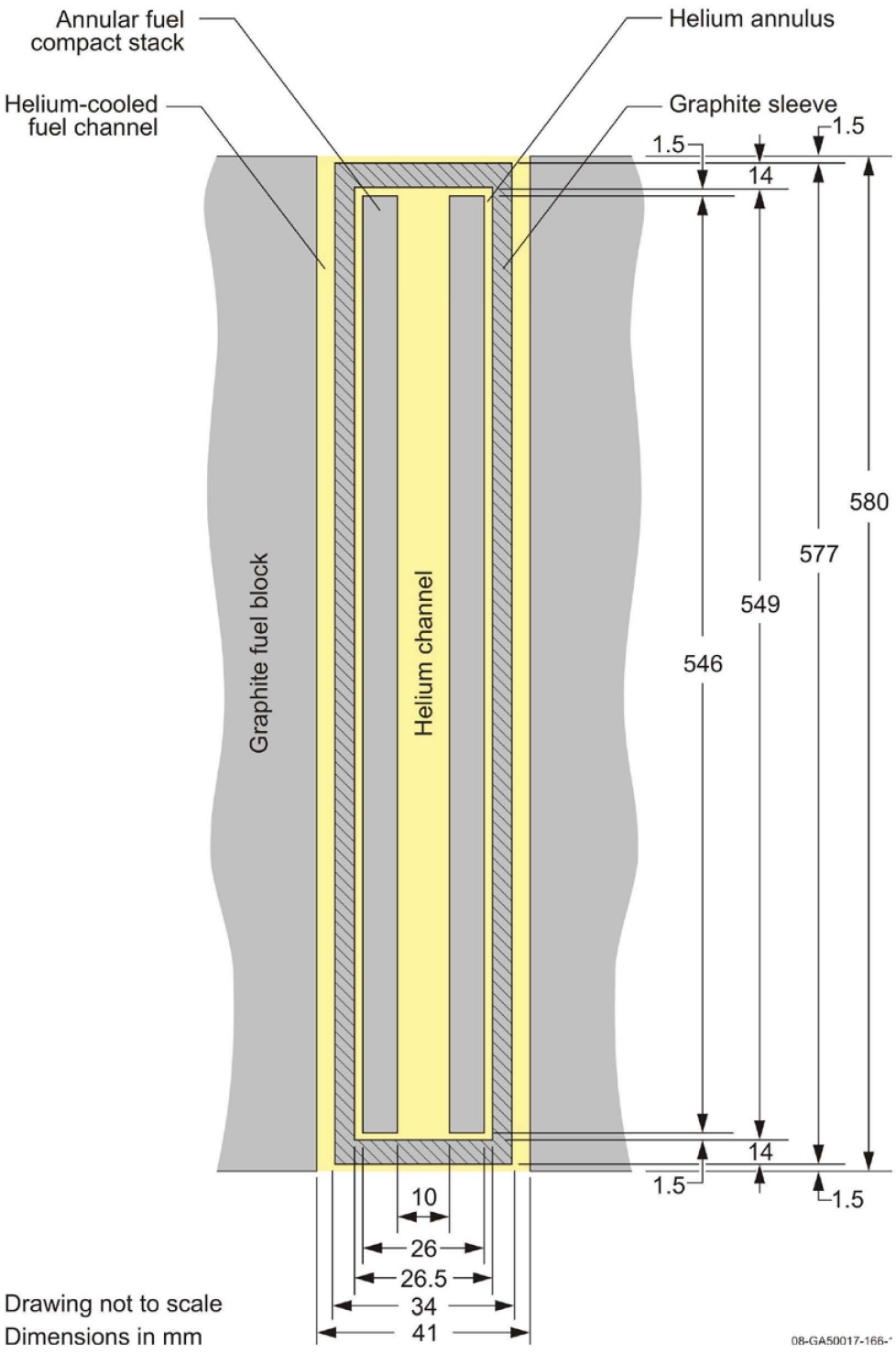

Figure 3.3. Benchmark HTTR Fuel Rod.

3.1.2.2 Burnable Poisons

The burnable poison pellets and graphite disks were modeled as individual stacks contained within a pin position in the fuel blocks (Figure 3.4). Each fuel block contained two BP pins and one empty pin position.

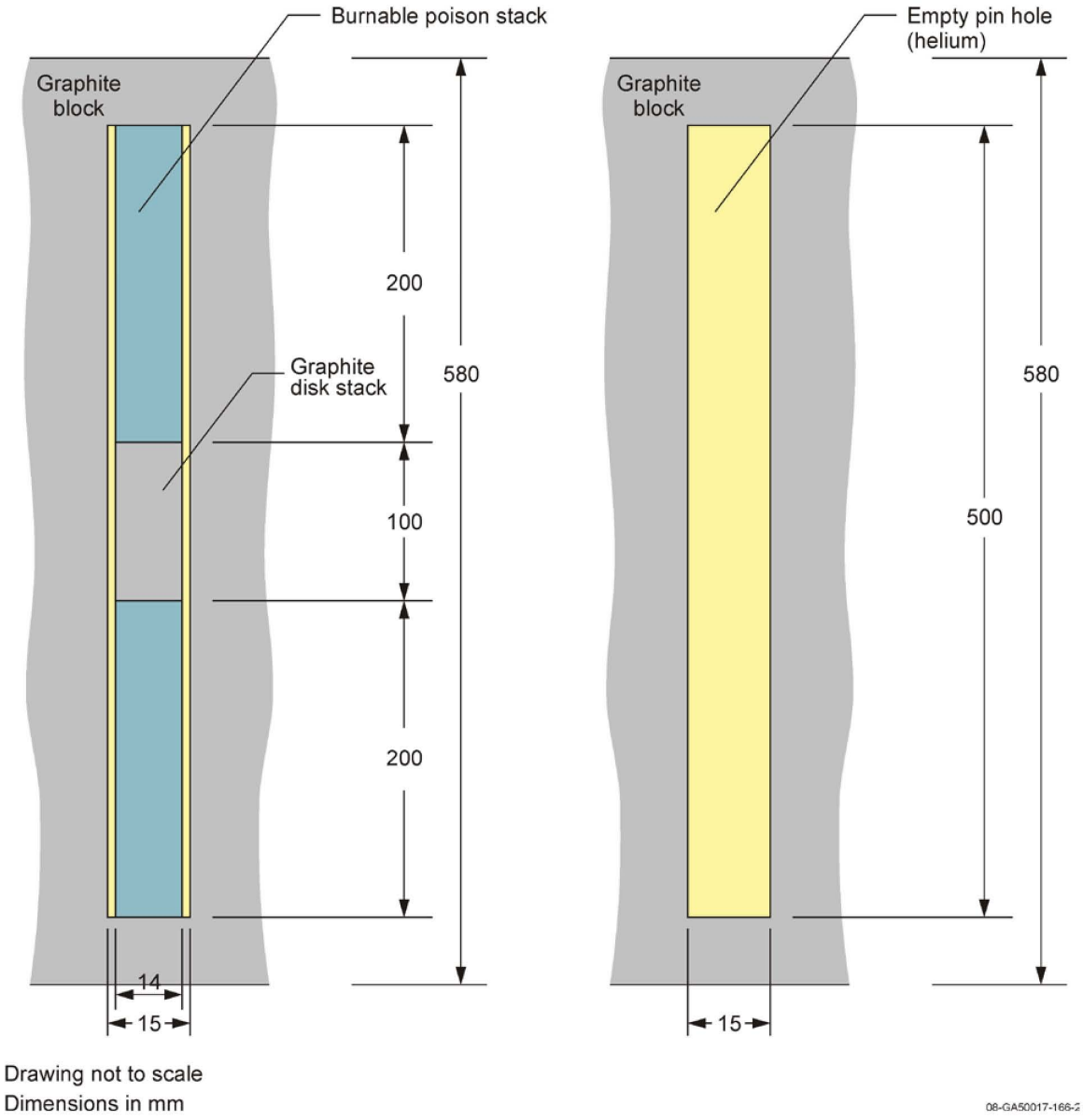

Figure 3.4. Burnable Poison Pin (Left) and Empty Pin Position (Right).

3.1.2.3 Fuel Blocks

The HTTR contains two types of regular hexagonal fuel blocks: 33-pin (Zones 1 and 2) and 31-pin (Zones 3 and 4). Diagrams of each fuel block design implemented in the benchmark model are shown in Figures 3.5 and 3.6, respectively. The pitch for all positions is 51.5 mm.

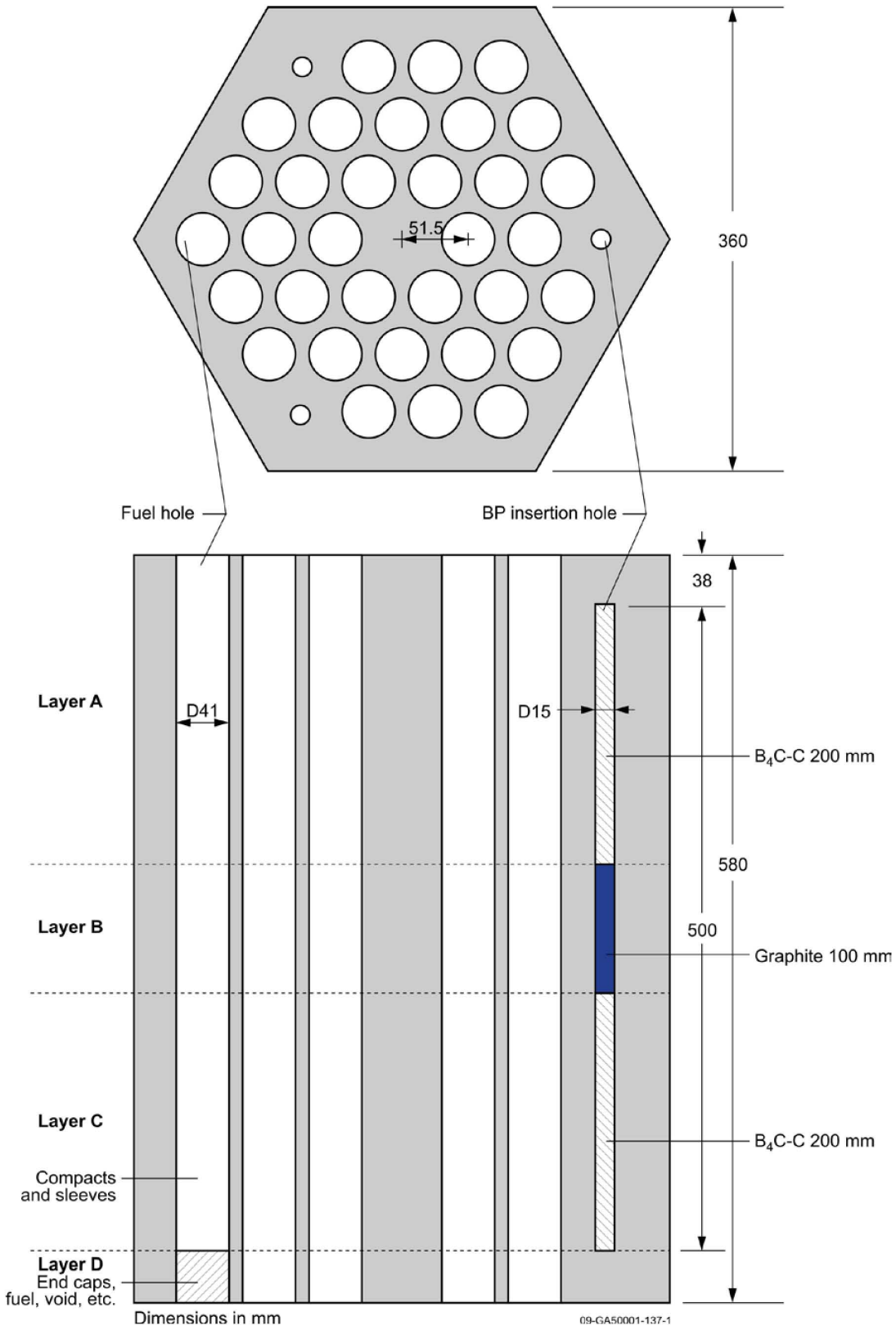

Figure 3.5. Fuel Block for 33-Pin Fuel Assembly. Dxx represents the diameter in xx (mm).

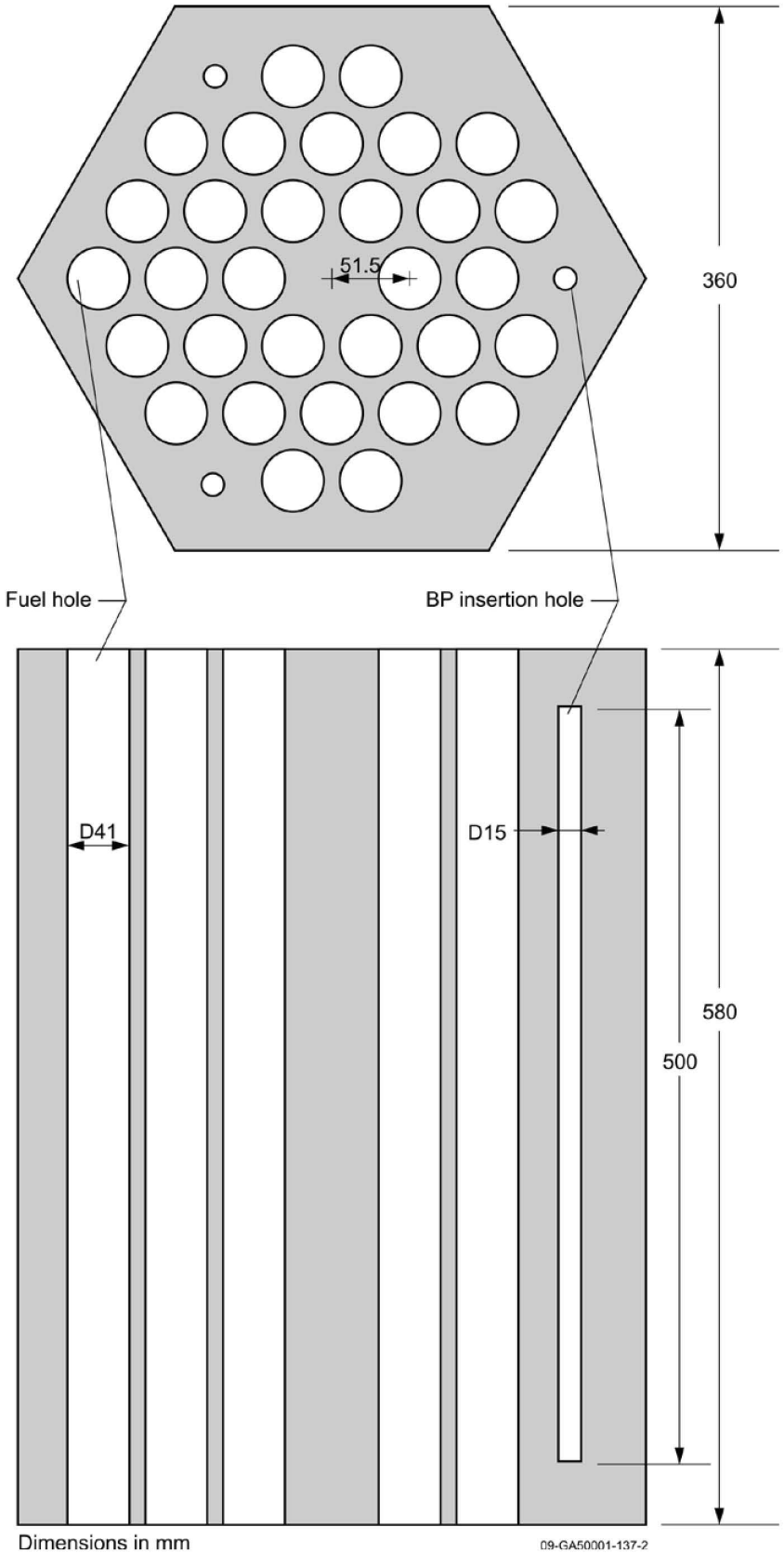

Figure 3.6. Fuel Block for 31-Pin Fuel Assembly. Dxx represents the diameter in xx (mm).

3.1.2.4 Dummy Blocks

The 30-fuel-column core does not contain dummy blocks.

3.1.2.5 Control Rod System

Control Rods

A diagram of a control rod section is shown in Figure 3.7. The absorber compacts are modeled as a single unit. Detailed dimensions regarding the cladding infrastructure for each section was unavailable, and the clad is therefore modeled without detail. A single control rod is comprised of ten sections (Figure 3.8) with a total height of 3.1 m.

The control rods are divided up into four sets: center position (C), ring 1 (R1), ring 2 (R2), and ring 3 (R3). The center position contains two control rods. The other rings are comprised of six, six, and three positions, containing a total of twelve, twelve, and six control rods, respectively. Control rods in each set are synchronously moved.

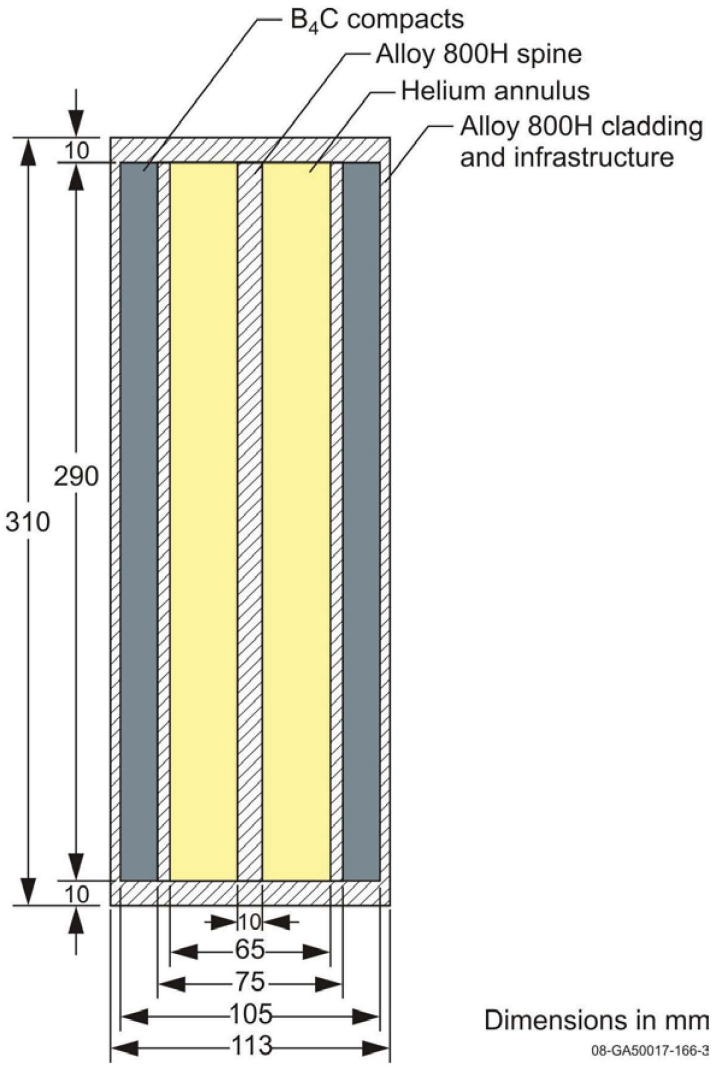

Figure 3.7. Control Rod Section.

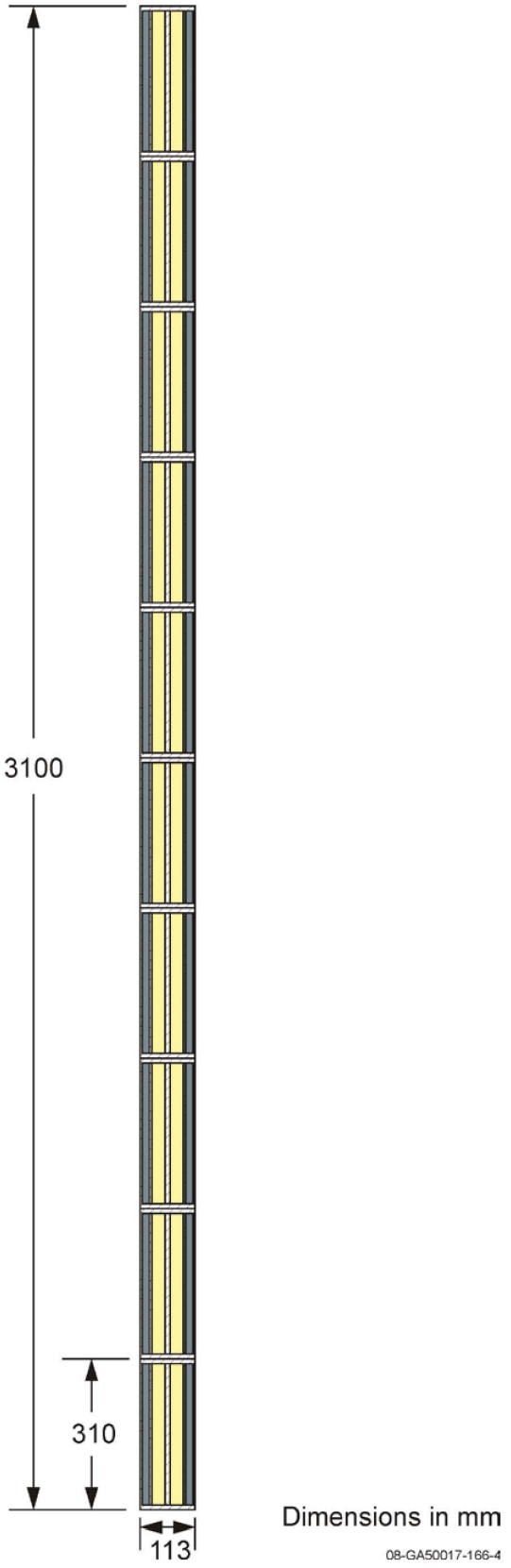

Figure 3.8. Control Rod Comprised of Ten Sections.

Control Rod Columns

Individual control rod blocks were not modeled. A single control rod column was modeled with three holes to accommodate two control rods and an empty position (for the reserved shutdown system). A diagram of a generic control column (without control rods) is shown in Figure 3.9. The holes in the control rod and instrumentation columns are equidistant from each other, with an angle of 120º.

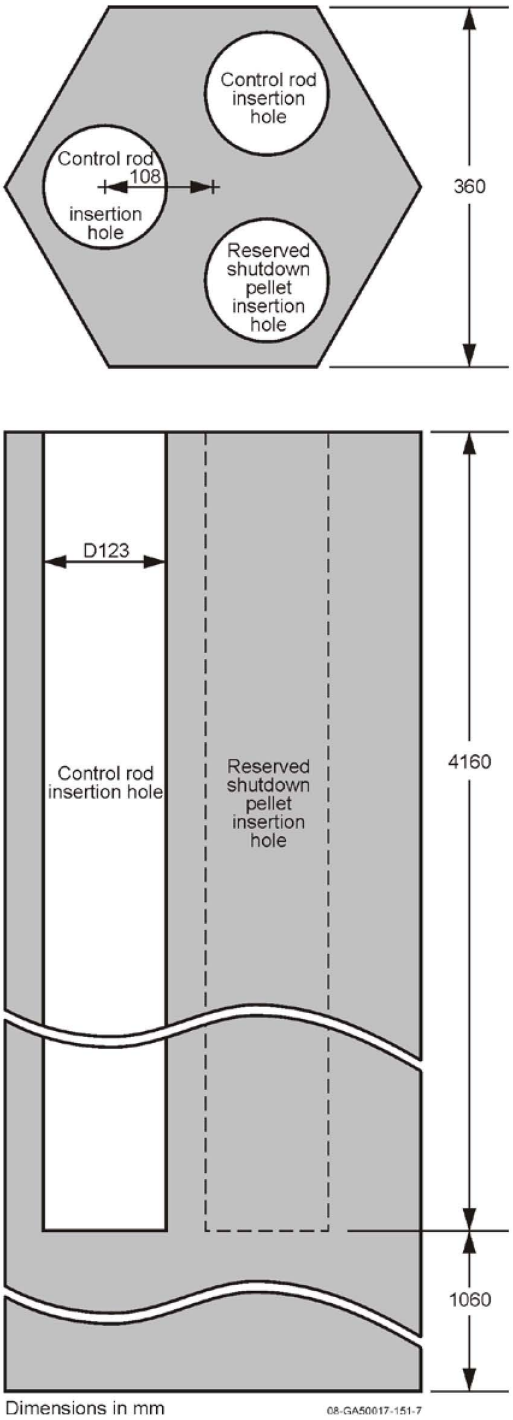

Figure 3.9. Control Rod Column. Dxx represents the diameter in xx (mm).

3.1.2.6 Instrumentation

Instrumentation Components

Instrumentation was not included in the benchmark model of the HTTR. An approximate bias with uncertainty was determined applied to the benchmark model (see Sections 2.1.2.1 and 3.1.1.1).

Instrumentation Columns

Instrumentation columns are modeled as a single unit without blocks, similar to the control rod columns. However, all three positions are empty (Figure 3.10).

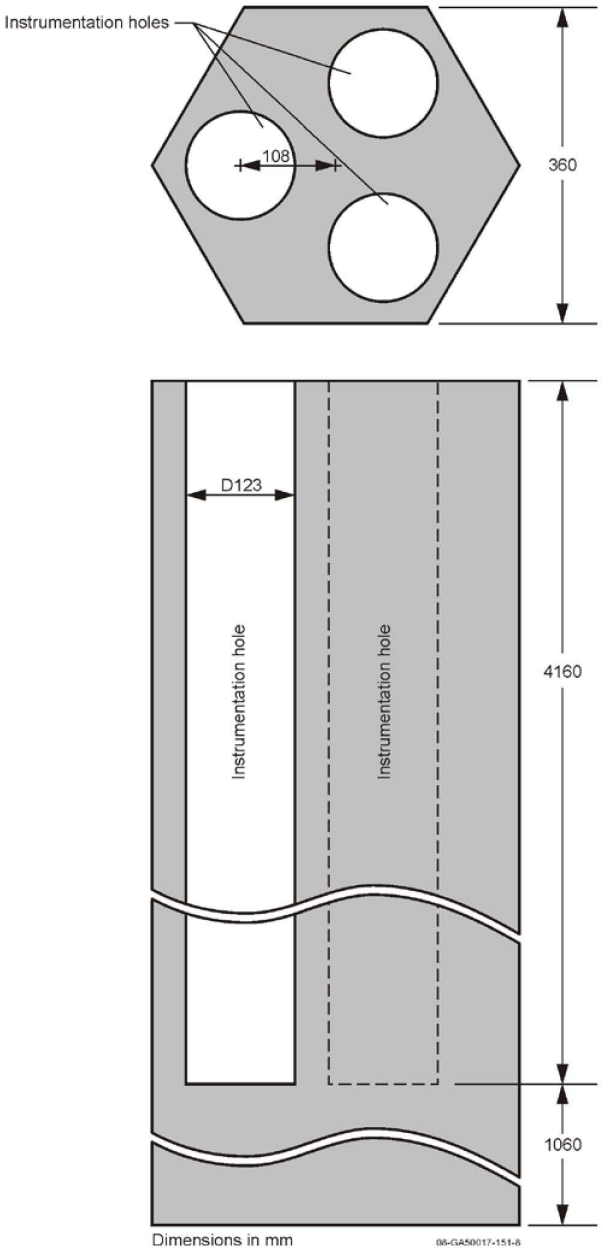

Figure 3.10. Instrumentation Column. Dxx represents the diameter in xx (mm).

3.1.2.7 Replaceable Reflector Columns

The replaceable reflector columns are modeled as a solid unit and not as individual blocks, similar to the control rod and instrumentation columns but without any channels (Figure 3.11).

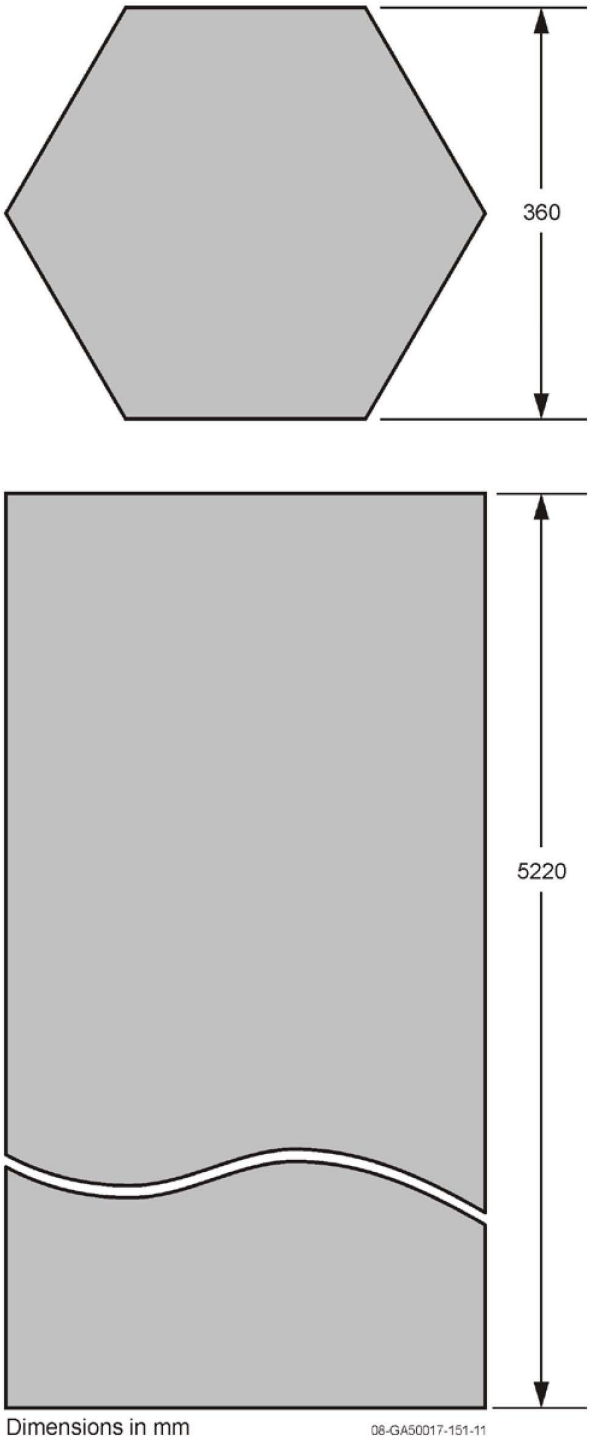

Figure 3.11. Replaceable Reflector Column.

3.1.2.8 Replaceable Reflectors Blocks in Fuel Columns

The replaceable reflector blocks, located at the top and the bottom fuel columns, are shown in Figures 3.12 and 3.13, for the 33-pin and 31-pin fuel assemblies, respectively. The replaceable reflector blocks have the same regular hexagonal shape and pitch as described for the fuel blocks.

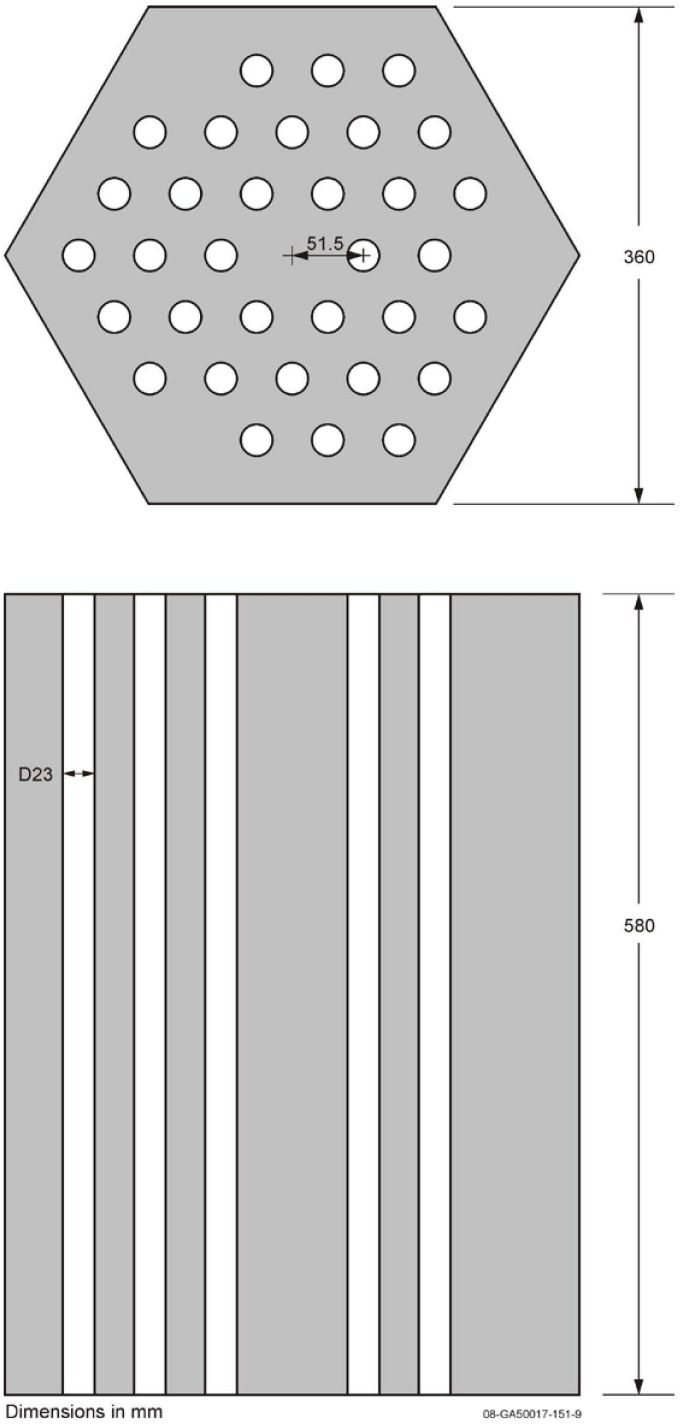

Figure 3.12. Replaceable Reflector Block for 33-Pin Fuel Assembly.
Dxx represents the diameter in xx (mm).

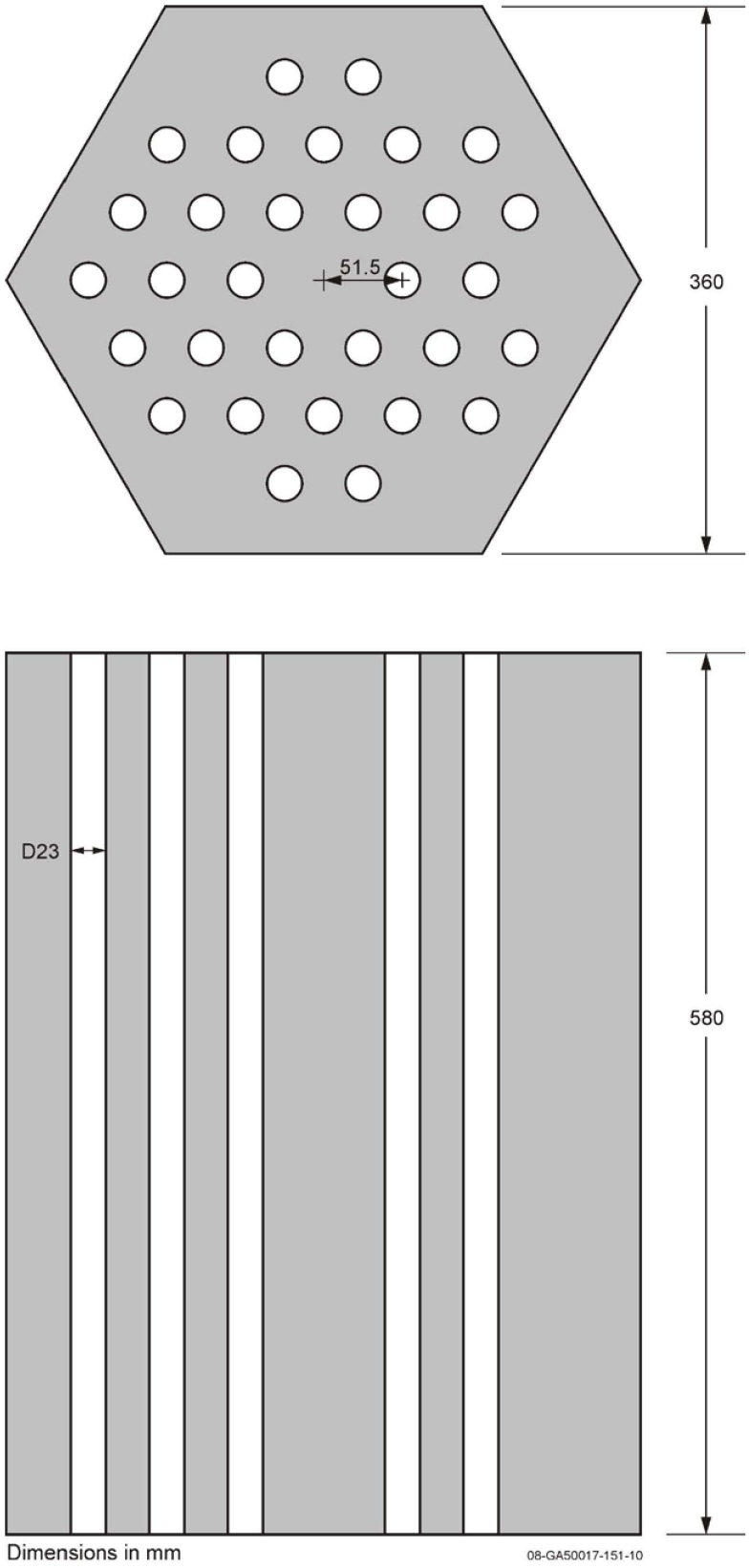

Figure 3.13. Replaceable Reflector Block for 31-Pin Fuel Assembly. Dxx represents the diameter in xx (mm).

3.1.2.9 Fuel Columns

The fuel columns are separated into four zones (as shown in Figure 1.46 of HTTR-GCR-RESR-001). Each zone has a specified pattern of uranium enrichment. Each column contains two top replaceable reflector blocks (Figure 3.12 for Zones 1 and 2 or Figure 3.13 for Zones 3 and 4), five fuel blocks (Figure 3.5 for Zones 1 and 2 and Figure 3.6 for Zones 3 and 4), and two bottom replaceable reflector blocks (Figure 3.12 for Zones 1 and 2 or Figure 3.13 for Zones 3 and 4). The second and third fuel blocks from the top contain burnable poison pellets that are more enriched than the pellets in the other three positions. Figure 3.14 shows the enrichment of the uranium (wt.%) in the TRISO fuel (upper left) and the natural boron content (wt.%) in the burnable pellets (lower right).

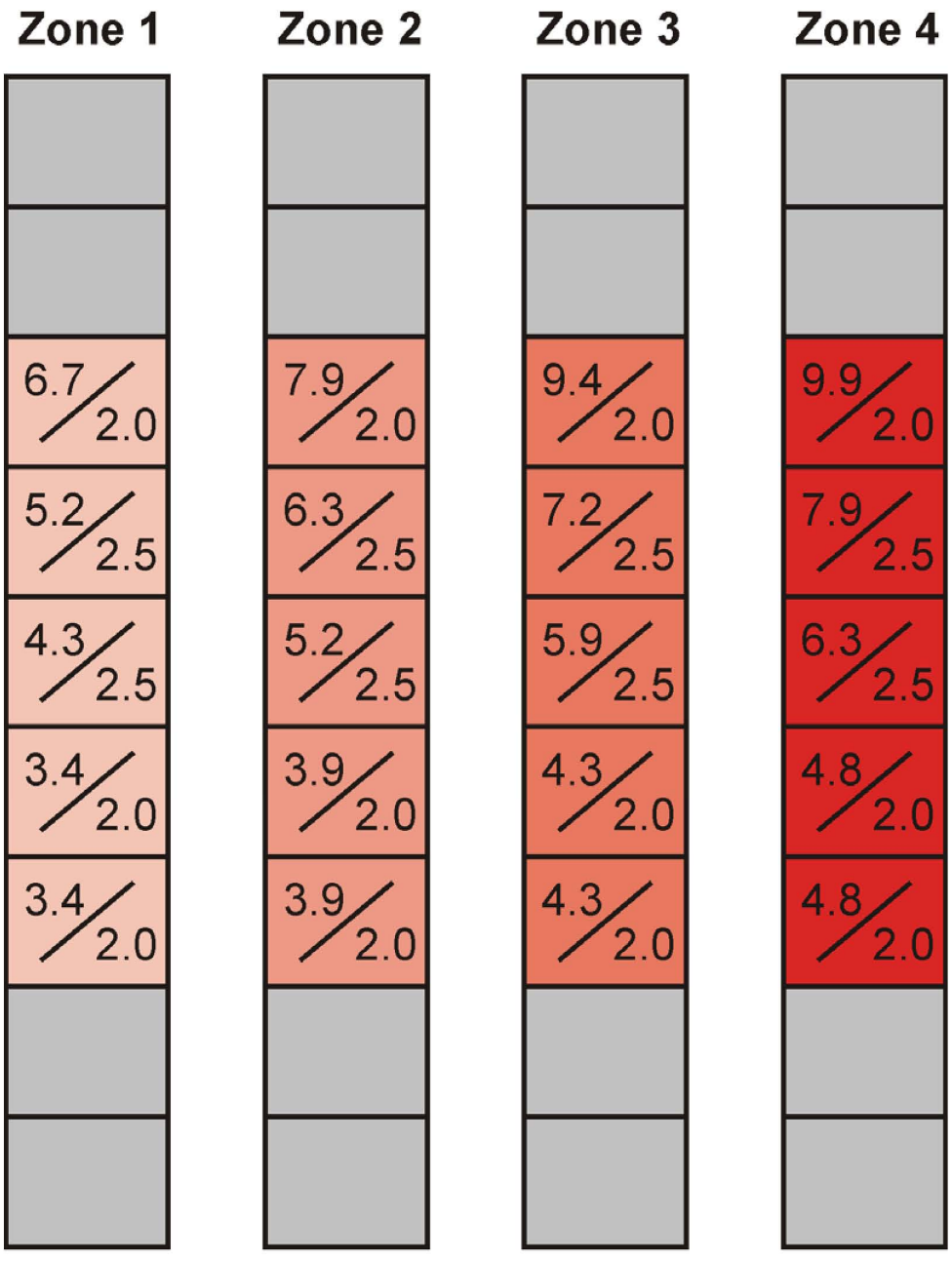

Figure 3.14. HTTR Fuel Zones.

3.1.2.10 Reactor Core Configuration

The HTTR core configuration is shown in Figures 3.15, 3.16, 3.17. The first figure identifies the positions in the core for a given column type. The second figure provides the orientation of each column within its respective position in the core. The third figure shows the column identification number for each position in the core. Figure 3.18 shows a basic cross section of the HTTR core.

The permanent reflector surrounding the core has been circularized with a radius of 2125 mm and height of 5220 mm.

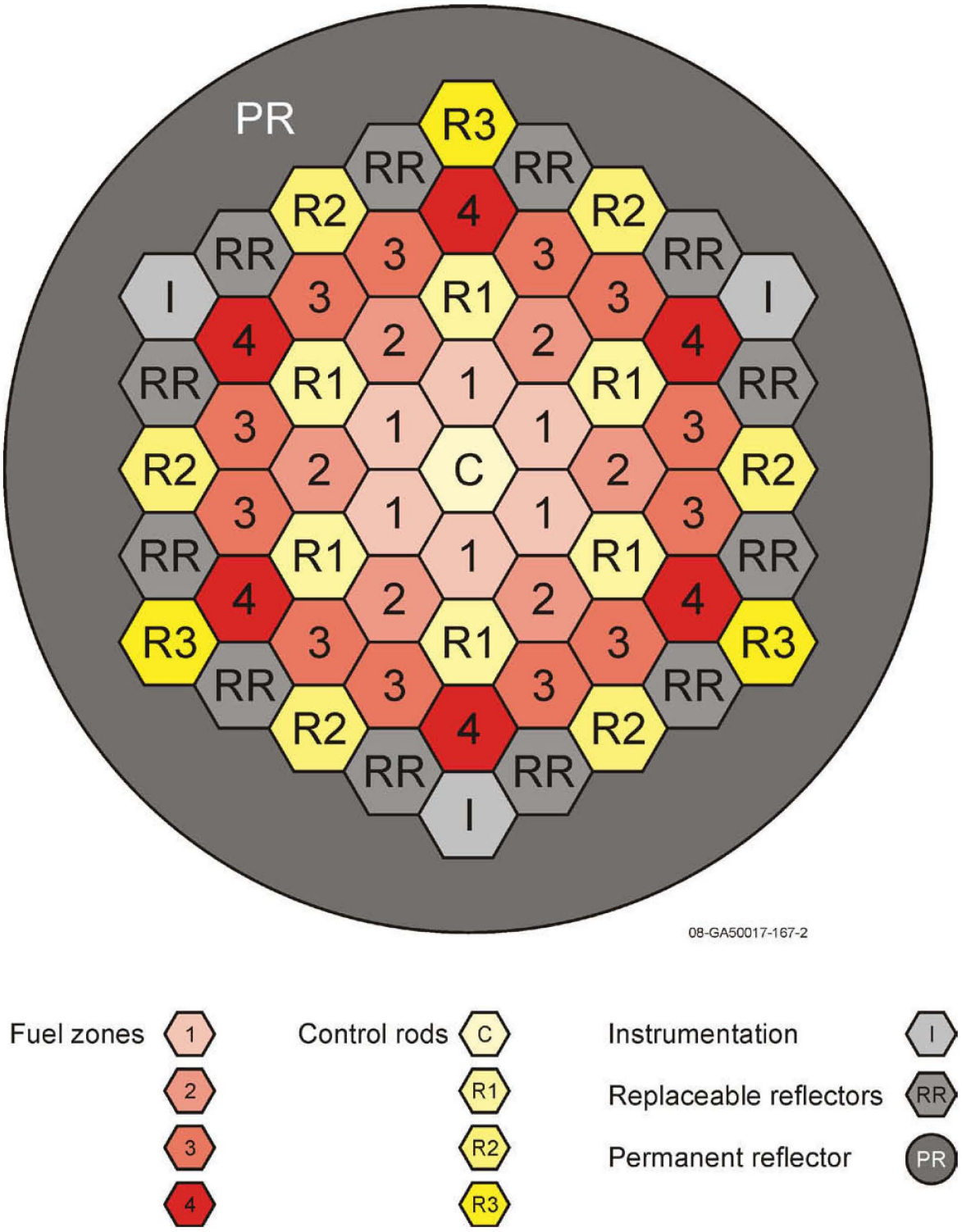

Figure 3.15. HTTR Core Positions (Fully-Loaded, 30-Fuel-Column Core – No Dummy Fuel Columns).

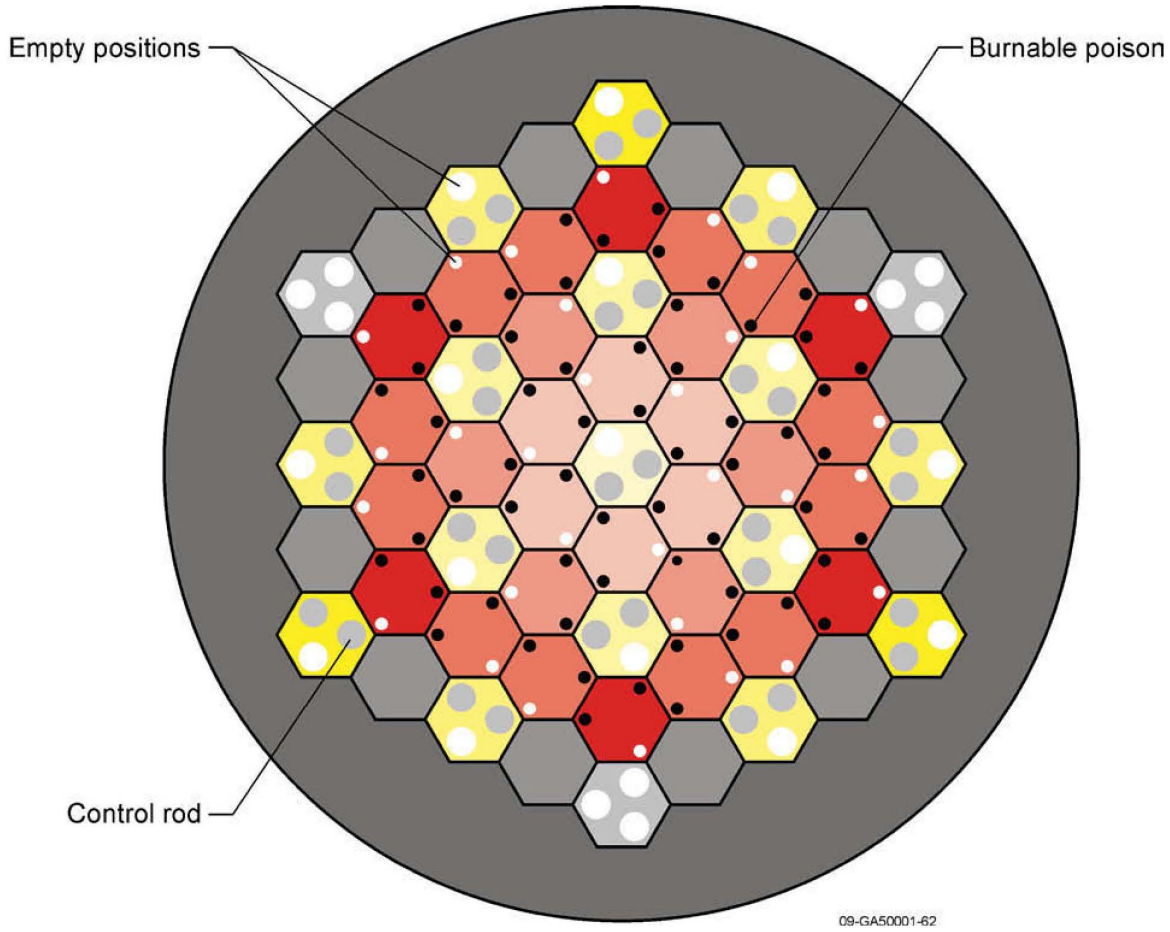

Figure 3.16. Fuel and Control Rod Column Orientations.

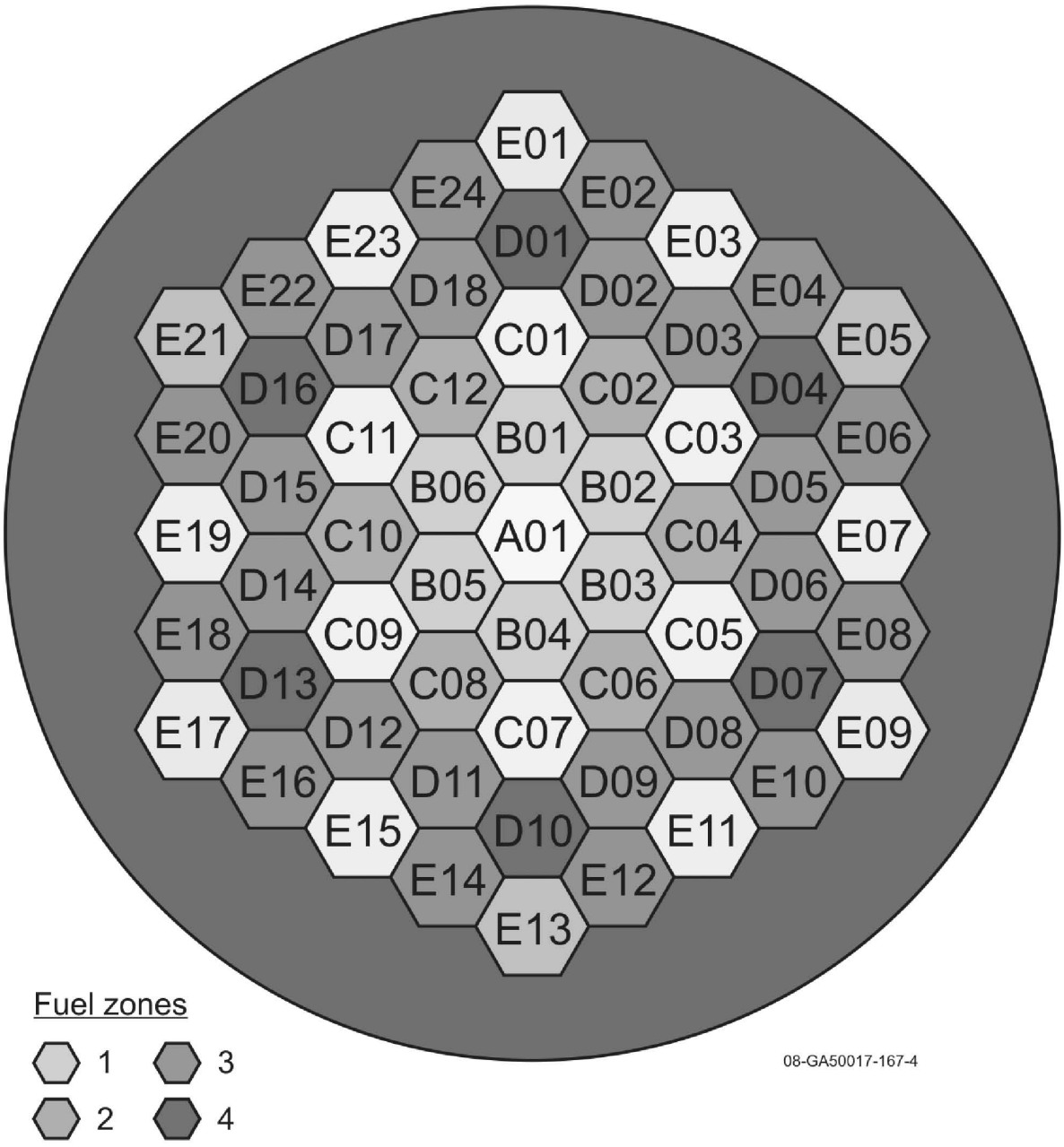

Figure 3.17. HTTR Column Identification.

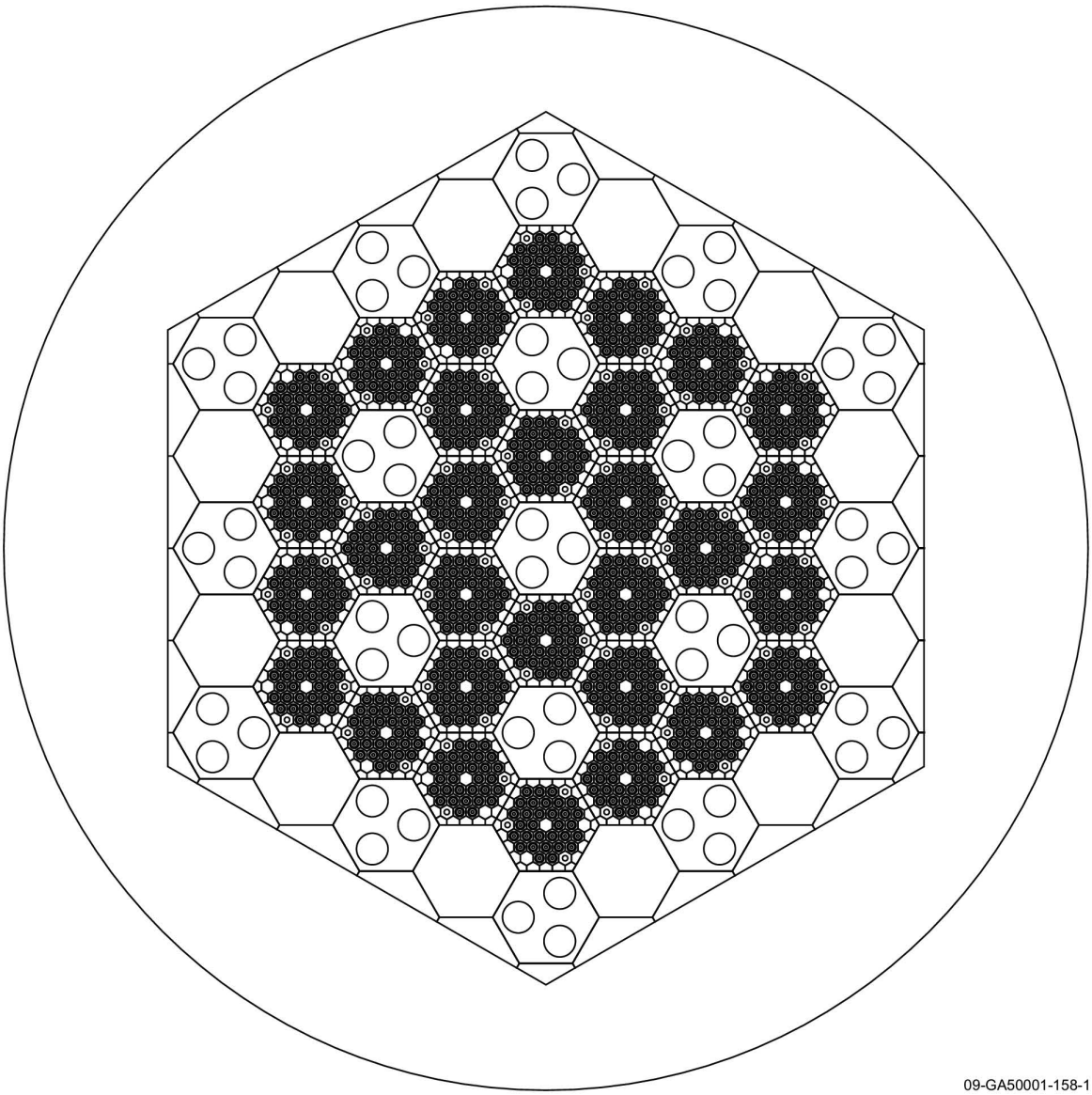

09-GA50001-158-1

Figure 3.18. Cross Section of the HTTR Fully-Loaded, 30-Fuel-Column Core.

3.1.2.12 Critical Rod Positions

The critical rod positions for configurations 1 and 2 are shown in Figures 3.19 and 3.20, respectively. Control rod positions are described with the zero position defined as level with the bottom place of the lowest fuel block (i.e. 1160 mm from the bottom of the core graphite, the lowest fuel block). These figures provide reference between the various column types in the core and the control rod positions; the dummy fuel column and fuel column are interchangeable in these figures, with no change in the dimensions.

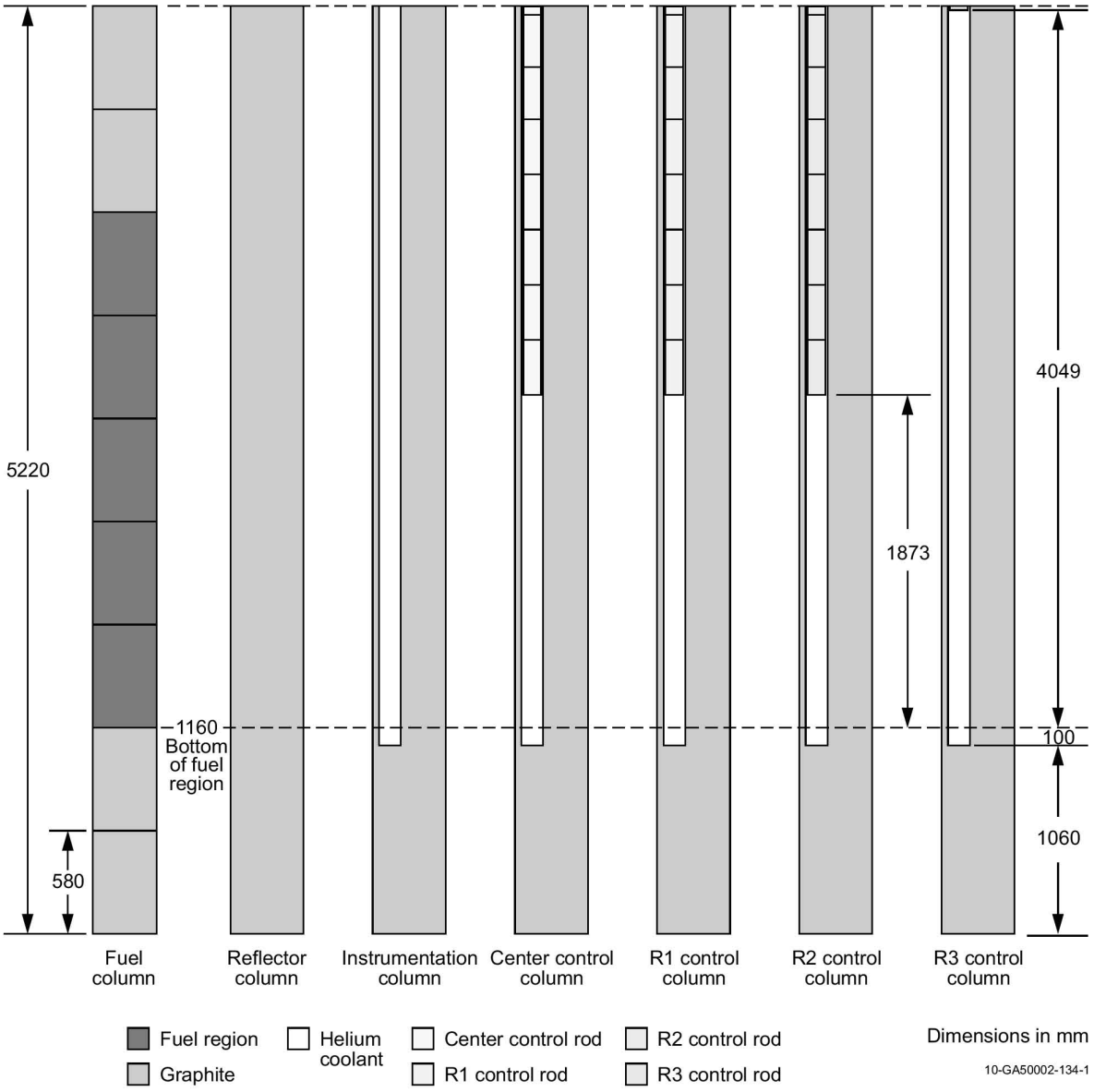

Figure 3.19. Axial Profile of Columns and Control Rod Positions (Configuration 1).

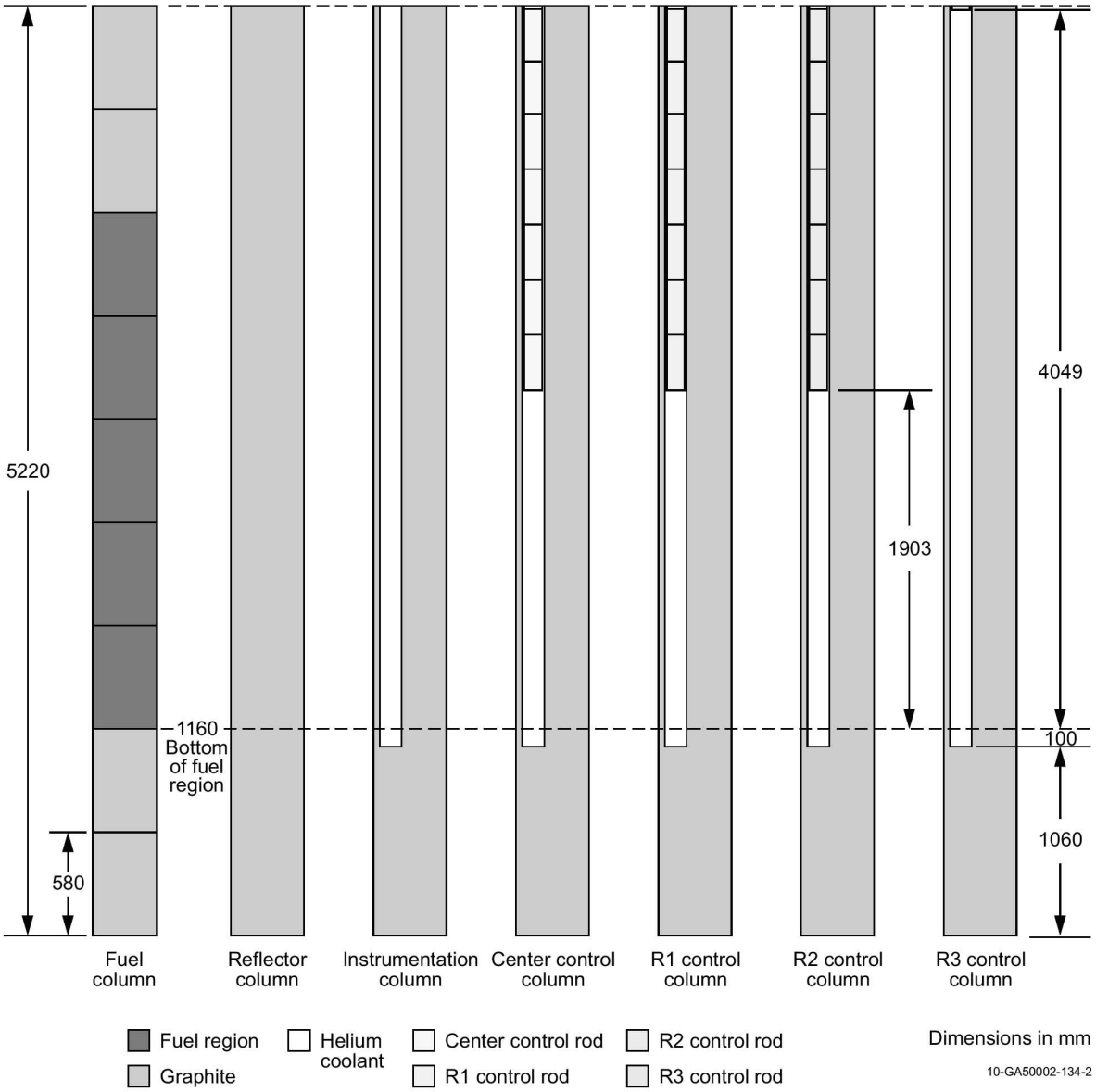

Figure 3.20. Axial Profile of Columns and Control Rod Positions (Configuration 2).

3.1.3 Material Data

3.1.3.1 Pin-in-Block Fuel

TRISO Particles

The mass density of the TRISO-coated UO_2 fuel kernels is 10.40363 g/cm^3 (such that the total uranium mass per fuel rod is 188.58 g) with an O/U ratio of 2.00 and an equivalent natural-boron impurity content of 0.00015 wt.%. A summary of the atom densities and compositions for the twelve enrichments found throughout the core are provided in Table 3.4.

Table 3.4. Atom Densities (atoms/b-cm) of the UO_2 Kernels for Varying Enrichments.

Isotope	3.40 wt.%	3.90 wt.%	4.30 wt.%	4.80 wt.%	5.20 wt.%	5.90 wt.%
^{10}B	1.7299E-07	1.7299E-07	1.7299E-07	1.7299E-07	1.7299E-07	1.7299E-07
O	4.6404E-02	4.6404E-02	4.6404E-02	4.6404E-02	4.6404E-02	4.6404E-02
^{234}U	6.1026E-06	7.0000E-06	7.7180E-06	8.6154E-06	9.3334E-06	1.0590E-05
^{235}U	7.9888E-04	9.1637E-04	1.0104E-03	1.1278E-03	1.2218E-03	1.3863E-03
^{238}U	2.2405E-02	2.2288E-02	2.2195E-02	2.2078E-02	2.1984E-02	2.1821E-02
Total	6.9614E-02	6.9616E-02	6.9617E-02	6.9618E-02	6.9619E-02	6.9622E-02

Table 3.4. (cont.) Atom Densities (atoms/b-cm) of the UO_2 Kernels for Varying Enrichments.

Isotope	6.30 wt.%	6.70 wt.%	7.20 wt.%	7.90 wt.%	9.40 wt.%	9.90 wt.%
^{10}B	1.7299E-07	1.7299E-07	1.7299E-07	1.7299E-07	1.7299E-07	1.7299E-07
O	4.6404E-02	4.6404E-02	4.6404E-02	4.6404E-02	4.6404E-02	4.6404E-02
^{234}U	1.1308E-05	1.2026E-05	1.2923E-05	1.4180E-05	1.6872E-05	1.7769E-05
^{235}U	1.4803E-03	1.5743E-03	1.6918E-03	1.8562E-03	2.2087E-03	2.3262E-03
^{238}U	2.1727E-02	2.1634E-02	2.1517E-02	2.1353E-02	2.1002E-02	2.0886E-02
Total	6.9623E-02	6.9624E-02	6.9625E-02	6.9628E-02	6.9632E-02	6.9634E-02

The material properties of the TRISO layers and graphite overcoat are provided in Table 3.5.

Table 3.5. Material Properties of the TRISO Coatings and Graphite Overcoat.

Property	Buffer	IPyC	SiC	OPyC	Overcoat
Mass Density (g/cm^3)	1.1	1.85	3.2	1.85	1.7
B-nat Impurity (wppm)	1.5	1.5	1.5	1.5	1.5
Atom Density (atoms/b-cm)	5.5153E-02	9.2758E-02	9.6122E-02	9.2758E-02	8.5237E-02
^{10}B	1.8290E-08	3.0761E-08	5.3208E-08	3.0761E-08	2.8267E-08
C-nat	5.5153E-02	9.2758E-02	4.8061E-02	9.2758E-02	8.5237E-02
Si	--	--	4.8061E-02	--	--

Compacts

A key parameter is that the total fuel mass of a single fuel rod (14 stacked compacts) is 188.58 g.

The mass density of the fuel compact graphite matrix is 1.7 g/cm^3 with an equivalent natural-boron impurity content of 0.000082 wt.%. The atom density and composition of the compact matrix is shown in Table 3.6.

Table 3.6. Atom Densities of the Fuel Compact Graphite Matrix.

Isotope	Atoms/b-cm
^{10}B	1.5452E-08
C-nat	8.5237E-02
Total	8.5237E-02

Fuel Rod

The IG-110 graphite sleeve and end caps for the fuel rods have a mass density of 1.77 g/cm^3 and an equivalent natural-boron content of 0.000037 wt.%. The atom density and composition of the graphite used in the fuel rod is shown in Table 3.7.

Table 3.7. Atom Densities of the Graphite Fuel Sleeve.

Isotope	Atoms/b-cm
^{10}B	7.2596E-09
C-nat	8.8747E-02
Total	8.8747E-02

3.1.3.2 Burnable Poisons

The burnable poison pellets have a mass density of 1.80 g/cm^3; a summary of the atom densities and compositions for the two natural-boron concentrations employed in the core are provided in Table 3.8. The mass density of the graphite disks used to separate the burnable poison pellets is 1.77 g/cm^3 with an equivalent natural-boron content of 0.000037 wt.%. The atom density and composition of the graphite disks is also found in Table 3.8

Table 3.8. Atom Densities (atoms/b-cm) of the Burnable Poison Pellets and Graphite Disks.

Isotope	2.00 wt.%	2.50 wt.%	Disks
^{10}B	3.9906E-04	4.9882E-04	7.2596E-09
^{11}B	1.6063E-03	2.0078E-03	--
C-nat	8.8446E-02	8.7995E-02	8.8747E-02
Total	9.0451E-02	9.0501E-02	8.8747E-02

3.1.3.3 Fuel Blocks

The IG-110 graphite fuel blocks have a mass density of 1.7512 g/cm^3 (1.76 g/cm^3 base density decreased by a calculated 0.5% void fraction) and an equivalent natural-boron content of 0.000059 wt.%. The atom density and composition of the graphite fuel blocks is shown in Table 3.9.

Table 3.9. Atom Densities of the Graphite Fuel Blocks.

Isotope	Atoms/b-cm
^{10}B	1.1453E-08
C-nat	8.7804E-02
Total	8.7804E-02

3.1.3.4 Dummy Blocks

The 30-fuel-column core does not contain dummy blocks.

3.1.3.5 Control Rod System

Control Rods

The absorber compacts have a mass density of 1.9 g/cm^3 and have a composition and atom density as described in Table 3.10.

Table 3.10. Atom Densities of the Absorber Compacts.

Isotope	Atoms/b-cm
^{10}B	6.3184E-03
^{11}B	2.5432E-02
C-nat	6.6685E-02
Total	9.8436E-02

The Alloy 800H cladding of the control rods has a mass density of 8.03 g/cm^3 with a composition and atom density as shown in Table 3.11.

Table 3.11. Atom Densities of the Alloy 800H Clad.

Isotope	Atoms/b-cm
C-nat	3.2210E-04
Al	6.7209E-04
Si	6.0263E-04
P	3.1225E-05
S	1.5081E-05
Ti	3.7884E-04
Cr	1.9530E-02
Mn	8.8022E-04
Fe	3.8092E-02
Ni	2.6777E-02
Cu	2.2830E-04
Total	8.7530E-02

Control Rod Columns

The IG-110 graphite fuel columns are modeled with the same physical properties as the fuel blocks in Section 3.1.3.3 and Table 3.9.

3.1.3.6 Instrumentation

Instrumentation Components

Insufficient information was available to adequately model instrumentation in the HTTR. An approximate bias with uncertainty was determined applied to the benchmark model (see Sections 2.1.2.1 and 3.1.1.1).

Instrumentation Columns

The IG-110 graphite instrumentation columns are modeled with the same physical properties as the fuel blocks in Section 3.1.3.3 and Table 3.9.

3.1.3.7 Replaceable Reflector Columns

The IG-110 replaceable reflector columns are modeled with the same physical properties as the fuel blocks in Section 3.1.3.3 and Table 3.9.

3.1.3.8 Replaceable Reflectors Blocks in Fuel Columns

The IG-110 replaceable reflector blocks are modeled with the same physical properties as the fuel blocks in Section 3.1.3.3 and Table 3.9.

3.1.3.9 Permanent Reflector

The PGX graphite permanent reflector has a mass density of 1.71789 g/cm^3 (1.76 g/cm^3 base density decreased by a provided 0.7% void fraction) and an equivalent natural-boron content of 0.000191 wt.%. The atom density and composition of the permanent reflector is shown in Table 3.12.

Table 3.12. Atom Densities of the Permanent Reflector.

Isotope	Atoms/b-cm
^{10}B	3.6372E-08
C-nat	8.6134E-02
Total	8.6134E-02

3.1.3.10 Helium Coolant

The helium coolant has an atom density of 7.2432×10^{-4} atoms/b-cm (mass density of 4.8142×10^{-3} g/cm^3) at a system pressure of 4 MPa and a temperature of 400 K (see calculations in Equation 3.1). No impurities are modeled in the coolant. Similar calculations can be performed for the densities at 420 K. These values are summarized in Table 3.13.

$$\frac{n}{V}=\frac{P\cdot N_A}{R\cdot T}=\frac{\left(4MPa\right)\cdot\left(\frac{1atm}{0.101325MPa}\right)\cdot\left(0.60221\frac{atoms\cdot cm^2}{mol\cdot b}\right)}{\left(0.082054\frac{L\cdot atm}{mol\cdot K}\right)\cdot\left(400K\right)}\cdot\left(\frac{1L}{1000cm^3}\right)=7.2432\times10^{-4}\frac{atoms}{b\cdot cm}$$

.

$$\rho=\frac{n}{V}\cdot\frac{M}{N_A}=7.2432\times10^{-4}\frac{atoms}{b\cdot cm}\cdot\frac{4.002602\frac{g}{mol}}{\left(0.60221\frac{atoms\cdot cm^2}{mol\cdot b}\right)}=4.8142\times10^{-3}\frac{g}{cm^3}. \qquad (3.1)$$

Table 3.13. Helium Coolant Density.

Case	g/cm^3	Atoms/b-cm
1	4.8142E-03	7.2432E-04
2	4.5850E-03	6.8983E-04

3.1.4 Temperature Data

The benchmark model temperature is 400 and 420 K for configurations 1 and 2, respectively.

3.1.5 Experimental and Benchmark-Model k_{eff} and / or Subcritical Parameters

The experimental k_{eff} was approximately at unity, made to delayed critical. A comprehensive bias assessment could not be performed; therefore, the experimental k_{eff} values were adjusted for the bias incurred by removing the instrumentation in the core (Table 3.1). Other biases due to model development are believed to be negligible. The uncertainty in the benchmark models (Tables 2.12 and 2.13) is the same as the uncertainty evaluated for the experimental, as the bias uncertainty for instrumentation has already been included and the uncertainty in the temperature correction bias is negligible. The benchmark eigenvalues for the annular HTTR core loadings are shown in Table 3.14.

Table 3.14. HTTR Benchmark Values.

Case	Isothermal Temperature (K)	k_{eff}	-σ	+σ
1	395.15	1.0025	0.0057	0.0068
2	418.05	1.0026	0.0057	0.0067

3.2 Benchmark-Model Specifications for Buckling and Extrapolation-Length Measurements

Buckling and extrapolation length measurements were not made.

3.3 Benchmark-Model Specifications for Spectral Characteristics Measurements

Spectral characteristics measurements were not made.

3.4 Benchmark-Model Specifications for Reactivity Effects Measurements

Reactivity effects measurements were not made.

3.5 Benchmark-Model Specifications for Reactivity Coefficient Measurements

Six isothermal temperature coefficients have been evaluated for the fully-loaded core configuration of the HTTR. The model used to obtain isothermal temperature coefficients is identical to warm critical benchmarks with the same material properties and dimensions to the cold-critical core; only the isothermal temperatures of the core and positions to which the control rods are withdrawn have changed.

3.5.1 Description of the Benchmark Model Simplifications

Simplifications of the benchmark model for determination of the reactivity effects measurements in the HTTR are identical to those of the critical fully-loaded core configuration described in Section 3.1.1.

3.5.2 Dimensions

The dimensions of the benchmark model for determination of the reactivity effects measurements in the HTTR are identical to those of the critical fully-loaded core configuration described in Section 3.1.2, except for control rod positions, which are varied as a function of temperature, as described in Section 2.5.1 (also see Figure 3.19 regarding in-core positioning of control rods with respect to core fuel).

3.5.3 Material Data

The materials of the benchmark model for determination of the reactivity effects measurements in the HTTR are identical to those of the critical fully-loaded core configuration described in Section 3.1.3.

3.5.4 Temperature Data

The reference temperatures for the isothermal temperature coefficients are in Table 3.15.

3.5.5 Experimental and Benchmark-Model for Reactivity Coefficients

The benchmark values for the isothermal temperature coefficient are in Table 3.15. The benchmark values represent the experimental values without any bias corrections. The third data point does not represent a high quality benchmark value as the coefficient does not conform to the other coefficients and it has a very large uncertainty.

Table 3.15. Benchmark Experiment Isothermal Temperature Coefficients.

Data Point	Temperature (K)	Reactivity Coefficient (% Δk/k/K)	±	1σ Uncertainty
1	346	-0.0123	±	0.0032
2	407	-0.0132	±	0.0033
3	421	-0.0217	±	0.0130
4	533	-0.0165	±	0.0029
5	642	-0.0103	±	0.0028
6	736	-0.0086	±	0.0027

3.6 Benchmark-Model Specifications for Kinetics Measurements

Kinetics measurements were not made.

3.7 Benchmark-Model Specifications for Reaction-Rate Distribution Measurements

Reaction-rate distribution measurements were not made.

3.8 Benchmark-Model Specifications for Power Distribution Measurements

Power distribution measurements were not made.

3.9 Benchmark-Model Specifications for Isotopic Measurements

Isotopic measurements were not made.

3.10 Benchmark-Model Specifications for Other Miscellaneous Types of Measurements

Other miscellaneous types of measurements were not made.

4.0 RESULTS OF SAMPLE CALCULATIONS

4.1 Results of Calculations of the Critical or Subcritical Configurations

Random particles cannot be easily modeled in MCNP. Therefore an ordered-lattice approach for modeling the benchmark was implemented, and results are provided

Eigenvalues were calculated using the benchmark model specifications of the zero-power, elevated-temperature cores with MCNP5 and ENDF/B-VII.0 neutron cross section library data (processed to the desired evaluation temperature using NJOY). All calculations are compared against the benchmark values reported in Section 3.1.5. The total uncertainty in the benchmark value of k_{eff} is taken from Section 2.1.7. The MCNP5 calculations were performed with 1,050 generations (skipping the first 50) and 50,000 neutrons per generation.

Doppler-broadened neutron cross sections were generated for ^{234}U, ^{235}U, and ^{238}U with the NJOY computer code at 400 and 420 K. These two temperatures were selected to correspond to the warm critical temperatures of 391.15 and 418.05 K, respectively. The thermal neutron scattering data [S(α,β)] for graphite and uranium dioxide were also generated with the NJOY computer code at the temperatures of 400 and 500 K. Thermal scattering data scaled linearly with temperature, and eigenvalue calculations at 420 K were corrected to the appropriate temperature. Additional uncertainty due to thermal scattering scaling was negligible.

It is currently difficult to obtain the necessary information to further improve the confidence in the benchmark model and effectively reduce the overall uncertainty; the necessary data is proprietary and its released is being restricted, because the benchmark configuration of the HTTR core is the same that is currently in operation. Once this information is made available, the HTTR benchmark can be adjusted as appropriate.

4.1.1 Ordered TRISO Lattice within the Fuel Compacts

The TRISO particles are modeled in rectangular lattices with the dimensions of 0.106 cm (length) × 0.106 cm (width) × 0.1 cm (height) to generate a volumetric packing fraction of 30% (not including the graphite overcoat) when only complete particles are placed within the compact. A cross-sectional view of the TRISO particle unit cell is shown in Figure 4.1. The graphite overcoat isn't completely represented in the lattice.

A horizontal cross section of a compact is shown in Figure 4.2. As can be seen, selective placement of TRISO particles was necessary to conserve the fuel rod mass of 188.58 g. For the current configuration, 12,987 TRISO particles are present within a standard fuel compact; this value is slightly less than the reported value of approximately 13,000.

The effective multiplication factor for configurations 1 and 2 are shown in Table 4.1, respectively. The benchmark values in Table 3.14 were adjusted to 400 and 420 K, respectively with a minor temperature adjustment (Table 3.2). Calculated values of k_{eff} differ from the adjusted benchmark model values by approximately 1.8%, which is comparable to results obtained in previous benchmark analyses: HTTR-GCR-RESR-001 and HTTR-GCR-RESR-002. Reevaluation of the HTTR model as additional information becomes available might improve the quality of this benchmark. The benchmark models are most sensitive to graphite impurities, and graphite cross section data may also contributed to the bias.

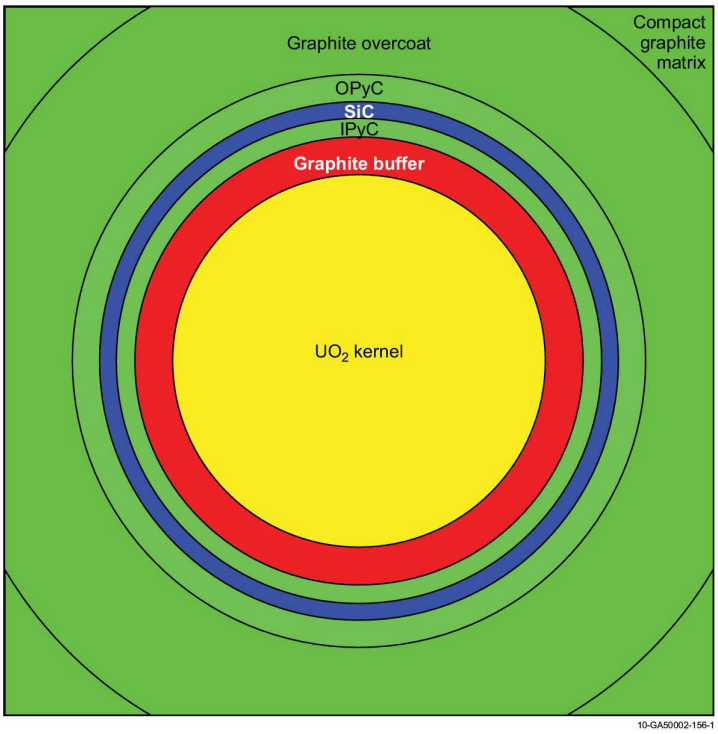

Figure 4.1. MCNP TRISO Particle Unit Cell.

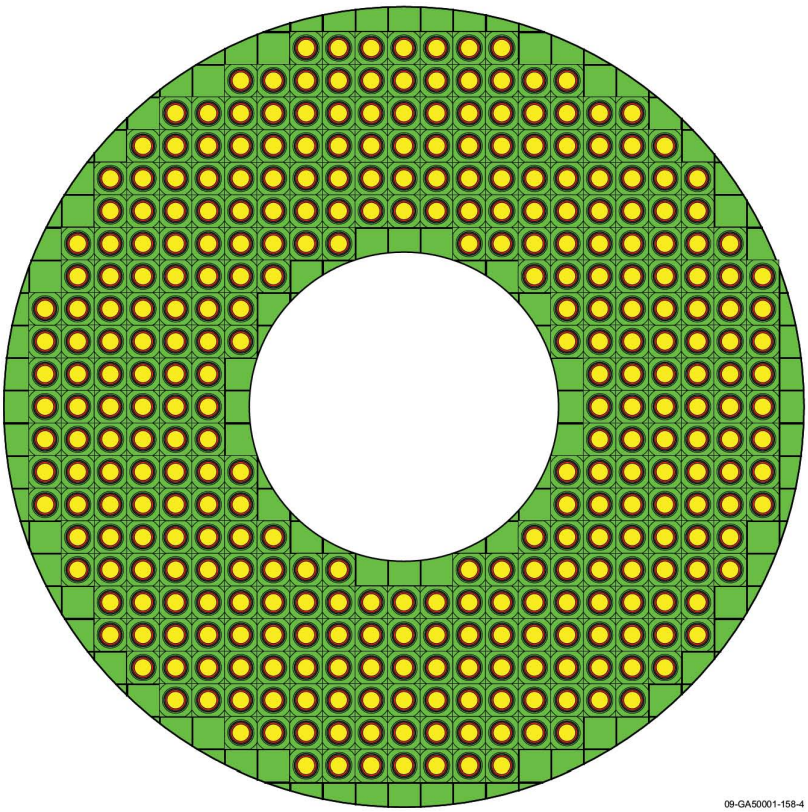

Figure 4.2. MCNP Fuel Compact (Single Particle Layer).

Table 4.1. Results for the HTTR Models using an Ordered Lattice (MCNP5 with ENDF/B-VII.0).

Configuration	Temperature (K)	Calculated k_{eff} ± σ	Benchmark k_{eff}	Uncertainty -σ (%)	Uncertainty +σ (%)	(C-E)/E (%)
1	400	1.01945 ± 0.00011	1.0019[(a)]	0.0057	0.0068	1.75
2	420	1.02009 ± 0.00011	1.0024[(a)]	0.0057	0.0067	1.77

(a) No biases have been currently evaluated for correcting the experimental k_{eff}, besides the bias for removing the reactor instrumentation in the instrumentation columns and a minor adjustment from benchmark to calculation temperatures.

4.2 Results of Buckling and Extrapolation Length Calculations

Buckling and extrapolation length measurements were not made.

4.3 Results of Spectral-Characteristics Calculations

Spectral characteristics measurements were not made.

4.4 Results of Reactivity-Effects Calculations

Reactivity effects measurements were not made.

4.5 Results of Reactivity Coefficient Calculations

Isothermal temperature coefficients were calculated using the benchmark model specifications of the zero-power, elevated-temperature cores using MCNP5 with ENDF/B-VII.0 neutron cross section library data (processed to the desired evaluation temperature using NJOY) and the same modeling approach as described in Section 4.1.1 for the TRISO particle distribution. Cross section were generated, including Doppler broadening of the uranium isotopes, with the NJOY computer code at 380, 400, 480, 580, 680, and 780 K. The thermal neutron scattering data [S(α,β)] for graphite and uranium dioxide were also generated with the NJOY computer code at the temperatures of 400, 500, 600, 700, 800, and 1000 K. Thermal scattering data scaled linearly with temperature, and eigenvalue calculations were corrected to the appropriate temperature. Additional uncertainty due to thermal scattering scaling was negligible.

Coefficients were calculated using the methods described in Section 2.5.1. All calculations are compared against the benchmark experiment values reported in Section 3.5.5. A comparison of the calculated results and benchmark values are shown in Table 4.2 and Figure 4.3. Calculated coefficients are within 2σ for the all six data points; however, the uncertainty in the third data point is very large and does not conform to the pattern of the other measurements. Unknown internal heating effects not mentioned by the authors in Ref. 1 may also contribute to the difference between benchmark experiment and calculated values at elevated temperatures. Additional unknown contributions to the uncertainty may include uncertainties in nuclear data and analysis tools and unknown experimental uncertainties in the measurement and evaluation of the isothermal temperature coefficients.

Comparison of just the last four data points indicate a trend that may or may not exist. A trend cannot be verified as the data point at 421 K has such a large uncertainty.

Table 4.2. Zero-Power Isothermal Temperature Coefficients for the HTTR.

Data Point	Temperature (K)	Benchmark Experiment α_E (% Δk/k/K)	Calculated α_C (% Δk/k/K)	$\frac{C-E}{E}(\%)$
1	346	-0.0123 ± 0.0032	-0.0116 ± 0.0002	-5.8
2	407	-0.0132 ± 0.0033	-0.0128 ± 0.0002	-3.3
3	421	-0.0217 ± 0.0130	-0.0128 ± 0.0002	-41.3
4	533	-0.0165 ± 0.0029	-0.0129 ± 0.0002	-21.7
5	642	-0.0103 ± 0.0028	-0.0126 ± 0.0002	22.1
6	736	-0.0086 ± 0.0027	-0.0121 ± 0.0002	40.1

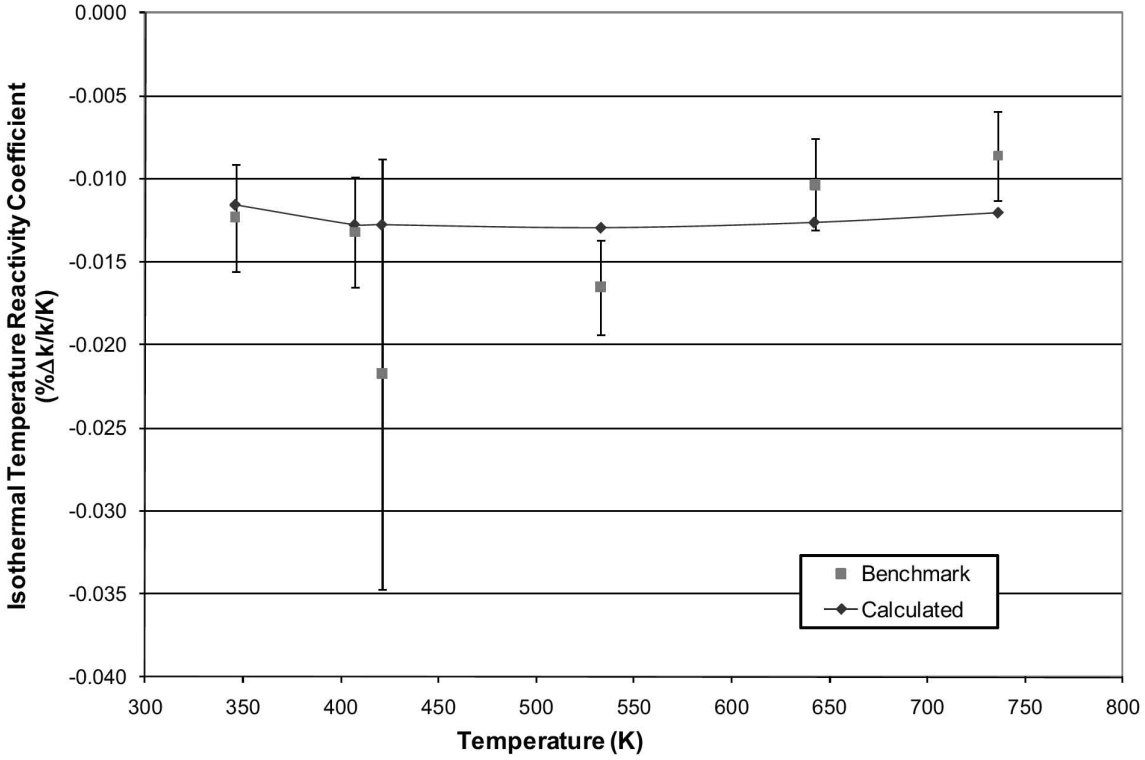

Figure 4.3. Zero-Power Isothermal Temperature Coefficients of the HTTR.

4.6 Results of Kinetics Parameter Calculations

Kinetics measurements were not made.

4.7 Results of Reaction-Rate Distribution Calculations

Reaction-rate distribution measurements were not made.

4.8 Results of Power Distribution Calculations

Power distribution measurements were not made.

4.9 Results of Isotopic Calculations

Isotopic measurements were not made.

4.10 Results of Calculations for Other Miscellaneous Types of Measurements

Other miscellaneous types of measurements were not made.

5.0 REFERENCES

1. N. Nojiri, S. Shimakawa, N. Fujimoto, and M. Goto, "Characteristic Test of Initial HTTR Core," *Nucl. Eng. Des.*, **233**: 283-290 (2004).

2. N. Fujimoto, N. Nojiri, E. Takada, K. Saito, S. Kobayashi, H. Sawahata, and S. Kokusen, "Control Rod Position and Temperature Coefficients in HTTR Power-Rise Tests – Interim Report," JAERI Tech 2000-091 (2001).

APPENDIX A: COMPUTER CODES, CROSS SECTIONS, AND TYPICAL INPUT LISTINGS

A.1 Critical Configuration

A.1.1 Name(s) of code system(s) used.

1. Monte Carlo n-Particle, version 5.1.40 (MCNP5)
2. NJOY-99.296.

A.1.2 Bibliographic references for the codes used.

1. X-5 Monte Carlo Team, "MCNP – a General Monte Carlo n-Particle Transport Code, version 5," LA-UR-03-1987, Los Alamos National Laboratory (2003).
2. R. E. MacFarlane and D. W. Muir, "The NJOY Nuclear Data Processing System Version 91," LA-12740-M (October 1994).

A.1.3 Origin of cross-section data.

The Evaluated Neutron Data File library, ENDF/B-VII.0,[a] processed by NJOY to desired temperatures.

A.1.4 Spectral calculations and data reduction methods used.

Not applicable

A.1.5 Number of energy groups or if continuous-energy cross sections are used in the different phases of the calculation.

Continuous-energy cross sections

A.1.6 Component calculations.

- Type of cell calculation – Reactor core and reflectors
- Geometry – Cylindrical
- Theory used – Not applicable
- Method used – Monte Carlo
- Calculation characteristics – histories/cycles/cycles skipped = 50,000/1,050/50
  continuous-energy cross sections

A.1.7 Other assumptions and characteristics.

Not applicable

[a] M. B. Chadwick, et al., "ENDF/B-VII.0: Next Generation Evaluated Nuclear Data Library for Nuclear Science and Technology," *Nucl. Data Sheets*, **107**: 2931-3060 (2006).

A.1.8 Typical input listings.

MCNP5 Input Deck for the 30-fuel-column core, Configuration 1, of the HTTR (T=400K):

```
HTTR 400 K Core Critical (30 fuel columns) --
c
c John Darrell Bess - Idaho National Laboratory
c Last Updated: August 11, 2010
c
c Cell Cards ******************************************************************
c --- Fuel Column ------------------------------------------------------------
c ------ TRISO Particles ------
1    1  6.9614E-02   -1 imp:n=1 u=13 tmp=3.447E-08 $ 3.4% kernel
2    13 5.5153E-02 1 -2 imp:n=1 u=13 tmp=3.447E-08 $ buffer
3    14 9.2758E-02 2 -3 imp:n=1 u=13 tmp=3.447E-08 $ IPyC
4    15 9.6122E-02 3 -4 imp:n=1 u=13 tmp=3.447E-08 $ SiC
5    16 9.2758E-02 4 -5 imp:n=1 u=13 tmp=3.447E-08 $ OPyC
6    17 8.5237E-02 5 -6 imp:n=1 u=13 tmp=3.447E-08 $ overcoat
7    18 8.5237E-02 6 901 -902 903 -904 905 -906 imp:n=1 u=13 tmp=3.447E-08 $ compact fill
11   like 1 but mat=2 u=14 rho=6.9616E-02 $ 3.9% kernel ---
12   like 2 but u=14 $ buffer
13   like 3 but u=14 $ IPyC
14   like 4 but u=14 $ SiC
15   like 5 but u=14 $ OPyC
16   like 6 but u=14 $ overcoat
17   like 7 but u=14 $ compact fill
21   like 1 but mat=3 u=15 rho=6.9617E-02 $ 4.3% kernel ---
22   like 2 but u=15 $ buffer
23   like 3 but u=15 $ IPyC
24   like 4 but u=15 $ SiC
25   like 5 but u=15 $ OPyC
26   like 6 but u=15 $ overcoat
27   like 7 but u=15 $ compact fill
31   like 1 but mat=4 u=16 rho=6.9618E-02 $ 4.8% kernel ---
32   like 2 but u=16 $ buffer
33   like 3 but u=16 $ IPyC
34   like 4 but u=16 $ SiC
35   like 5 but u=16 $ OPyC
36   like 6 but u=16 $ overcoat
37   like 7 but u=16 $ compact fill
41   like 1 but mat=5 u=17 rho=6.9619E-02 $ 5.2% kernel ---
42   like 2 but u=17 $ buffer
43   like 3 but u=17 $ IPyC
44   like 4 but u=17 $ SiC
45   like 5 but u=17 $ OPyC
46   like 6 but u=17 $ overcoat
47   like 7 but u=17 $ compact fill
51   like 1 but mat=6 u=18 rho=6.9622E-02 $ 5.9% kernel ---
52   like 2 but u=18 $ buffer
53   like 3 but u=18 $ IPyC
54   like 4 but u=18 $ SiC
55   like 5 but u=18 $ OPyC
56   like 6 but u=18 $ overcoat
57   like 7 but u=18 $ compact fill
61   like 1 but mat=7 u=19 rho=6.9623E-02 $ 6.3% kernel ---
62   like 2 but u=19 $ buffer
63   like 3 but u=19 $ IPyC
64   like 4 but u=19 $ SiC
65   like 5 but u=19 $ OPyC
66   like 6 but u=19 $ overcoat
67   like 7 but u=19 $ compact fill
71   like 1 but mat=8 u=20 rho=6.9624E-02 $ 6.7% kernel ---
72   like 2 but u=20 $ buffer
73   like 3 but u=20 $ IPyC
74   like 4 but u=20 $ SiC
75   like 5 but u=20 $ OPyC
76   like 6 but u=20 $ overcoat
77   like 7 but u=20 $ compact fill
81   like 1 but mat=9 u=21 rho=6.9625E-02 $ 7.2% kernel ---
82   like 2 but u=21 $ buffer
83   like 3 but u=21 $ IPyC
84   like 4 but u=21 $ SiC
85   like 5 but u=21 $ OPyC
86   like 6 but u=21 $ overcoat
```

```
87   like 7 but u=21 $ compact fill
91   like 1 but mat=10 u=22 rho=6.9628E-02 $ 7.9% kernel ---
92   like 2 but u=22 $ buffer
93   like 3 but u=22 $ IPyC
94   like 4 but u=22 $ SiC
95   like 5 but u=22 $ OPyC
96   like 6 but u=22 $ overcoat
97   like 7 but u=22 $ compact fill
101  like 1 but mat=11 u=23 rho=6.9632E-02 $ 9.4% kernel ---
102  like 2 but u=23 $ buffer
103  like 3 but u=23 $ IPyC
104  like 4 but u=23 $ SiC
105  like 5 but u=23 $ OPyC
106  like 6 but u=23 $ overcoat
107  like 7 but u=23 $ compact fill
111  like 1 but mat=12 u=24 rho=6.9634E-02 $ 9.9% kernel ---
112  like 2 but u=24 $ buffer
113  like 3 but u=24 $ IPyC
114  like 4 but u=24 $ SiC
115  like 5 but u=24 $ OPyC
116  like 6 but u=24 $ overcoat
117  like 7 but u=24 $ compact fill
c
c ------ Compacts ------
120  18 8.5237E-02 901 -902 903 -904 905 -906 imp:n=1 u=300 tmp=3.447E-08 $ compact fill
163  0 911 -912 913 -914 915 -916 imp:n=1 u=25 lat=1 tmp=3.447E-08
     fill=-13:13 -13:13 0:0
     300 26r 300 26r 300 9r 13 6r 300 9r 300 7r 13 10r 300 7r
     300 5r 13 14r 300 5r 300 4r 13 16r 300 4r 300 3r 13 18r 300 3r
     300 3r 13 18r 300 3r 300 2r 13 8r 300 2r 13 8r 300 2r
     300 1r 13 7r 300 6r 13 6r 300 2r 300 1r 13 6r 300 8r 13 6r 300 1r
     300 1r 13 6r 300 8r 13 6r 300 1r 300 1r 13 5r 300 10r 13 5r 300 1r
     300 1r 13 5r 300 10r 13 5r 300 1r 300 1r 13 5r 300 10r 13 5r 300 1r
     300 1r 13 6r 300 8r 13 6r 300 1r 300 1r 13 6r 300 8r 13 6r 300 1r
     300 2r 13 6r 300 6r 13 6r 300 2r 300 2r 13 8r 300 2r 13 8r 300 2r
     300 3r 13 18r 300 3r 300 3r 13 18r 300 3r 300 4r 13 16r 300 4r
     300 5r 13 14r 300 5r 300 7r 13 10r 300 7r 300 9r 13 6r 300 9r
     300 26r 300 26r
164  like 163 but u=26 fill=-13:13 -13:13 0:0
     300 26r 300 26r 300 9r 14 6r 300 9r 300 7r 14 10r 300 7r
     300 5r 14 14r 300 5r 300 4r 14 16r 300 4r 300 3r 14 18r 300 3r
     300 3r 14 18r 300 3r 300 2r 14 8r 300 2r 14 8r 300 2r
     300 1r 14 7r 300 6r 14 6r 300 2r 300 1r 14 6r 300 8r 14 6r 300 1r
     300 1r 14 6r 300 8r 14 6r 300 1r 300 1r 14 5r 300 10r 14 5r 300 1r
     300 1r 14 5r 300 10r 14 5r 300 1r 300 1r 14 5r 300 10r 14 5r 300 1r
     300 1r 14 6r 300 8r 14 6r 300 1r 300 1r 14 6r 300 8r 14 6r 300 1r
     300 2r 14 6r 300 6r 14 6r 300 2r 300 2r 14 8r 300 2r 14 8r 300 2r
     300 3r 14 18r 300 3r 300 3r 14 18r 300 3r 300 4r 14 16r 300 4r
     300 5r 14 14r 300 5r 300 7r 14 10r 300 7r 300 9r 14 6r 300 9r
     300 26r 300 26r
165  like 163 but u=27 fill=-13:13 -13:13 0:0
     300 26r 300 26r 300 9r 15 6r 300 9r 300 7r 15 10r 300 7r
     300 5r 15 14r 300 5r 300 4r 15 16r 300 4r 300 3r 15 18r 300 3r
     300 3r 15 18r 300 3r 300 2r 15 8r 300 2r 15 8r 300 2r
     300 1r 15 7r 300 6r 15 6r 300 2r 300 1r 15 6r 300 8r 15 6r 300 1r
     300 1r 15 6r 300 8r 15 6r 300 1r 300 1r 15 5r 300 10r 15 5r 300 1r
     300 1r 15 5r 300 10r 15 5r 300 1r 300 1r 15 5r 300 10r 15 5r 300 1r
     300 1r 15 6r 300 8r 15 6r 300 1r 300 1r 15 6r 300 8r 15 6r 300 1r
     300 2r 15 6r 300 6r 15 6r 300 2r 300 2r 15 8r 300 2r 15 8r 300 2r
     300 3r 15 18r 300 3r 300 3r 15 18r 300 3r 300 4r 15 16r 300 4r
     300 5r 15 14r 300 5r 300 7r 15 10r 300 7r 300 9r 15 6r 300 9r
     300 26r 300 26r
166  like 163 but u=28 fill=-13:13 -13:13 0:0
     300 26r 300 26r 300 9r 16 6r 300 9r 300 7r 16 10r 300 7r
     300 5r 16 14r 300 5r 300 4r 16 16r 300 4r 300 3r 16 18r 300 3r
     300 3r 16 18r 300 3r 300 2r 16 8r 300 2r 16 8r 300 2r
     300 1r 16 7r 300 6r 16 6r 300 2r 300 1r 16 6r 300 8r 16 6r 300 1r
     300 1r 16 6r 300 8r 16 6r 300 1r 300 1r 16 5r 300 10r 16 5r 300 1r
     300 1r 16 5r 300 10r 16 5r 300 1r 300 1r 16 5r 300 10r 16 5r 300 1r
     300 1r 16 6r 300 8r 16 6r 300 1r 300 1r 16 6r 300 8r 16 6r 300 1r
     300 2r 16 6r 300 6r 16 6r 300 2r 300 2r 16 8r 300 2r 16 8r 300 2r
     300 3r 16 18r 300 3r 300 3r 16 18r 300 3r 300 4r 16 16r 300 4r
     300 5r 16 14r 300 5r 300 7r 16 10r 300 7r 300 9r 16 6r 300 9r
     300 26r 300 26r
167  like 163 but u=29 fill=-13:13 -13:13 0:0
     300 26r 300 26r 300 9r 17 6r 300 9r 300 7r 17 10r 300 7r
```

```
     300 5r 17 14r 300 5r 300 4r 17 16r 300 4r 300 3r 17 18r 300 3r
     300 3r 17 18r 300 3r 300 2r 17 8r 300 2r 17 8r 300 2r
     300 1r 17 7r 300 6r 17 6r 300 2r 300 1r 17 6r 300 8r 17 6r 300 1r
     300 1r 17 6r 300 8r 17 6r 300 1r 300 1r 17 5r 300 10r 17 5r 300 1r
     300 1r 17 5r 300 10r 17 5r 300 1r 300 1r 17 5r 300 10r 17 5r 300 1r
     300 1r 17 6r 300 8r 17 6r 300 1r 300 1r 17 6r 300 8r 17 6r 300 1r
     300 2r 17 6r 300 6r 17 6r 300 2r 300 2r 17 8r 300 2r 17 8r 300 2r
     300 3r 17 18r 300 3r 300 3r 17 18r 300 3r 300 4r 17 16r 300 4r
     300 5r 17 14r 300 5r 300 7r 17 10r 300 7r 300 9r 17 6r 300 9r
     300 26r 300 26r
168  like 163 but u=30 fill=-13:13 -13:13 0:0
     300 26r 300 26r 300 9r 18 6r 300 9r 300 7r 18 10r 300 7r
     300 5r 18 14r 300 5r 300 4r 18 16r 300 4r 300 3r 18 18r 300 3r
     300 3r 18 18r 300 3r 300 2r 18 8r 300 2r 18 8r 300 2r
     300 1r 18 7r 300 6r 18 6r 300 2r 300 1r 18 6r 300 8r 18 6r 300 1r
     300 1r 18 6r 300 8r 18 6r 300 1r 300 1r 18 5r 300 10r 18 5r 300 1r
     300 1r 18 5r 300 10r 18 5r 300 1r 300 1r 18 5r 300 10r 18 5r 300 1r
     300 1r 18 6r 300 8r 18 6r 300 1r 300 1r 18 6r 300 8r 18 6r 300 1r
     300 2r 18 6r 300 6r 18 6r 300 2r 300 2r 18 8r 300 2r 18 8r 300 2r
     300 3r 18 18r 300 3r 300 3r 18 18r 300 3r 300 4r 18 16r 300 4r
     300 5r 18 14r 300 5r 300 7r 18 10r 300 7r 300 9r 18 6r 300 9r
     300 26r 300 26r
169  like 163 but u=31 fill=-13:13 -13:13 0:0
     300 26r 300 26r 300 9r 19 6r 300 9r 300 7r 19 10r 300 7r
     300 5r 19 14r 300 5r 300 4r 19 16r 300 4r 300 3r 19 18r 300 3r
     300 3r 19 18r 300 3r 300 2r 19 8r 300 2r 19 8r 300 2r
     300 1r 19 7r 300 6r 19 6r 300 2r 300 1r 19 6r 300 8r 19 6r 300 1r
     300 1r 19 6r 300 8r 19 6r 300 1r 300 1r 19 5r 300 10r 19 5r 300 1r
     300 1r 19 5r 300 10r 19 5r 300 1r 300 1r 19 5r 300 10r 19 5r 300 1r
     300 1r 19 6r 300 8r 19 6r 300 1r 300 1r 19 6r 300 8r 19 6r 300 1r
     300 2r 19 6r 300 6r 19 6r 300 2r 300 2r 19 8r 300 2r 19 8r 300 2r
     300 3r 19 18r 300 3r 300 3r 19 18r 300 3r 300 4r 19 16r 300 4r
     300 5r 19 14r 300 5r 300 7r 19 10r 300 7r 300 9r 19 6r 300 9r
     300 26r 300 26r
180  like 163 but u=32 fill=-13:13 -13:13 0:0
     300 26r 300 26r 300 9r 20 6r 300 9r 300 7r 20 10r 300 7r
     300 5r 20 14r 300 5r 300 4r 20 16r 300 4r 300 3r 20 18r 300 3r
     300 3r 20 18r 300 3r 300 2r 20 8r 300 2r 20 8r 300 2r
     300 1r 20 7r 300 6r 20 6r 300 2r 300 1r 20 6r 300 8r 20 6r 300 1r
     300 1r 20 6r 300 8r 20 6r 300 1r 300 1r 20 5r 300 10r 20 5r 300 1r
     300 1r 20 5r 300 10r 20 5r 300 1r 300 1r 20 5r 300 10r 20 5r 300 1r
     300 1r 20 6r 300 8r 20 6r 300 1r 300 1r 20 6r 300 8r 20 6r 300 1r
     300 2r 20 6r 300 6r 20 6r 300 2r 300 2r 20 8r 300 2r 20 8r 300 2r
     300 3r 20 18r 300 3r 300 3r 20 18r 300 3r 300 4r 20 16r 300 4r
     300 5r 20 14r 300 5r 300 7r 20 10r 300 7r 300 9r 20 6r 300 9r
     300 26r 300 26r
181  like 163 but u=33 fill=-13:13 -13:13 0:0
     300 26r 300 26r 300 9r 21 6r 300 9r 300 7r 21 10r 300 7r
     300 5r 21 14r 300 5r 300 4r 21 16r 300 4r 300 3r 21 18r 300 3r
     300 3r 21 18r 300 3r 300 2r 21 8r 300 2r 21 8r 300 2r
     300 1r 21 7r 300 6r 21 6r 300 2r 300 1r 21 6r 300 8r 21 6r 300 1r
     300 1r 21 6r 300 8r 21 6r 300 1r 300 1r 21 5r 300 10r 21 5r 300 1r
     300 1r 21 5r 300 10r 21 5r 300 1r 300 1r 21 5r 300 10r 21 5r 300 1r
     300 1r 21 6r 300 8r 21 6r 300 1r 300 1r 21 6r 300 8r 21 6r 300 1r
     300 2r 21 6r 300 6r 21 6r 300 2r 300 2r 21 8r 300 2r 21 8r 300 2r
     300 3r 21 18r 300 3r 300 3r 21 18r 300 3r 300 4r 21 16r 300 4r
     300 5r 21 14r 300 5r 300 7r 21 10r 300 7r 300 9r 21 6r 300 9r
     300 26r 300 26r
182  like 163 but u=34 fill=-13:13 -13:13 0:0
     300 26r 300 26r 300 9r 22 6r 300 9r 300 7r 22 10r 300 7r
     300 5r 22 14r 300 5r 300 4r 22 16r 300 4r 300 3r 22 18r 300 3r
     300 3r 22 18r 300 3r 300 2r 22 8r 300 2r 22 8r 300 2r
     300 1r 22 7r 300 6r 22 6r 300 2r 300 1r 22 6r 300 8r 22 6r 300 1r
     300 1r 22 6r 300 8r 22 6r 300 1r 300 1r 22 5r 300 10r 22 5r 300 1r
     300 1r 22 5r 300 10r 22 5r 300 1r 300 1r 22 5r 300 10r 22 5r 300 1r
     300 1r 22 6r 300 8r 22 6r 300 1r 300 1r 22 6r 300 8r 22 6r 300 1r
     300 2r 22 6r 300 6r 22 6r 300 2r 300 2r 22 8r 300 2r 22 8r 300 2r
     300 3r 22 18r 300 3r 300 3r 22 18r 300 3r 300 4r 22 16r 300 4r
     300 5r 22 14r 300 5r 300 7r 22 10r 300 7r 300 9r 22 6r 300 9r
     300 26r 300 26r
183  like 163 but u=35 fill=-13:13 -13:13 0:0
     300 26r 300 26r 300 9r 23 6r 300 9r 300 7r 23 10r 300 7r
     300 5r 23 14r 300 5r 300 4r 23 16r 300 4r 300 3r 23 18r 300 3r
     300 3r 23 18r 300 3r 300 2r 23 8r 300 2r 23 8r 300 2r
     300 1r 23 7r 300 6r 23 6r 300 2r 300 1r 23 6r 300 8r 23 6r 300 1r
     300 1r 23 6r 300 8r 23 6r 300 1r 300 1r 23 5r 300 10r 23 5r 300 1r
```

```
     300 1r 23 5r 300 10r 23 5r 300 1r 300 1r 23 5r 300 10r 23 5r 300 1r
     300 1r 23 6r 300 8r 23 6r 300 1r 300 1r 23 6r 300 8r 23 6r 300 1r
     300 2r 23 6r 300 6r 23 6r 300 2r 300 2r 23 8r 300 2r 23 8r 300 2r
     300 3r 23 18r 300 3r 300 3r 23 18r 300 3r 300 4r 23 16r 300 4r
     300 5r 23 14r 300 5r 300 7r 23 10r 300 7r 300 9r 23 6r 300 9r
     300 26r 300 26r
184  like 163 but u=36 fill=-13:13 -13:13 0:0
     300 26r 300 26r 300 9r 24 6r 300 9r 300 7r 24 10r 300 7r
     300 5r 24 14r 300 5r 300 4r 24 16r 300 4r 300 3r 24 18r 300 3r
     300 3r 24 18r 300 3r 300 2r 24 8r 300 2r 24 8r 300 2r
     300 1r 24 7r 300 6r 24 6r 300 2r 300 1r 24 6r 300 8r 24 6r 300 1r
     300 1r 24 6r 300 8r 24 6r 300 1r 300 1r 24 5r 300 10r 24 5r 300 1r
     300 1r 24 5r 300 10r 24 5r 300 1r 300 1r 24 5r 300 10r 24 5r 300 1r
     300 1r 24 6r 300 8r 24 6r 300 1r 300 1r 24 6r 300 8r 24 6r 300 1r
     300 2r 24 6r 300 6r 24 6r 300 2r 300 2r 24 8r 300 2r 24 8r 300 2r
     300 3r 24 18r 300 3r 300 3r 24 18r 300 3r 300 4r 24 16r 300 4r
     300 5r 24 14r 300 5r 300 7r 24 10r 300 7r 300 9r 24 6r 300 9r
     300 26r 300 26r
9163 0 921 -922 923 -924 925 -926 imp:n=1 u=925 lat=1 tmp=3.447E-08 fill=25
9164 like 9163 but u=926 fill=26
9165 like 9163 but u=927 fill=27
9166 like 9163 but u=928 fill=28
9167 like 9163 but u=929 fill=29
9168 like 9163 but u=930 fill=30
9169 like 9163 but u=931 fill=31
9180 like 9163 but u=932 fill=32
9181 like 9163 but u=933 fill=33
9182 like 9163 but u=934 fill=34
9183 like 9163 but u=935 fill=35
9184 like 9163 but u=936 fill=36
185  0 12 -13 imp:n=1 u=37 tmp=3.447E-08 fill=925
186  like 185 but u=38 fill=926
187  like 185 but u=39 fill=927
188  like 185 but u=40 fill=928
189  like 185 but u=41 fill=929
190  like 185 but u=42 fill=930
191  like 185 but u=43 fill=931
192  like 185 but u=44 fill=932
193  like 185 but u=45 fill=933
194  like 185 but u=46 fill=934
195  like 185 but u=47 fill=935
196  like 185 but u=48 fill=936
c
c ------ Fuel Pins ------
251  27 7.2432E-04 -12 imp:n=1 u=37 tmp=3.447E-08 $ central hole
252  like 251 but u=38
253  like 251 but u=39
254  like 251 but u=40
255  like 251 but u=41
256  like 251 but u=42
257  like 251 but u=43
258  like 251 but u=44
259  like 251 but u=45
260  like 251 but u=46
261  like 251 but u=47
262  like 251 but u=48
263  27 7.2432E-04 13 -21 imp:n=1 u=37 tmp=3.447E-08 $ annulus between compact and sleeve
264  like 263 but u=38
265  like 263 but u=39
266  like 263 but u=40
267  like 263 but u=41
268  like 263 but u=42
269  like 263 but u=43
270  like 263 but u=44
271  like 263 but u=45
272  like 263 but u=46
273  like 263 but u=47
274  like 263 but u=48
275  19 8.8747E-02 21 -22 imp:n=1 u=37 tmp=3.447E-08 $ graphite sleeve
1275 like 275 but u=38
276  like 275 but u=39
277  like 275 but u=40
278  like 275 but u=41
279  like 275 but u=42
280  like 275 but u=43
281  like 275 but u=44
```

```
282  like 275 but u=45
283  like 275 but u=46
284  like 275 but u=47
285  like 275 but u=48
c
c ------ Coolant Channels ------
286  27 7.2432E-04 22 -31 imp:n=1 u=37 tmp=3.447E-08 $ annulus between sleeve and block
287  like 286 but u=38
288  like 286 but u=39
289  like 286 but u=40
290  like 286 but u=41
291  like 286 but u=42
292  like 286 but u=43
293  like 286 but u=44
294  like 286 but u=45
295  like 286 but u=46
296  like 286 but u=47
297  like 286 but u=48
298  25 8.7804E-02 31 imp:n=1 u=37 tmp=3.447E-08 $ graphite block
299  like 298 but u=38
300  like 298 but u=39
301  like 298 but u=40
302  like 298 but u=41
303  like 298 but u=42
304  like 298 but u=43
305  like 298 but u=44
306  like 298 but u=45
307  like 298 but u=46
308  like 298 but u=47
309  like 298 but u=48
c
c ------ BP Pins ------
351  20 9.0451E-02 -41 imp:n=1 u=50 tmp=3.447E-08 $ 2.0%
352  like 351 but mat=21 rho=9.0501E-02 u=51 $ 2.5%
353  22 8.8747E-02 -42 imp:n=1 u=50 tmp=3.447E-08 $ graphite disks
354  like 353 but u=51
355  20 9.0451E-02 -43 imp:n=1 u=50 tmp=3.447E-08 $ 2.0%
356  like 355 but mat=21 rho=9.0501E-02 u=51 $ 2.5%
357  27 7.2432E-04 41 42 43 -44 imp:n=1 u=50 tmp=3.447E-08 $ pin gap
358  like 357 but u=51
359  27 7.2432E-04 -44 imp:n=1 u=52 tmp=3.447E-08 $ empty pin position
360  25 8.7804E-02 44 imp:n=1 u=50 tmp=3.447E-08 $ graphite block
361  like 360 but u=51
362  like 360 but u=52
c
c ------ Blocks ------
401  25 8.7804E-02 -501 imp:n=1 u=61 lat=2 tmp=3.447E-08 fill= -5:5 -5:5 0:0 $ Zone 1 Lvl 4/5
     61 10r
     61 10r
     61  4r       50  37  37  37       61 1r
     61  3r     37  37  37  37  37     61 1r
     61  2r   37  37  37  37  37  37   61 1r
     61  1r 37  37  37  61  37  37  52 61 1r
     61  1r   37  37  37  37  37  37   61 2r
     61  1r     37  37  37  37  37     61 3r
     61  1r       50  37  37  37       61 4r
     61 10r
     61 10r
402  25 8.7804E-02 -501 imp:n=1 u=62 lat=2 tmp=3.447E-08 fill= -5:5 -5:5 0:0 $ Zone 1 Lvl 3
     62 10r
     62 10r
     62  4r       51  39  39  39       62 1r
     62  3r     39  39  39  39  39     62 1r
     62  2r   39  39  39  39  39  39   62 1r
     62  1r 39  39  39  62  39  39  52 62 1r
     62  1r   39  39  39  39  39  39   62 2r
     62  1r     39  39  39  39  39     62 3r
     62  1r       51  39  39  39       62 4r
     62 10r
     62 10r
403  25 8.7804E-02 -501 imp:n=1 u=63 lat=2 tmp=3.447E-08 fill= -5:5 -5:5 0:0 $ Zone 1 Lvl 2
     63 10r
     63 10r
     63  4r       51  41  41  41       63 1r
     63  3r     41  41  41  41  41     63 1r
     63  2r   41  41  41  41  41  41   63 1r
```

```
     63  1r 41  41  41  63  41  41  52 63 1r
     63  1r   41  41  41  41  41  41   63 2r
     63  1r     41  41  41  41  41     63 3r
     63  1r       51  41  41  41       63 4r
     63 10r
     63 10r
404  25 8.7804E-02 -501 imp:n=1 u=64 lat=2 tmp=3.447E-08 fill= -5:5 -5:5 0:0 $ Zone 1 Lvl 1
     64 10r
     64 10r
     64  4r       50  44  44  44       64 1r
     64  3r     44  44  44  44  44     64 1r
     64  2r   44  44  44  44  44  44   64 1r
     64  1r 44  44  44  64  44  44  52 64 1r
     64  1r   44  44  44  44  44  44   64 2r
     64  1r     44  44  44  44  44     64 3r
     64  1r       50  44  44  44       64 4r
     64 10r
     64 10r
405  25 8.7804E-02 -501 imp:n=1 u=65 lat=2 tmp=3.447E-08 fill= -5:5 -5:5 0:0 $ Zone 2 Lvl 4/5
     65 10r
     65 10r
     65  4r       50  38  38  38       65 1r
     65  3r     38  38  38  38  38     65 1r
     65  2r   38  38  38  38  38  38   65 1r
     65  1r 38  38  38  65  38  38  52 65 1r
     65  1r   38  38  38  38  38  38   65 2r
     65  1r     38  38  38  38  38     65 3r
     65  1r       50  38  38  38       65 4r
     65 10r
     65 10r
406  25 8.7804E-02 -501 imp:n=1 u=66 lat=2 tmp=3.447E-08 fill= -5:5 -5:5 0:0 $ Zone 2 Lvl 3
     66 10r
     66 10r
     66  4r       51  41  41  41       66 1r
     66  3r     41  41  41  41  41     66 1r
     66  2r   41  41  41  41  41  41   66 1r
     66  1r 41  41  41  66  41  41  52 66 1r
     66  1r   41  41  41  41  41  41   66 2r
     66  1r     41  41  41  41  41     66 3r
     66  1r       51  41  41  41       66 4r
     66 10r
     66 10r
407  25 8.7804E-02 -501 imp:n=1 u=67 lat=2 tmp=3.447E-08 fill= -5:5 -5:5 0:0 $ Zone 2 Lvl 2
     67 10r
     67 10r
     67  4r       51  43  43  43       67 1r
     67  3r     43  43  43  43  43     67 1r
     67  2r   43  43  43  43  43  43   67 1r
     67  1r 43  43  43  67  43  43  52 67 1r
     67  1r   43  43  43  43  43  43   67 2r
     67  1r     43  43  43  43  43     67 3r
     67  1r       51  43  43  43       67 4r
     67 10r
     67 10r
408  25 8.7804E-02 -501 imp:n=1 u=68 lat=2 tmp=3.447E-08 fill= -5:5 -5:5 0:0 $ Zone 2 Lvl 1
     68 10r
     68 10r
     68  4r       50  46  46  46       68 1r
     68  3r     46  46  46  46  46     68 1r
     68  2r   46  46  46  46  46  46   68 1r
     68  1r 46  46  46  68  46  46  52 68 1r
     68  1r   46  46  46  46  46  46   68 2r
     68  1r     46  46  46  46  46     68 3r
     68  1r       50  46  46  46       68 4r
     68 10r
     68 10r
409  25 8.7804E-02 -501 imp:n=1 u=69 lat=2 tmp=3.447E-08 fill= -5:5 -5:5 0:0 $ Zone 3 Lvl 4/5
     69 10r
     69 10r
     69  4r       50  39  39  69       69 1r
     69  3r     39  39  39  39  39     69 1r
     69  2r   39  39  39  39  39  39   69 1r
     69  1r 39  39  39  69  39  39  52 69 1r
     69  1r   39  39  39  39  39  39   69 2r
     69  1r     39  39  39  39  39     69 3r
     69  1r       50  39  39  69       69 4r
```

```
     69 10r
     69 10r
410  25 8.7804E-02 -501 imp:n=1 u=70 lat=2 tmp=3.447E-08 fill= -5:5 -5:5 0:0 $ Zone 3 Lvl 3
     70 10r
     70 10r
     70  4r       51  42  42  70       70 1r
     70  3r     42  42  42  42  42     70 1r
     70  2r   42  42  42  42  42  42   70 1r
     70  1r 42  42  42  70  42  42  52 70 1r
     70  1r   42  42  42  42  42  42   70 2r
     70  1r     42  42  42  42  42     70 3r
     70  1r       51  42  42  70       70 4r
     70 10r
     70 10r
411  25 8.7804E-02 -501 imp:n=1 u=71 lat=2 tmp=3.447E-08 fill= -5:5 -5:5 0:0 $ Zone 3 Lvl 2
     71 10r
     71 10r
     71  4r       51  45  45  71       71 1r
     71  3r     45  45  45  45  45     71 1r
     71  2r   45  45  45  45  45  45   71 1r
     71  1r 45  45  45  71  45  45  52 71 1r
     71  1r   45  45  45  45  45  45   71 2r
     71  1r     45  45  45  45  45     71 3r
     71  1r       51  45  45  71       71 4r
     71 10r
     71 10r
412  25 8.7804E-02 -501 imp:n=1 u=72 lat=2 tmp=3.447E-08 fill= -5:5 -5:5 0:0 $ Zone 3 Lvl 1
     72 10r
     72 10r
     72  4r       50  47  47  72       72 1r
     72  3r     47  47  47  47  47     72 1r
     72  2r   47  47  47  47  47  47   72 1r
     72  1r 47  47  47  72  47  47  52 72 1r
     72  1r   47  47  47  47  47  47   72 2r
     72  1r     47  47  47  47  47     72 3r
     72  1r       50  47  47  72       72 4r
     72 10r
     72 10r
413  25 8.7804E-02 -501 imp:n=1 u=73 lat=2 tmp=3.447E-08 fill= -5:5 -5:5 0:0 $ Zone 4 Lvl 4/5
     73 10r
     73 10r
     73  4r       50  40  40  73       73 1r
     73  3r     40  40  40  40  40     73 1r
     73  2r   40  40  40  40  40  40   73 1r
     73  1r 40  40  40  73  40  40  52 73 1r
     73  1r   40  40  40  40  40  40   73 2r
     73  1r     40  40  40  40  40     73 3r
     73  1r       50  40  40  73       73 4r
     73 10r
     73 10r
414  25 8.7804E-02 -501 imp:n=1 u=74 lat=2 tmp=3.447E-08 fill= -5:5 -5:5 0:0 $ Zone 4 Lvl 3
     74 10r
     74 10r
     74  4r       51  43  43  74       74 1r
     74  3r     43  43  43  43  43     74 1r
     74  2r   43  43  43  43  43  43   74 1r
     74  1r 43  43  43  74  43  43  52 74 1r
     74  1r   43  43  43  43  43  43   74 2r
     74  1r     43  43  43  43  43     74 3r
     74  1r       51  43  43  74       74 4r
     74 10r
     74 10r
415  25 8.7804E-02 -501 imp:n=1 u=75 lat=2 tmp=3.447E-08 fill= -5:5 -5:5 0:0 $ Zone 4 Lvl 2
     75 10r
     75 10r
     75  4r       51  46  46  75       75 1r
     75  3r     46  46  46  46  46     75 1r
     75  2r   46  46  46  46  46  46   75 1r
     75  1r 46  46  46  75  46  46  52 75 1r
     75  1r   46  46  46  46  46  46   75 2r
     75  1r     46  46  46  46  46     75 3r
     75  1r       51  46  46  75       75 4r
     75 10r
     75 10r
416  25 8.7804E-02 -501 imp:n=1 u=76 lat=2 tmp=3.447E-08 fill= -5:5 -5:5 0:0 $ Zone 4 Lvl 1
     76 10r
```

```
     76 10r
     76  4r       50  48  48  76       76 1r
     76  3r     48  48  48  48  48     76 1r
     76  2r   48  48  48  48  48  48   76 1r
     76  1r 48  48  48  76  48  48  52 76 1r
     76  1r   48  48  48  48  48  48   76 2r
     76  1r     48  48  48  48  48     76 3r
     76  1r       50  48  48  76       76 4r
     76 10r
     76 10r
451  0 -502 imp:n=1 u=81 tmp=3.447E-08 fill=61
452  like 451 but u=82 fill=62
453  like 451 but u=83 fill=63
454  like 451 but u=84 fill=64
455  like 451 but u=85 fill=65
456  like 451 but u=86 fill=66
457  like 451 but u=87 fill=67
458  like 451 but u=88 fill=68
459  like 451 but u=89 fill=69
460  like 451 but u=90 fill=70
461  like 451 but u=91 fill=71
462  like 451 but u=92 fill=72
463  like 451 but u=93 fill=73
464  like 451 but u=94 fill=74
465  like 451 but u=95 fill=75
466  like 467 but u=96 fill=76
467  27 7.2432E-04 502 imp:n=1 u=81 tmp=3.447E-08
468  like 467 but u=82
469  like 467 but u=83
470  like 467 but u=84
471  like 467 but u=85
472  like 467 but u=86
473  like 467 but u=87
474  like 467 but u=88
475  like 467 but u=89
476  like 467 but u=90
477  like 467 but u=91
478  like 467 but u=92
479  like 467 but u=93
480  like 467 but u=94
481  like 467 but u=95
482  like 467 but u=96
c
c ------ Reflectors ------
483  27 7.2432E-04 -201 imp:n=1 u=97 tmp=3.447E-08 $ coolant channels
484  25 8.7804E-02  201 imp:n=1 u=97 tmp=3.447E-08 $ graphite block
485  25 8.7804E-02 -501 imp:n=1 u=98 lat=2 tmp=3.447E-08 fill= -5:5 -5:5 0:0 $ 33-hole
     98 10r
     98 10r
     98  4r       98  97  97  97       98 1r
     98  3r     97  97  97  97  97     98 1r
     98  2r   97  97  97  97  97  97   98 1r
     98  1r 97  97  97  98  97  97  98 98 1r
     98  1r   97  97  97  97  97  97   98 2r
     98  1r     97  97  97  97  97     98 3r
     98  1r       98  97  97  97       98 4r
     98 10r
     98 10r
486  25 8.7804E-02 -501 imp:n=1 u=99 lat=2 tmp=3.447E-08 fill= -5:5 -5:5 0:0 $ 31-hole
     99 10r
     99 10r
     99  4r       99  97  97  99       99 1r
     99  3r     97  97  97  97  97     99 1r
     99  2r   97  97  97  97  97  97   99 1r
     99  1r 97  97  97  99  97  97  99 99 1r
     99  1r   97  97  97  97  97  97   99 2r
     99  1r     97  97  97  97  97     99 3r
     99  1r       99  97  97  99       99 4r
     99 10r
     99 10r
489  0 -502 imp:n=1 u=100 tmp=3.447E-08 fill=98
490  0 -502 imp:n=1 u=101 tmp=3.447E-08 fill=99
491  like 467 but u=100
492  like 467 but u=101
c
c ------ Columns ------
```

```
501  27 7.2432E-04 -503 imp:n=1 u=121 lat=2 tmp=3.447E-08 fill= -1:1 -1:1 -5:5 $ Zone 1
     121 121 121 121 121 121 121 121 121
     121 121 121 121 100 121 121 121 121
     121 121 121 121 100 121 121 121 121
     121 121 121 121  81 121 121 121 121
     121 121 121 121  81 121 121 121 121
     121 121 121 121  82 121 121 121 121
     121 121 121 121  83 121 121 121 121
     121 121 121 121  84 121 121 121 121
     121 121 121 121 100 121 121 121 121
     121 121 121 121 100 121 121 121 121
     121 121 121 121 121 121 121 121 121
502  27 7.2432E-04 -503 imp:n=1 u=122 lat=2 tmp=3.447E-08 fill= -1:1 -1:1 -5:5 $ Zone 2
     122 122 122 122 122 122 122 122 122
     122 122 122 122 100 122 122 122 122
     122 122 122 122 100 122 122 122 122
     122 122 122 122  85 122 122 122 122
     122 122 122 122  85 122 122 122 122
     122 122 122 122  86 122 122 122 122
     122 122 122 122  87 122 122 122 122
     122 122 122 122  88 122 122 122 122
     122 122 122 122 100 122 122 122 122
     122 122 122 122 100 122 122 122 122
     122 122 122 122 122 122 122 122 122
503  27 7.2432E-04 -503 imp:n=1 u=123 lat=2 tmp=3.447E-08 fill= -1:1 -1:1 -5:5 $ Zone 3
     123 123 123 123 123 123 123 123 123
     123 123 123 123 100 123 123 123 123
     123 123 123 123 100 123 123 123 123
     123 123 123 123  89 123 123 123 123
     123 123 123 123  89 123 123 123 123
     123 123 123 123  90 123 123 123 123
     123 123 123 123  91 123 123 123 123
     123 123 123 123  92 123 123 123 123
     123 123 123 123 101 123 123 123 123
     123 123 123 123 101 123 123 123 123
     123 123 123 123 123 123 123 123 123
504  27 7.2432E-04 -503 imp:n=1 u=124 lat=2 tmp=3.447E-08 fill= -1:1 -1:1 -5:5 $ Zone 4
     124 124 124 124 124 124 124 124 124
     124 124 124 124 100 124 124 124 124
     124 124 124 124 100 124 124 124 124
     124 124 124 124  93 124 124 124 124
     124 124 124 124  93 124 124 124 124
     124 124 124 124  94 124 124 124 124
     124 124 124 124  95 124 124 124 124
     124 124 124 124  96 124 124 124 124
     124 124 124 124 101 124 124 124 124
     124 124 124 124 101 124 124 124 124
     124 124 124 124 124 124 124 124 124
525  0 -950 imp:n=1 u=125 tmp=3.447E-08 fill=121 $ B04
526  like 525 but u=126 fill=121 *trcl=(0 0 0 180 90 90 270 180 90 90 90 0) $ B01
527  like 525 but u=127 fill=121 *trcl=(0 0 0 120 30 90 210 120 90 90 90 0) $ B02
528  like 525 but u=128 fill=121 *trcl=(0 0 0 60 330 90 150 60 90 90 90 0) $ B03
529  like 525 but u=129 fill=121 *trcl=(0 0 0 300 210 90 30 300 90 90 90 0) $ B05
530  like 525 but u=130 fill=121 *trcl=(0 0 0 240 150 90 330 240 90 90 90 0) $ B06
531  0 -950 imp:n=1 u=131 tmp=3.447E-08 fill=122 $ C02
532  like 531 but u=132 fill=122 *trcl=(0 0 0 300 210 90 30 300 90 90 90 0) $ C04
533  like 531 but u=133 fill=122 *trcl=(0 0 0 240 150 90 330 240 90 90 90 0) $ C06
534  like 531 but u=134 fill=122 *trcl=(0 0 0 180 90 90 270 180 90 90 90 0) $ C08
535  like 531 but u=135 fill=122 *trcl=(0 0 0 120 30 90 210 120 90 90 90 0) $ C10
536  like 531 but u=136 fill=122 *trcl=(0 0 0 60 330 90 150 60 90 90 90 0) $ C12
537  0 -950 imp:n=1 u=137 tmp=3.447E-08 fill=123 $ D05/09
538  like 537 but u=138 fill=123 *trcl=(0 0 0 60 330 90 150 60 90 90 90 0) $ D02/06
539  like 537 but u=139 fill=123 *trcl=(0 0 0 120 30 90 210 120 90 90 90 0) $ D03/17
540  like 537 but u=140 fill=123 *trcl=(0 0 0 300 210 90 30 300 90 90 90 0) $ D08/12
541  like 537 but u=141 fill=123 *trcl=(0 0 0 240 150 90 330 240 90 90 90 0) $ D11/15
542  like 537 but u=142 fill=123 *trcl=(0 0 0 180 90 90 270 180 90 90 90 0) $ D14/18
543  0 -950 imp:n=1 u=143 tmp=3.447E-08 fill=124 $ D07
544  like 543 but u=144 fill=124 *trcl=(0 0 0 120 30 90 210 120 90 90 90 0) $ D01
545  like 543 but u=145 fill=124 *trcl=(0 0 0 60 330 90 150 60 90 90 90 0) $ D04
546  like 543 but u=146 fill=124 *trcl=(0 0 0 300 210 90 30 300 90 90 90 0) $ D10
547  like 543 but u=147 fill=124 *trcl=(0 0 0 240 150 90 330 240 90 90 90 0) $ D13
548  like 543 but u=148 fill=124 *trcl=(0 0 0 180 90 90 270 180 90 90 90 0) $ D16
c
c --- Control Column ------------------------------------------------------------
c ------ Control Rod Segments ------
601  24 8.7530E-02 -103 imp:n=1 u=150 tmp=3.447E-08 $ spine
```

```
602  27 7.2432E-04 103 -104 imp:n=1 u=150 tmp=3.447E-08 $ helium gap
603  24 8.7530E-02 104 -101 imp:n=1 u=150 tmp=3.447E-08 $ inner clad
604  23 9.8436E-02 101 -102 imp:n=1 u=150 tmp=3.447E-08 $ absorber
605  24 8.7530E-02 102 -105 imp:n=1 u=150 tmp=3.447E-08 $ outer clad
606  27 7.2432E-04 105 imp:n=1 u=150 tmp=3.447E-08 $ helium
607  0 -151 imp:n=1 u=151 lat=2 tmp=3.447E-08 fill=150 $ rod segment
608  0 -152 imp:n=1 u=152 tmp=3.447E-08 fill=151 $ control rod
609  27 7.2432E-04 152 imp:n=1 u=152 tmp=3.447E-08 $ helium
c
c ------ Positions ------
610  0 -999 imp:n=1 u=153 tmp=3.447E-08 fill=152 (0 0 187.3) $ C
611  0 -154 imp:n=1 u=154 tmp=3.447E-08 fill=153 (10.8 0 0)
612  0 -155 imp:n=1 u=154 tmp=3.447E-08 fill=153 (-5.4 -9.35307 0)
613  27 7.2432E-04 -156 imp:n=1 u=154 tmp=3.447E-08 $ RSS
614  like 610 but u=155 fill=152 (0 0 187.3) $ R1
615  like 611 but u=156 fill=155 (10.8 0 0)
616  like 612 but u=156 fill=155 (-5.4 -9.35307 0)
617  like 613 but u=156
618  like 610 but u=157 fill=152 (0 0 187.3) $ R2
619  like 611 but u=158 fill=157 (10.8 0 0)
620  like 612 but u=158 fill=157 (-5.4 -9.35307 0)
621  like 613 but u=158
622  like 610 but u=159 fill=152 (0 0 404.9) $ R3
623  like 611 but u=160 fill=159 (10.8 0 0)
624  like 612 but u=160 fill=159 (-5.4 -9.35307 0)
625  like 613 but u=160
c
c ------ C Column ------
626  25 8.7804E-02 154 155 156 -550 imp:n=1 u=154 tmp=3.447E-08 $ graphite blocks
627  27 7.2432E-04 550 imp:n=1 u=154 tmp=3.447E-08
628  0 -950 imp:n=1 u=161 tmp=3.447E-08 fill=154 $ A01
c
c ------ R1 Columns ------
629  25 8.7804E-02 154 155 156 -550 imp:n=1 u=156 tmp=3.447E-08 $ graphite blocks
630  like 627 but u=156
631  like 628 but u=162 fill=156 $ C01
632  like 631 but u=163 *trcl=(0 0 0 300 210 90 30 300 90 90 90 0) $ C03
633  like 631 but u=164 *trcl=(0 0 0 240 150 90 330 240 90 90 90 0) $ C05
634  like 631 but u=165 *trcl=(0 0 0 180 90 90 270 180 90 90 90 0) $ C07
635  like 631 but u=166 *trcl=(0 0 0 120 30 90 210 120 90 90 90 0) $ C09
636  like 631 but u=167 *trcl=(0 0 0 60 330 90 150 60 90 90 90 0) $ C11
c
c ------ R2 Columns ------
637  25 8.7804E-02 154 155 156 -550 imp:n=1 u=158 tmp=3.447E-08 $ graphite blocks
638  like 627 but u=158
639  like 628 but u=168 fill=158 $ E23
640  like 639 but u=169 *trcl=(0 0 0 300 210 90 30 300 90 90 90 0) $ E03
641  like 639 but u=170 *trcl=(0 0 0 240 150 90 330 240 90 90 90 0) $ E07
642  like 639 but u=171 *trcl=(0 0 0 180 90 90 270 180 90 90 90 0) $ E11
643  like 639 but u=172 *trcl=(0 0 0 120 30 90 210 120 90 90 90 0) $ E15
644  like 639 but u=173 *trcl=(0 0 0 60 330 90 150 60 90 90 90 0) $ E19
c
c ------ R3 Columns ------
645  25 8.7804E-02 154 155 156 -550 imp:n=1 u=160 tmp=3.447E-08 $ graphite blocks
646  like 627 but u=160
647  like 628 but u=174 fill=160 $ E01
648  like 647 but u=175 *trcl=(0 0 0 240 150 90 330 240 90 90 90 0) $ E09
649  like 647 but u=176 *trcl=(0 0 0 120 30 90 210 120 90 90 90 0) $ E17
c
c --- Instrumentation Column ----------------------------------------------------
c ------ Positions ------
661  27 7.2432E-04 -155 imp:n=1 u=181 tmp=3.447E-08
662  27 7.2432E-04 -154 imp:n=1 u=181 tmp=3.447E-08
663  27 7.2432E-04 -156 imp:n=1 u=181 tmp=3.447E-08
c
c ------ Columns ------
664  25 8.7804E-02 154 155 156 -550 imp:n=1 u=181 tmp=3.447E-08 $ graphite blocks
665  like 627 but u=181
666  0 -950 imp:n=1 u=182 tmp=3.447E-08 fill=181
c
c --- Reflector Column ----------------------------------------------------------
c ------ Columns ------
671  25 8.7804E-02 -550 imp:n=1 u=183 tmp=3.447E-08 $ graphite blocks
672  like 627 but u=183
673  0 -950 imp:n=1 u=184 tmp=3.447E-08 fill=183
c
```

```
c --- HTTR Core ------------------------------------------------------------
c ------ Core Map ------
701  26 8.6134E-02 -551 imp:n=1 lat=2 u=200 tmp=3.447E-08 fill=-6:6 -6:6 0:0
     200 12r
     200 12r
     200 5r          175 184 170 184 182          200 1r
     200 4r        184 143 138 137 145 184        200 1r
     200 3r      171 140 164 132 163 139 169      200 1r
     200 2r    184 137 133 128 127 131 138 184    200 1r
     200 1r  182 146 165 125 161 126 162 144 174  200 1r
     200 1r    184 141 134 129 130 136 142 184    200 2r
     200 1r      172 140 166 135 167 139 168      200 3r
     200 1r       184 147 142 141 148 184         200 4r
     200 1r         176 184 173 184 182           200 5r
     200 12r
     200 12r
c
c ------ Core Map Legend ---
c    u 12r
c    u 12r
c    u 5r      Z G Y G I      u 1r
c    u 4r     G 4 3 3 4 G     u 1r
c    u 3r    Y 3 X 2 X 3 Y    u 1r           |
c    u 2r   G 3 2 1 1 2 3 G   u 1r           |     \
c    u 1r  I 4 X 1 C 1 X 4 Z  u 1r   --------+------> N
c    u 1r   G 3 2 1 1 2 3 G   u 2r           |     /
c    u 1r    Y 3 X 2 X 3 Y    u 3r           |
c    u 1r     G 4 3 3 4 G     u 4r
c    u 1r      Z G Y G I      u 5r
c    u 12r
c    u 12r
c
c    1 = Fuel Columns #1
c    2 = Fuel Columns #2
c    3 = Fuel Columns #3
c    4 = Fuel Columns #4
c    C = Central Control Column
c    X = R1 Control Columns
c    Y = R2 Control Columns
c    Z = R3 Control Columns
c    I = Instrumentation Columns
c    G = Removable Reflector Columns
c
702  0  -602 imp:n=1 fill=200
c
c --- Permanent Reflector --------------------------------------------------
711  26 8.6134E-02 602 -651 imp:n=1 tmp=3.447E-08
c
c --- The Great Void -------------------------------------------------------
999  0 651 imp:n=0
c

c Surface Cards ****************************************************************
c --- Fuel Blocks ----------------------------------------------------------
c ------ TRISO Particles ------
1    so 0.03   $ UO2 kernal
2    so 0.036  $ buffer
3    so 0.039  $ IPyC
4    so 0.0415 $ SiC
5    so 0.046  $ OPyC
6    so 0.066  $ overcoat
901 px -0.125
902 px  0.125
903 py -0.125
904 py  0.125
905 pz -0.125
906 pz  0.125
c
c ------ Compacts ------
911 px -0.053
912 px  0.053
913 py -0.053
914 py  0.053
915 pz -0.05
916 pz 0.05
921 px -1.31
```

```
922 px 1.31
923 py -1.31
924 py 1.31
925 pz -0.05
926 pz 0.05
12   rcc 0 0 -27.3 0 0 54.6 0.5 $ inside
13   rcc 0 0 -27.3 0 0 54.6 1.3 $ outside
c
c ------ Fuel Pins ------
21   rcc 0 0 -27.45 0 0 54.9 1.325 $ inside
22   rcc 0 0 -28.85 0 0 57.7 1.7   $ outside
c
c ------ Coolant Channels ------
31   rcc 0 0 -31 0 0 62 2.05
c
c ------ BP Pins ------
41   rcc 0 0 -25 0 0 20 0.7  $ BP
42   rcc 0 0  -5 0 0 10 0.7  $ graphite
43   rcc 0 0   5 0 0 20 0.7  $ BP
44   rcc 0 0 -25 0 0 50 0.75 $ pin
c
c --- Control Blocks ---------------------------------------------------------
c ------ Control Rod Segments ------
101  rcc 0 0 11 0 0 29 3.75 $ inside
102  rcc 0 0 11 0 0 29 5.25 $ outside
103  rcc 0 0 11 0 0 29 0.5 $ spine
104  rcc 0 0 11 0 0 29 3.25 $ inside clad
105  rcc 0 0 10 0 0 31 5.65 $ outside clad
c
c ------ Positions ------
151  hex 0 0 10 0 0 31 10 $ "box"
152  rcc 0 0 -145 0 0 310 6.30 $ control rod
154  rcc 10.8 0 -155 0 0 416 6.15 $ control rod hole
155  rcc -5.4 -9.35307 -155 0 0 416 6.15 $ control rod hole
156  rcc -5.4 9.35307 -155 0 0 416 6.15 $ control rod hole
c
c --- Reflector Blocks -------------------------------------------------------
c ------ Coolant Channels ------
201  rcc 0 0 -31 0 0 62 1.15
c
c --- Blocks -----------------------------------------------------------------
501  hex 0 0 -30 0 0 60 2.575 0 0 $ pitch
502  hex 0 0 -29.5 0 0 59 0 18 0 $ graphite
503  hex 0 0 -29 0 0 58 0 18.2 0 $ helium
c
c --- Columns ----------------------------------------------------------------
550  hex 0 0 -261.5 0 0 523 0 18 0
551  hex 0 0 -261 0 0 522 0 18.1 0
c
c --- HTTR Core --------------------------------------------------------------
602  hex 0 0 -261 0 0 522 -148 0 0
c
c --- Permanent Reflector ----------------------------------------------------
651  rcc 0 0 -261 0 0 522 212.5
c
c --- Auxiliary Organization -------------------------------------------------
950  rcc 0 0 -1000 0 0 2000 25 $ small cylinder
999  rcc 0 0 -2500 0 0 5000 2500 $ big cylinder
c

c Data Cards *****************************************************************
c --- Material Cards ---------------------------------------------------------
c ------ Kernel (3.4%) ------
m1    5010.85c 1.7299E-07
      8016.85c 4.6386E-02
      8017.85c 1.7633E-05
     92234.85c 6.1026E-06
     92235.85c 7.9888E-04
     92238.85c 2.2405E-02
c    Total     6.9614E-02
mt1   OUO2.80t
      UUO2.80t
c
c ------ Kernel (3.9%) ------
m2    5010.85c 1.7299E-07
      8016.85c 4.6386E-02
```

```
      8017.85c 1.7633E-05
     92234.85c 7.0000E-06
     92235.85c 9.1637E-04
     92238.85c 2.2288E-02
c    Total     6.9616E-02
mt2   OUO2.80t
      UUO2.80t
c
c ------ Kernel (4.3%) ------
m3    5010.85c 1.7299E-07
      8016.85c 4.6386E-02
      8017.85c 1.7633E-05
     92234.85c 7.7180E-06
     92235.85c 1.0104E-03
     92238.85c 2.2195E-02
c    Total     6.9617E-02
mt3   OUO2.80t
      UUO2.80t
c
c ------ Kernel (4.8%) ------
m4    5010.85c 1.7299E-07
      8016.85c 4.6386E-02
      8017.85c 1.7633E-05
     92234.85c 8.6154E-06
     92235.85c 1.1278E-03
     92238.85c 2.2078E-02
c    Total     6.9618E-02
mt4   OUO2.80t
      UUO2.80t
c
c ------ Kernel (5.2%) ------
m5    5010.85c 1.7299E-07
      8016.85c 4.6386E-02
      8017.85c 1.7633E-05
     92234.85c 9.3334E-06
     92235.85c 1.2218E-03
     92238.85c 2.1984E-02
c    Total     6.9619E-02
mt5   OUO2.80t
      UUO2.80t
c
c ------ Kernel (5.9%) ------
m6    5010.85c 1.7299E-07
      8016.85c 4.6386E-02
      8017.85c 1.7633E-05
     92234.85c 1.0590E-05
     92235.85c 1.3863E-03
     92238.85c 2.1821E-02
c    Total     6.9622E-02
mt6   OUO2.80t
      UUO2.80t
c
c ------ Kernel (6.3%) ------
m7    5010.85c 1.7299E-07
      8016.85c 4.6386E-02
      8017.85c 1.7633E-05
     92234.85c 1.1308E-05
     92235.85c 1.4803E-03
     92238.85c 2.1727E-02
c    Total     6.9623E-02
mt7   OUO2.80t
      UUO2.80t
c
c ------ Kernel (6.7%) ------
m8    5010.85c 1.7299E-07
      8016.85c 4.6386E-02
      8017.85c 1.7633E-05
     92234.85c 1.2026E-05
     92235.85c 1.5743E-03
     92238.85c 2.1634E-02
c    Total     6.9624E-02
mt8   OUO2.80t
      UUO2.80t
c
c ------ Kernel (7.2%) ------
m9    5010.85c 1.7299E-07
```

```
      8016.85c 4.6386E-02
      8017.85c 1.7633E-05
     92234.85c 1.2923E-05
     92235.85c 1.6918E-03
     92238.85c 2.1517E-02
c    Total     6.9625E-02
mt9   OUO2.80t
      UUO2.80t
c
c ------ Kernel (7.9%) ------
m10   5010.85c 1.7299E-07
      8016.85c 4.6386E-02
      8017.85c 1.7633E-05
     92234.85c 1.4180E-05
     92235.85c 1.8562E-03
     92238.85c 2.1353E-02
c    Total     6.9628E-02
mt10  OUO2.80t
      UUO2.80t
c
c ------ Kernel (9.4%) ------
m11   5010.85c 1.7299E-07
      8016.85c 4.6386E-02
      8017.85c 1.7633E-05
     92234.85c 1.6872E-05
     92235.85c 2.2087E-03
     92238.85c 2.1002E-02
c    Total     6.9632E-02
mt11  OUO2.80t
      UUO2.80t
c
c ------ Kernel (9.9%) ------
m12   5010.85c 1.7299E-07
      8016.85c 4.6386E-02
      8017.85c 1.7633E-05
     92234.85c 1.7769E-05
     92235.85c 2.3262E-03
     92238.85c 2.0886E-02
c    Total     6.9634E-02
mt12  OUO2.80t
      UUO2.80t
c
c ------ Buffer Layer ------
m13   5010.85c 1.8290E-08
      6000.85c 5.5153E-02
c    Total     5.5153E-02
mt13 Graph.80t
c
c ------ IPyC Layer ------
m14   5010.85c 3.0761E-08
      6000.85c 9.2758E-02
c    Total     9.2758E-02
mt14 Graph.80t
c
c ------ SiC Layer ------
m15   5010.85c 5.3208E-08
      6000.85c 4.8061E-02
     14028.85c 4.4327E-02
     14029.85c 2.2508E-03
     14030.85c 1.4837E-03
c    Total     9.6122E-02
mt15 Graph.80t
c
c ------ OPyC Layer ------
m16   5010.85c 3.0761E-08
      6000.85c 9.2758E-02
c    Total     9.2758E-02
mt16 Graph.80t
c
c ------ Graphite Overcoat ------
m17   5010.85c 2.8267E-08
      6000.85c 8.5237E-02
c    Total     8.5237E-02
mt17 Graph.80t
c
c ------ Graphite Compact ------
```

```
m18   5010.85c 1.5452E-08
      6000.85c 8.5237E-02
c    Total     8.5237E-02
mt18 Graph.80t
c
c ------ Graphite Sleeve ------
m19   5010.85c 7.2596E-09
      6000.85c 8.8747E-02
c    Total     8.8747E-02
mt19 Graph.80t
c
c ------ Burnable Poison (2.0%) ------
m20   5010.85c 3.9906E-04
      5011.85c 1.6063E-03
      6000.85c 8.8446E-02
c    Total     9.0451E-02
mt20 Graph.80t
c
c ------ Burnable Poison (2.5%) ------
m21   5010.85c 4.9882E-04
      5011.85c 2.0078E-03
      6000.85c 8.7995E-02
c    Total     9.0501E-02
mt21 Graph.80t
c
c ------ Graphite Disks ------
m22   5010.85c 7.2596E-09
      6000.85c 8.8747E-02
c    Total     8.8747E-02
mt22 Graph.80t
c
c ------ Neutron Absorber ------
m23   5010.85c 6.3184E-03
      5011.85c 2.5432E-02
      6000.85c 6.6685E-02
c    Total     9.8436E-02
mt23 Graph.80t
c
c ------ Alloy 800H ------
m24   6000.85c 3.2210E-04
     13027.85c 6.7209E-04
     14028.85c 5.5580E-04
     14029.85c 2.8222E-05
     14030.85c 1.8604E-05
     15031.85c 3.1225E-05
     16032.85c 1.4316E-05
     16033.85c 1.1462E-07
     16034.85c 6.4698E-07
     16036.85c 3.0162E-09
     22046.85c 3.1254E-05
     22047.85c 2.8186E-05
     22048.85c 2.7928E-04
     22049.85c 2.0495E-05
     22050.85c 1.9624E-05
     24050.85c 8.4860E-04
     24052.85c 1.6364E-02
     24053.85c 1.8556E-03
     24054.85c 4.6189E-04
     25055.85c 8.8022E-04
     26054.85c 2.2265E-03
     26056.85c 3.4951E-02
     26057.85c 8.0717E-04
     26058.85c 1.0742E-04
     28058.85c 1.8229E-02
     28060.85c 7.0217E-03
     28061.85c 3.0523E-04
     28062.85c 9.7320E-04
     28064.85c 2.4785E-04
     29063.85c 1.5791E-04
     29065.85c 7.0383E-05
c    Total     8.7530E-02
c
c ------ IG-110 Graphite ------
m25   5010.85c 1.1453E-08
      6000.85c 8.7804E-02
c    Total     8.7804E-02
```

```
mt25 Graph.80t
c
c ------ PGX Graphite ------
m26   5010.85c 3.6372E-08
      6000.85c 8.6134E-02
c    Total     8.6134E-02
mt26 Graph.80t
c
c ------ Helium Coolant ------
m27   2003.85c 9.9232E-10
      2004.85c 7.2432E-04
c    Total     7.2432E-04
c
c --- Control Cards ------------------------------------------------------------
mode  n
kcode 50000 1 50 1050
ksrc  93.545       0 -20  93.545       0 20
     -93.545       0 -20 -93.545       0 20
      55.050  76.350 -20  55.050  76.350 20
     -55.050  76.350 -20 -55.050  76.350 20
      55.050 -76.350 -20  55.050 -76.350 20
     -55.050 -76.350 -20 -55.050 -76.350 20
c print
```

Example NJOY Input File for Processing Cross Section Data at 400 K:

```
--
-- basic NJOY input file to create fast ACER files
reconr
 20 21
 'pendf tape for endf/b-vii.0 U-235'/
 9228 4 0/
 0.001 /
 'U-235 from endf/b-vii.0'/
 'processed by NJOY on July 29, 2009'/
 'by John Darrell Bess'/
 'see original library tape for evaluation details'/
 0 /
--
-- create pendf at desired temperature
broadr
 20 21 22
 9228 1 /
 0.001 /
 400 /
 0 /
--
-- generate heat production and radiation damage
heatr
 20 22 23 99
 9228 6 0 1 0 0 /
 302 303 304 402 443 444 /
--
-- unresolved region probability tables for MCNP
purr
 20 23 24
 9228 1 1 20 64 /
 400 /
 1.e10 /
 0 /
--
-- free gas inelastic scattering
thermr
 0 24 25
 0 9228 20 1 1 0 1 221 2 /
 400 /
 0.001 10. /
--
-- add gas production reactions
gaspr
 20 25 26
--
-- prepare fast ACE library and xsdir for MCNP
acer
 20 26 0 27 28
```

```
 1 0 1 .85 /
 'endf/b-vii.0 U-235'/
 9228 400 /
 /
 /
--
-- all done
stop
```

A.2 Buckling and Extrapolation Length Configurations

Buckling and extrapolation length measurements were not made.

A.3 Spectral-Characteristics Configurations

Spectral characteristics measurements were not made.

A.4 Reactivity-Effects Configurations

Reactivity effects measurements were not made.

A.5 Reactivity Coefficient Configurations

MCNP5 Input for Evaluating the Isothermal Temperature Coefficient:

Input decks for analysis of the isothermal temperature coefficients are that of the fully-loaded critical configuration (Appendix A.1) with modifications to the temperature of model cell cards, the temperature at which the evaluated neutron cross section data was evaluated, and the withdrawn position of the control rods.

Example NJOY Input File for Processing Cross Section Data:

The input files for processing neutron cross section libraries is identical to that used for processing the data at 400 K (Appendix A.1) but at the desired analysis temperatures.

A.6 Kinetics Parameter Configurations

Kinetics measurements have not been evaluated.

A.7 Reaction-Rate Configurations

Reaction-rate distribution measurements were not made.

A.8 Power Distribution Configuration

Power distribution measurements were not made.

A.9 Isotopic Configurations

Isotopic measurements were not made.

A.10 Configurations of Other Miscellaneous Types of Measurements

Other miscellaneous types of measurements were not made.

APPENDIX B: CALCULATED SPECTRAL DATA

B.1 Spectral Data for the Critical and Subcritical Configurations

The neutron spectral calculations provided below were obtained from the output files for the MCNP5 input decks provided in Appendix A.1 and results in Section 4.1 using the ENDF/B-VII.0 neutron cross section library. The cross sections are all continuous and the cross sections are processed with NJOY to correspond to the temperature of the benchmark configuration.

Table B.1. Spectral Data for the HTTR Benchmark Models using an Ordered Lattice.

Configuration		1	2
Temperature (K)		400	420
Neutron Cross Section Library		ENDF/B-VII.0	ENDF/B-VII.0
k_{eff}		1.01945	1.01965
$\pm\sigma_k$		0.00011	0.00011
Fission Fraction, by Energy (%)	**Thermal (<0.625 eV)**	92.17	92.16
	Intermediate	6.91	6.93
	Fast (>100 keV)	0.92	0.92
Average Number of Neutrons Produced per Fission		2.439	2.439
Energy of Average Neutron Lethargy Causing Fission (eV)		0.092158	0.092332

APPENDIX C: DATA FROM THE 16TH EDITION CHART OF THE NUCLIDES[a]

C.1 Isotopic Abundances and Atomic Weights

This evaluation incorporated atomic weights and isotopic abundances found in the 16th edition of the Chart of the Nuclides. A list of the values used in the benchmark model or in the generation of the MCNP input deck is compiled in Table C.1.

[a] Nuclides and Isotopes: Chart of the Nuclides, 16th edition, (2002).

Table C.1. Summary of Data Employed from the 16th Ed. of the Chart of the Nuclides.

Isotope or Element	Atomic Weight	Isotopic Abundance
He	4.002602	--
^{3}He	--	0.000137
^{4}He	--	99.999863
^{10}B	10.0129370	19.9
^{11}B	11.0093055	80.1
C	12.0107	--
N	14.0067	--
^{14}N	--	99.632
^{15}N	--	0.368
O	15.9994	--
^{16}O	--	99.757
^{17}O	--	0.038
^{18}O[(a)]	--	0.205
Na	22.989770	--
Al	26.981538	--
Si	28.0855	--
^{28}Si	--	92.2297
^{29}Si	--	4.6832
^{30}Si	--	3.0872
P	30.973761	--
S	32.065	--
^{32}S	--	94.93
^{33}S	--	0.76
^{34}S	--	4.29
^{36}S	--	0.02
Ca	40.078	--
^{40}Ca	--	96.941
^{42}Ca	--	0.647
^{43}Ca	--	0.135
^{44}Ca	--	2.086
^{46}Ca	--	0.004
^{48}Ca	--	0.187

(a) Neutronically, ^{18}O is treated as ^{16}O.

Table C.1 (cont.). Summary of Data Employed from the 16th Ed. of the Chart of the Nuclides.

Isotope or Element	Atomic Weight	Isotopic Abundance
Ti	47.867	--
^{46}Ti	--	8.25
^{47}Ti	--	7.44
^{48}Ti	--	73.72
^{49}Ti	--	5.41
^{50}Ti	--	5.18
Cr	51.9961	--
^{50}Cr	--	4.345
^{52}Cr	--	83.789
^{53}Cr	--	9.501
^{54}Cr	--	2.365
Mn	54.938049	--
Fe	55.845	--
^{54}Fe	--	5.845
^{56}Fe	--	91.754
^{57}Fe	--	2.119
^{58}Fe	--	0.282
Ni	58.6934	--
^{58}Ni	--	68.0769
^{60}Ni	--	26.2231
^{61}Ni	--	1.1399
^{62}Ni	--	3.6345
^{64}Ni	--	0.9256
Cu	63.546	--
^{63}Cu	--	69.17
^{65}Cu	--	30.83
^{234}U	234.040946	0.0055[(b)]
^{235}U	235.043923	0.7200[(b)]
^{238}U	238.050783	99.2745[(b)]

(b) Natural isotopic abundance of U.